DSPACE

https://dspace.org/

Morphological characteristics of humeri and ulnae relating to supratrochlear aperture expression

Ndou, Robert

2015-09-18
http://hdl.handle.net/10539/18701

Downloaded from a DSpace repository. https://dspace.org/

Morphological Characteristics of Humeri and Ulnae Relating to Supratrochlear Aperture Expression

ROBERT NDOU

A Thesis submitted to the Faculty of Health Sciences,
University of the Witwatersrand, Johannesburg,
in accomplishment of the requirements for the degree
of
DOCTOR OF PHILOSOPHY
.

Supervisor: Professor L.A. Schepartz

25 May 2015

DECLARATION

I, Robert Ndou (Student number: 603220) am a student registered for the degree of doctor of philosophy in the academic year 2015.

I hereby declare the following:

- This work has not been submitted before for any degree or examination at any other University.
- I am aware that plagiarism (the use of someone else's work without their permission and/or without acknowledging the original source) is wrong.
- I confirm that the work submitted for assessment for the above degree is my own unaided work except where I have explicitly indicated otherwise.
- I have followed the required conventions in referencing the thoughts and ideas of others.
- I understand that the University of the Witwatersrand may take disciplinary action against me if there is a belief that this is not my own unaided work or that I have failed to acknowledge the source of the ideas or words in my writing.
- I have included as an appendix a report from "Turnitin" (or other approved plagiarism detection) software indicating the level of plagiarism in my research document.

Signature: _____ Date: 25 May, 2015

ABSTRACT

The supratrochlear aperture (STA) is a perforation of the septum found between the olecranon and coronoid fossae of the humerus. Its prevalence is population specific and varies by sex. This study investigated the prevalence, shape and population-level variability of the STA, as well as the morphological attributes of dry humeri and ulnae according to STA expression, in South African populations (White, Mixed ethnicity and Black). The tissue found in the aperture was sampled from cadavers and studied by histochemical techniques. The objective was to identify the characteristics of STA bearing limbs in order to evaluate the possible etiology and function of the aperture.

The overall prevalence of the STA among South Africans was found to be 32.5%. Significant population differences exist, with Whites having the lowest rate of 16% and Sotho peoples expressing the highest prevalence of 41% among the Black group. The STA was more prevalent in females and on the left arm. In bilateral cases, females had twice the prevalence rate.

Osteometric measures of bone size were used to test the propositions that robust humeri are less prone to STA formation and that pressure from the ulnar olecranon and coronoid processes may result in an STA.

Most measures of overall humeral size, such as epicondylar breadth, humeral head circumference and the three shaft circumferences, were significantly larger when the STA was absent in all three populations. This supports the general proposition that gracile bones are prone to septal

perforation. However, an important result of this study is the finding from the discriminant analyses that determinants of STA status are population specific. For Blacks and the Mixed group, the olecranon process length was the sole main contributor to STA status. Lower loadings for this variable were found for the Mixed group. Therefore, this variable can more reliably predict STA status in Blacks compared to the Mixed group. In Whites, with a lower prevalence of the STA, more parameters are required for STA prediction compared to the Mixed group or Blacks. These additional parameters were proximal humeral shaft circumference (right) and trochlear notch depth (left).

The presence of dense connective tissue found crossing the aperture needs to be explained as it appears to be a feature unique to the distal humerus. It is possible that the STA forms as a result of incomplete remodeling in response to pressure from the olecranon process. The result would be bone resorption and subsequent osteoblastic secretion of collagen, but no incorporation of hydroxyapatite occurs – rendering the aperture region pliant and able to withstand the continuing force of the olecranon during joint motion. As to the function of the STA covering tissue, it may be of considerable structural strength in light of its dense regular connective tissue composition. It is strongly attached to the bony septum in a manner comparable to the way tendons attach to bone, suggesting a need for structural strength. One explanation for this particular feature of the tissue may be that it functions to prevent locking the olecranon process in the joint.

An additional aspect to be considered regarding function of the STA is that the mean extension angle in the STA bearing arms was greater. This implies that the olecranon process tip may penetrate the aperture (as observed on many dry humeri, when articulated with ulnae and elbow joints maximally extended), permitting a greater extension angle. It follows that the elbow range of motion is greater in STA individuals.

Based on orthopedic surgical experience, bones with the STA are thought to have a narrower medullary canal. Humeri with the STA in our study did appear to have narrower medullary canal dimensions. However, this was not the case after standardizing for bone size. The smaller medullary canal width observed in STA humeri is due to the bone size differences rather than the presence of the STA. We therefore propose that bone size be the major factor to consider when making choices of a rod for intramedullary fixation.

For my family and friends

CONTENTS

Item		Page
Declaration		ii
Abstract		iii
Dedication		iv
Figure List		vi
Table List		x
Publications and presentations arising from thesis		xii
Chapter 1	General introduction	1
Chapter 2	The supratrochlear aperture (STA) of the humerus among South Africans	
Chapter 3	Morphometric characteristics of the humerus and ulna in limbs bearing the supratrochlear aperture (STA)	
Chapter 4	A radiographic investigation of the relationships between humeral cortical bone thickness, medullary canal width and the supratrochlear aperture (STA)	
Chapter 5	The relationship between elbow extension angle and the supratrochlear aperture (STA)	
Chapter 6	Characterization of the tissue crossing the supratrochlear aperture of the humerus using histochemical techniques	
Chapter 7	Generalized discussion and conclusion	
References		
Appendix	P-values	

LIST OF FIGURES

Figure	Title	Page
Figure 1.1	Elbow – skeletal articulation	3
Figure 1.2	Long bone (Humerus) showing various parts	14
Figure 1.3	The Haversian system	17
Figure 1.4	Bone remodeling phases	19
Figure 1.5	Figure 1.5: Skeletal components of the elbow joint and their articulation	15
Figure 2.1	Measurements taken from the STA	27
Figure 2.2	Various shapes of the STA	32
Figure 3.1	Measurements taken from the humerus	44
Figure 3.2	Measuring the depth of the olecranon fossa using a palatometer	45
Figure 3.3	Measurements taken from the proximal aspect of the ulna	46
Figure 3.4	Humerus head circumference	49
Figure 3.5	Epicondylar breadth (EB).	51
Figure 3.6	Humeral length.	52
Figure 3.7	Humerus shaft circumferences - proximal, midshaft and distal	55
Figure 3.8	Olecranon fossa depth	57
Figure 3.9	Olecranon process length (O)	59
Figure 3.10	Coronoid process length	60
Figure 3.11	Olecranon-coronoid distance (O-C)	62
Figure 3.12	Trochlear notch depth (D)	64
Figure 3.13	Ulnar length	66
Figure 3.14	Population discrimination	69
Figure 3.15	Segregation by STA status	72
Figure 3.16	Classification of limbs by STA status in Whites	75
Figure 3.17	Classification of limbs by STA status in the Mixed group	78
Figure 3.18	Classification of limbs by STA presence and absence in Blacks	81
Figure 4.1	Representation of cone bean (a) and Lodox Statscan (b) configurations	95
Figure 4.2	Width of the humerus	103
Figure 4.3	The medullary canal	106
Figure 4.4	Differences in mean medullary canal width in Whites by humeral shaft region, stratified by STA status and age	107

Figure 4.5	Differences in mean medullary canal width in the Mixed group by humeral shaft region, stratified by STA status and age	109
Figure 4.6	Differences in mean medullary canal width in Blacks by humeral shaft region, stratified by STA status and age	111
Figure 4.7	Differences in mean medullary canal proportion in Whites by humeral shaft region, stratified by STA status and age	114
Figure 4.8	Mean differences in medullary canal width proportion in the Mixed group by humeral shaft region, stratified by STA status and age	115
Figure 4.9	Mean differences in medullary canal width proportion in Blacks by humeral shaft region, stratified by STA status and age	115
Figure 4.10	Standardized mean medullary canal width proportion in the proximal and distal shaft regions for combined age cohorts 46-60, stratified by population and STA status	116
Figure 5.1	Measurements taken from the proximal aspect of the ulna	138
Figure 5.2	Measuring the extension angle	139
Figure 5.3	Extension angle and the presence of STA (A) and by side (B)	140
Figure 5.4	Extension angle in males and females	141
Figure 5.5	Extension angle and the side of STA in males and females	142
Figure 5.6	Elbow extension in males and females	143
Figure 5.7	Magnitude of extension and STA parameters	144
Figure 5.8	Classification of limbs by STA presence and absence	146
Figure 5.9	Classification of limbs by degree of extension	148
Figure 6.1	The setup of the equipment used to radiograph	159
Figure 6.2	A dry bone used for radiographic standardization	160
Figure 6.3	Identification of the STA in radiographs	162
Figure 6.4	Demarcating the area of interest on the humerus for tissue harvesting	163
Figure 6.5	Harvesting and bisecting the tissue samples	164
Figure 6.6	STA (composite image) stained with Rapid One-Step Mallory-Heidenhain.	165
Figure 6.7	Control sample stained with Rapid One-Step Mallory-Heidenhain (composite image)	165

LIST OF TABLES

Table	Title	Page
Table 1.1	Types of connective tissue	13
Table 2.1	Total number of skeletonized individuals studied in each ethnic group	27
Table 2.2	Measurements taken and instruments used	28
Table 2.3	The prevalence and laterality of STA in males and females	30
Table 2.4	The prevalence of STA in each of the six ethnic groups studied	31
Table 2.5	Shapes of the STA in the six ethnic groups studied.	31
Table 2.6	The mean ($\overline{X}$) dimensions of the STA and the distal humerus in the six ethnic groups studied	33
Table 2.7	Dimensions of the STA and the distal humerus in males and females	33
Table 3.1	Sample	44
Table 3.2	Humerus head circumference	49
Table 3.3	Humerus epicondylar breadth	51
Table 3.4	Humeral length	52
Table 3.5	Proximal, Midshaft, and distal humeral circumferences	54
Table 3.6	Olecranon fossa depth.	57
Table 3.7	Olecranon process length (O)	59
Table 3.8	Coronoid process length	60
Table 3.9	Olecranon-coronoid distance (O-C)	62
Table 3.10	Trochlear notch depth (D)	64
Table 3.11	Ulnar length	66
Table 3.12	Structure matrix showing correlations between variables distinguishing populations and standardized canonical discriminant functions	68
Table 3.13	Population classification	69
Table 3.14	Structure matrix showing correlations between STA status discriminating variables and standardized canonical discriminant functions in the combined sample	71
Table 3.15	Classification by STA status	72
Table 3.16	Structure matrix showing correlations between variables distinguishing STA status and standardized canonical discriminant functions in Whites	74
Table 3.17	Classification of limbs by STA status in Whites	75

Table 3.18	Structure matrix showing correlations between variables discriminating STA status and standardized canonical discriminant functions in the Mixed group	77
Table 3.19	Classification of STA status in the Mixed group	78
Table 3.20	Structure matrix showing correlations between variables discriminating STA status and standardized canonical discriminant functions in Blacks	80
Table 3.21	Classification of STA by presence and STA side in Blacks	80
Table: 4.1	STA status of the sample	98
Table 4.2	Age profile by population, sex and STA status	98
Table 4.3	Measurements taken from the radiographs	100
Table 4.4	Proximal, Midshaft, and Distal Humeral Width.	102
Table 4.5	Proximal, Midshaft, and Distal medullary canal width	105
Table 4.6	Proportion of the medullary canal width to cortical bone thickness by population, and further stratified by sex and STA status	113
Table 4.7	Spearman's correlation for the cortical thickness (CT) and medullary canal width (MCW) by age cohorts and further stratified by STA status in Whites	118
Table 4.8	Spearman's correlation for the cortical thickness (CT) and medullary canal width (MCW) by age cohorts and further stratified by STA status among individuals of the Mixed group.	120
Table 4.9	Spearman's correlation for the cortical thickness (CT) and medullary canal width (MW) by age cohorts and further stratified by STA status in Blacks	123
Table 5.1	Number of humeri with and without STA.	136
Table 5.2	Correlations between variables discriminating STA status and standardized canonical discriminant functions	145
Table 5.3	Classification of STA by presence and STA side	146
Table 5.4	Correlations between variables predicting degree of extension and standardized canonical discriminant functions	147
Table 5.5	Classification according to degree of extension	148
Table 6.1	Samples taken from cadavers.	158

PUBLICATIONS AND CONFERENCE PRESENTATIONS EMANATING FROM THIS THESIS

PUBLICATIONS

Ndou R, Smith P, Gemell R, Mohatla O. 2013. The supratrochlear foramen of the humerus in a South African dry bone sample. Clin Anat 26:870-874.

CONFERENCE PRESENTATIONS

The 18th Congress of the International Federation of Associations of Anatomists (IFAA) 08-10 August, 2014: Characterization of the tissue crossing the septal aperture using radiography and histochemical techniques.

The 2nd International Conference on Forensic Research & Technology 7 - 9 October 2013, Las Vegas, Nevada, USA: Morphometric characteristics of the humerus and ulna in limbs bearing the supratrochlear aperture (STA).

The 40th annual conference of the Anatomical Society of Southern Africa (ASSA), 14–18 April 2012, Windhoek, Namibia: The supratrochlear foramen of the humerus: A South African Study.

CHAPTER 1

General Introduction:

Literature Review, Aims and Objectives

Contents_Toc414787196

1.0 GENERAL INTRODUCTION 3
1.1 LITERATURE REVIEW 6
1.1.1 The supratrochlear aperture (STA) 6
1.2 T-BOX 10
1.3 CONNECTIVE TISSUE AND BONE 11
1.3.1 Connective tissue and collagen 11
1.3.2 Bone 14
1.4 BIOMECHANICS OF BONE 22
1.5 AIM OF THE STUDY 23
1.5.1 Objectives 24

1.0 GENERAL INTRODUCTION

The humerus is the major long bone of the upper limb and comprises a shaft as well as a proximal and distal extremity. The distal extremity of the humerus articulates with the ulna anteriorly and posteriorly to form the elbow joint. Anteriorly, the ulnar coronoid process articulates with the coronoid fossa of the humerus in flexion (Fig. 1.1A), while in extension the olecranon process articulates posteriorly with the olecranon fossa (Fig. 1.1B). A bony septum separates the coronoid and olecranon fossae. This septum is occasionally perforated, forming the supratrochlear aperture (STA) of the humerus (Fig. 1.1C).

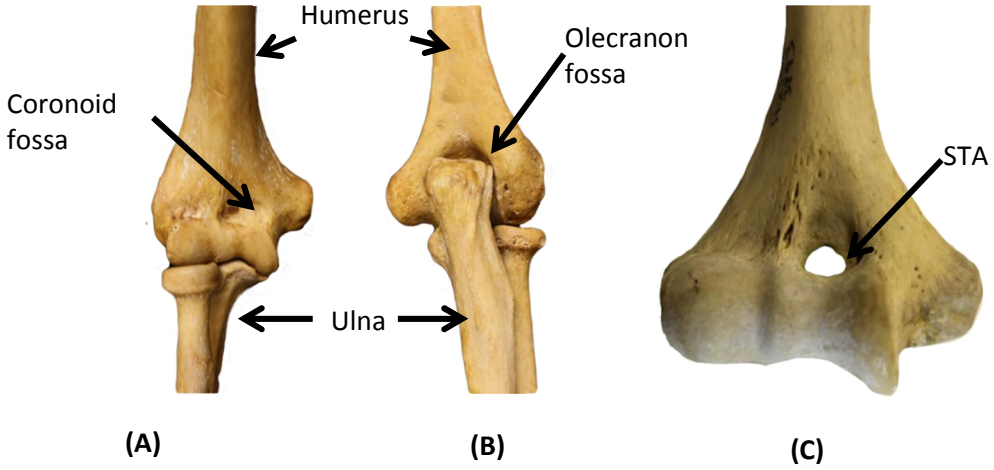


Figure 1.1: Elbow – skeletal articulation: A – anterior view; B – posterior view; C – supratrochlear aperture (STA) . Images not to scale.

The prevalence of the STA in human populations varies substantially, from very low in Greeks (less than 1%) to over 50% among Arkansas Indians (Nayak et al., 2009). A few patterns are known to characterize all populations: the size and shape of the STA is highly variable; females have higher STA frequencies than males; and the left exhibits the trait with a higher frequency than the right humerus in both sexes.

The function and etiology of the STA are not known, but it is generally understood that the STA and its formation are related to the functional development of the elbow joint. Some researchers suggested a mechanical explanation whereby the interaction of the humerus and ulnar at the elbow joint result in septal resorption (Glanville, 1967; Mays, 2008). Another possible cause is the heritability of the feature, as reflected in the observed population differences in its occurrence (Glanville, 1967). To address these issues, the morphological and structural characteristics of the STA region, as well as those of the humeri and ulnae in individuals bearing the STA, need to be determined and compared to cases lacking the STA.

This study investigates the STA in three different South African populations. We start by determining the frequencies of the aperture. Then, we test the hypothesis, based on the general observation that STAs are more common in females, that gracility of bones may predispose individuals to aperture formation. The internal humeral structure is studied with respect to the medullary canal width and cortical bone thickness as these dimensions may be smaller when an STA is present. We then examine aspects of the mechanical hypothesis (see section 1.1.1, proposed etiology) by documenting size variation in components of the joint as size may affect the range of flexion and extension. The ability of arms with the aperture to hyperextend is also investigated, and finally we examine the tissue that occupies the STA in cadaveric remains. As this tissue is subjected to pressure in elbow extension and flexion, we

hypothesize that it will have characteristics that give it resilience to such pressures.

.

1.1 LITERATURE REVIEW

1.1.1 The supratrochlear aperture (STA)

The STA is commonly referred to using various descriptive terms such as supratrochlear foramen (Singhal and Rao, 2007), septal aperture (Akabori, 1934; Sahajpal and Pichora, 2006), aperture in the coronoid-olecranon septum (Koyun et al., 2011) or intercondyloid foramen (Kumarasamy et al., 2011). Human skeletal biologists are routinely trained to record it as a non-metric skeletal trait that is more frequently observed in females (White et al., 2012), but there has been limited systematic research on its variability or function. The diversity of terms used to denote the same structure speaks to the lack of understanding about its function and etiology, as anatomically, foramina and apertures have different characteristics. Specifically, foramina are defined as conduits for vessels while apertures are merely openings in bone (White et al., 2012). No anatomical structure is known to pass through the STA. Instead, in life the STA is reported to be covered by a membrane (Nayak et al., 2009).

Worldwide prevalence

Worldwide prevalence of the STA varies (0.3% to 58%) among different populations (Christos et al., 2011; Nayak et al., 2009). In one Greek sample, Christos et al. (2011) found no STAs in 304 males but did find the aperture in 0.57% of 352 females resulting in an overall prevalence of 0.3%. A Chinese study of 264 humeri found STA in 17.5% with significant differences, 6.9% and 27.3%, between males and females respectively (Ming-Tzu, 1935). Similarly, the overall prevalence in Japanese populations has been found to be 18.1% (Singhal and Rao, 2007), with a

greater frequency of 20.6% observed in females as compared to males (13.5%) (Akabori, 1934). A prevalence of 32% was found in Central India, whereas a lower prevalence was found among the South (28%), North (27.5%), and East Indian (27.4%) populations, as reviewed by Singhal and Rao (2007). The highest recorded prevalence of 58% for Arkansas Indians was reported in Nayak et al. (2009).

Prevalence in South Africa

The overall prevalence of the STA has been determined to be 32.5% in a South African dry bone sample of 538 skeletonized individuals in the Raymond A Dart Collection for the White, Mixed ethnic group and Black populations. The STA occurred bilaterally in 15.1% of the sample, with twice as many females affected as males. In unilateral cases, the prevalence was higher on the left compared to the right. The prevalence was the lowest in Whites (16%) followed by the Mixed ethnic group (31%) and highest in Blacks (Sotho individuals with 41%) (Ndou et al., 2013).

The STA occurred in round, oval, triangular and irregular form, with the highest prevalence of the oval shape (Ndou et al., 2013). The Mixed ethnicity group had the largest transverse and vertical diameters of the STA compared to the other groups (Ndou et al., 2013).

Clinical significance

The medullary canal has been found to be shorter and narrower in STA humeri (Akpinar et al., 2003; Singhal and Rao, 2007; Sunday et al., 2014). This may have implications in orthopedic surgery, when a nail or rod is inserted into the medullary cavity (intramedullary fixation) in order to stabilize a diaphyseal fracture site. Knowledge of the dimensions of the

humerus and the medullary cavity are therefore important for choosing the nail or rod of appropriate length and diameter to avoid secondary fractures during the surgical procedure. It is recommended for radiologists to be aware of the occurrence of the aperture to help avoid misinterpretation of radiographs as it may be interpreted as an osteolytic lesion (De Wilde et al., 2004). The presence of this aperture is also a risk factor for low energy fractures of the distal aspect of the humerus (Sahajpal and Pichora, 2006).

It is proposed that individuals with the STA have the potential to hyperextend at the elbow joint (Glanville, 1967). The elbow forms an essential link in the upper limb between the hand, the wrist, and the shoulder. Primarily, it facilitates positioning of the hand in space such as in reaching out to grab an object. Therefore, loss of function at the elbow results in impairment, affecting the activities of daily living (Alt Murphy et al., 2011). Disease, congenital deformity or injury to the elbow may limit the range of motion (ROM), stability, and overall function. Certain diseases that involve disturbances in bone remodeling, such as familial expansile osteolysis, may affect joint motion and bone integrity (Colbert, 2007).

The clinical assessment of the condition of a joint often requires ROM measurements (Vasen et al., 1995). The integrity of the ROM is crucial since even minor deficiencies may affect the physical abilities of a patient. Females tend to have greater joint mobility irrespective of age, although aging decreases ROM in joints of both males and females (Soucie et al., 2011). When the STA is present, the ROM tends to be greater compared to when it is absent (Glanville, 1967). There are differences in elbow

extension angle between the left and right sides, with the left exhibiting a higher extension angle than the right side (Gunal et al., 1996).

Proposed etiologies of the STA

Two general theories regarding the formation of the STA have been proposed: the mechanical theory and the genetic theory (Glanville, 1967). According to the mechanical theory, the STA is formed as a consequence of perforation of the septum by articulation of the ulna and the humerus during excessive extension and flexion (Glanville, 1967; Mays, 2008; Singhal and Rao, 2007). Three findings are currently used to bolster the mechanical theory. The prevalence of the STA is greater on the generally more gracile left arm and is sometimes twice as prevalent in females. Secondly, smaller epicondylar breadths in females are associated with the aperture (Krishnamurthy et al., 2011; Mahajan, 2011; Ndou et al., 2013). Third, these characteristics together suggest that the STA is more prevalent in gracile bones (Benfer and McKern, 1966; Mays, 2008). It follows that robust bones are assumed to have a thicker and stronger olecranon septum that would withstand the stresses of humero-ulnar articulation.

Disturbances in bone development and in calcium metabolism have been cited as some of the other explanations of the STA etiology (Koyun et al., 2011). The former would affect ossification while the later may result in weak bones. Bone resorption in early adulthood is thought to be another possible explanation for the etiology (Mays, 2008). This bone resorption is said to be a result of articulation of the ulna and humerus in movement of the elbow. Some researchers (Mays, 2008) have found no STAs in

children, while others (Koyun et al., 2011) have seen it only in one female aged 16 years out of a sample of 709 participants. This suggests that the aperture generally forms after adolescence. Having not found signs of bone deposition around the aperture in adults, Mays (2008) suggested that once formed the aperture persists, as new bone formation would indicate an attempt for aperture obliteration.

In contrast, the genetic theory proposes that the STA is an inherited characteristic. Frequencies of unilateral and bilateral occurrences of the STA seen among various populations are thought to indicate genetic differences (Koyun et al., 2011). Since the STA occurs mostly on the left and among females, it is suggested that the gene is possibly not expressed on the stronger side (mostly right) or in males. It is possible that the genetic differences may be in overall skeletal size although there is no direct evidence of such genes. Atavism is also considered to be a possible etiology (Koyun et al., 2011).

1.2 T-BOX

T-Box genes may play a role in STA formation. Genes of the TBX family control the synthesis of proteins known as T-box proteins that are crucial for the development of the limbs and the heart huring both in-utero (Chapman et al., 1996) and postnatal development (Govoni et al., 2009). Since the STA is not present in neonates, it is possible that these genes may play a role in STA etiology in postnatal development. Animal studies show expression of *Tbx2* and *Tbx3* limb buds (Chapman et al., 1996;

Simon, 1999). In humans, *Tbx3* is important in the development of the distal aspects of the upper limb (He et al., 1999).

In animals, *Tbx4* and *Tbx5* are important in the differentiation between the hind limb and forelimb (Isaac et al., 1998) and this may be the case in humans as mutations in *TBX5* compromise the development of both the upper limb and the heart (Basson et al., 1997). Tbx3 is crucial in regulation of osteoblast proliferation or control of osteoblast cell number as there is an increase in the expression of Tbx3 in the course of osteoblast differentiation (Govoni et al., 2006). These findings suggest that T-box genes may potentially have a role in human variation with reference to the limbs such as the formation of the STA.

1.3 CONNECTIVE TISSUE AND BONE

To test the mechanical hypothesis of STA etiology and to investigate the tissues crossing this feature information on the basic structure of connective tissue and, bone structure, bone remodeling, and the mechanisms by which the latter two processes can be altered is necessary. The following section reviews those topics.

1.3.1 Connective tissue and collagen

Connective tissue occupies the STA. However, the role and composition of that tissue have not been previously studied. Connective tissue is composed of cells and extracellular matrix that fills the spaces between organs and tissues. The extracellular matrix is made up of fibers in a protein and polysaccharide medium (Mescher, 2013). Collagen is the main fibrous protein in the extracellular matrix and in connective tissue.

Generally, connective tissue is considered as loose or dense, depending on the arrangement of the fibers (Table 1.1). The composition of the extracellular matrix varies in connective tissues of different properties- such as bone in which the matrix is calcified (Kierszenbaum and Tres, 2012). The interstitial fluid of connective tissue provides metabolic support to cells as it serves as the medium for diffusion of nutrients and waste products (Mescher, 2013).

Loose connective tissue has sparse fibers and is generally found in the mucosa and submucosa of different organs and also surrounds blood vessels, nerves and muscle. In contrast, dense connective tissue has closely packed fibers and is further divided into dense regular and dense irregular tissue depending on the arrangement of the fibers (Kierszenbaum and Tres, 2012). In dense regular connective tissue, such as the type we have recently observed crossing the STA (Chapter 6), the fibers are arranged parallel to each other such as in tendon. In contrast, the fibers are randomly oriented in the dense irregular connective tissue of the skin (Kierszenbaum and Tres, 2012; Ovalle and Nahirney, 2013).

Connective tissue is composed of collagen, reticular, and elastic fibers (Paulsen, 2010). Whereas both collagen and reticular fibers are formed by proteins of the collagen family, elastic fibers are made of elastin. The distribution of these fibers is connective tissue type dependent, resulting in the predominant fiber type being responsible for specific tissue properties. For example, elastic fibers are abundant in the lungs where stretching is a required feature. Elastic fibers can stretch to 150% of their length without breaking and are able to recoil (Paulsen, 2010). Reticular fibers are thin

and highly glycosylated, forming delicate networks instead of bundles. These supportive fiber networks permit movement of cells and fluids in loosely arranged (e.g., hematopoietic) tissues (Kierszenbaum and Tres, 2012; Paulsen, 2010).

Table 1.1: Types of connective tissue. The typical characteristics and examples of their respective body sites or organs of occurrence (Ross and Pawlina, 2011).

Type		Characteristics	Site
Loose	Reticular fibers	Loosely arranged sparse fibers	Kidney and spleen
	Adipose	Thin mesh of polyhedral or oval shaped strands	Fat cells e.g. hypodermis
	Elastic	Fibers arranged parallel to each other	Ear and lungs
Dense	Dense regular	Fibers in randomly oriented	Cartilage and tendons
	Dense irregular	Fibers arranged parallel to each other	Skin and bone

1.3.2 Development of the humerus

The humerus begins as a cartilaginous bud in the first trimester and begins ossification in the 7th week of intrauterine life. Proximally, there is an epiphysis for the head and for the greater and lesser tubercles. Distally, there are four ossification centres (Baker et al., 2005). These are for the capitulum, trochlear, medial and lateral epicondyles. The metaphyseal surface of the distal aspect widens mediolaterally, resulting in a flattened appearance. The olecranon fossa is deepened by the removal of periosteal bone to the extent that the anteroposterior thickness of the bone in that region is less than that of the metaphysis (Gray and Gardner, 1969).

1.3.3 Bone structure

Bone is a rigid but vascularized and metabolically active connective tissue mineralized with calcium and phosphate. Most of the adult skeleton is composed of bone, a form of mineralized connective tissue that contains collagen and calcium. The basic functions of bones are support and protection, locomotion, hemopoiesis, and storage of minerals. Bone integrity is crucial for general health, normal function for locomotion, and relative movements at certain joints in activities of daily living. Anatomically, it is categorized into two distinct forms: compact and spongy (trabecular or cancellous) bone (Fig. 1.2).

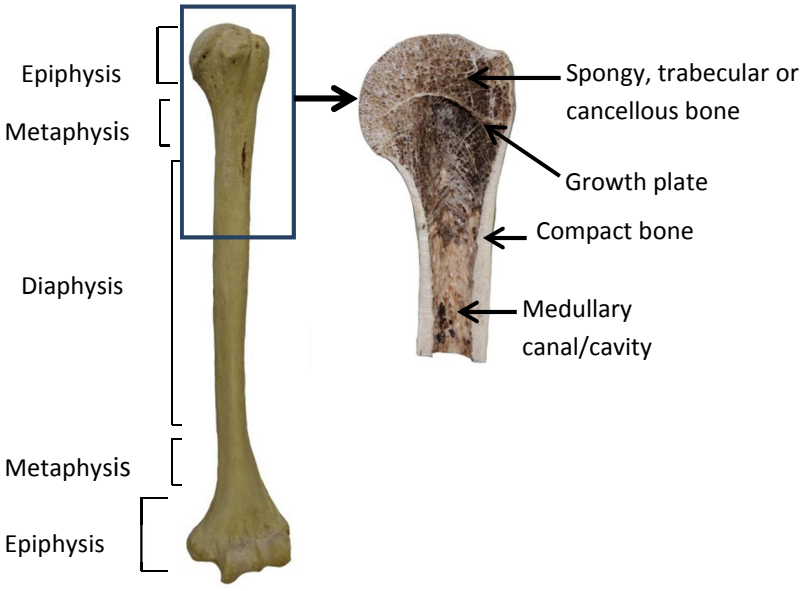


Figure 1.2: Long bone (Humerus) showing various parts

The former is a solid mass in appearance, whereas the latter has spicules or trabeculae with spaces containing bone marrow (Kierszenbaum and Tres, 2012; White et al., 2012). In long bones such as the humerus, a shaft or diaphysis consists of compact bone surrounding a marrow filled

space known as the medullary canal (Fig. 1.2). At either end of the shaft are the epiphyses, consisting of spongy bone covered by a thin layer of compact bone (White et al., 2012). In children, a cartilaginous epiphyseal plate known as the growth plate (for increasing bone length) separates the diaphysis from the epiphyses. The transitional zone is the metaphysis.

Articular cartilage made of hyaline cartilage covers the articular surfaces. A specialized connective tissue with osteogenic properties called periosteum surrounds the diaphysis whereas the medullary cavity is lined by endosteum. The periosteum consists of bone forming cells known as osteoblasts. In adults, the periosteum has an inner layer of osteogenic cells that have potential to differentiate in bone repair following an injury. The endosteum, composed of squamous cells and connective tissue fibers, covers all the haversian canals (Kierszenbaum and Tres, 2012).

Cellular components and microscopic structure

Osteoblasts initiate, control and deposit the mineralized matrix of bone called osteoid. Collagen type I, osteopontin and osteocalcin are the major products of osteoblasts. These cells derive from osteoprogenitor cells, and after they release osteoid and they become embedded in it they are known as osteocytes. These may live for several years before they are replaced. They regulate calcium and phosphorus homeostasis under the influence of parathyroid hormone (PTH) and calcitonin (Ortner, 2003). Osteoclasts derive from monocytes that reach the bone through the blood circulatory system and they have a role in bone remodeling. They are responsible for the breakdown and resorption of bone (Kierszenbaum and Tres, 2012).

Two types of bone can be distinguished microscopically namely: lamellar and woven bone. The former is found in mature bone and consists of regular collagen fibers and the latter characterizes developing bone with irregular collagen fibers (Gartner and Hiatt, 2014). Lamellar bone is mechanically stronger than woven bone which is formed rapidly and is produced during bone fracture healing. Lamellar bone consists of concentric layers called lamellae composed of a mineralized substance and osteocytes found in the lacuna (Fig 1.3) (Ross and Pawlina, 2011). These are cavities with radiating canaliculi that penetrate the lamellae of adjacent lacunae. Four distinct patterns may be observed in lamellar bone as follows:

i. **Haversian systems** – these are also called osteons and are formed by concentrically arranged lamellae around a blood vessel.
ii. **Interstitial lamellae** are found between haversian systems with a thin layer known as the cement line separating them.
iii. **The outer circumferential lamellae** that may be seen at the external surface of compact bone
iv. **The inner and outer circumferential lamellae** is found on the inner surface of the endosteum

The vasculature in compact bone consists of longitudinal capillaries and blood vessels in Volkmann's canals. Longitudinal capillaries are found in the center of a Haversian system within a space called the Haversian canal (Fig 1.3). These are connected by the transverse Volkmann's canals that contain blood vessels from the marrow and periosteum (Kierszenbaum and Tres, 2012; Ross et al., 1989).

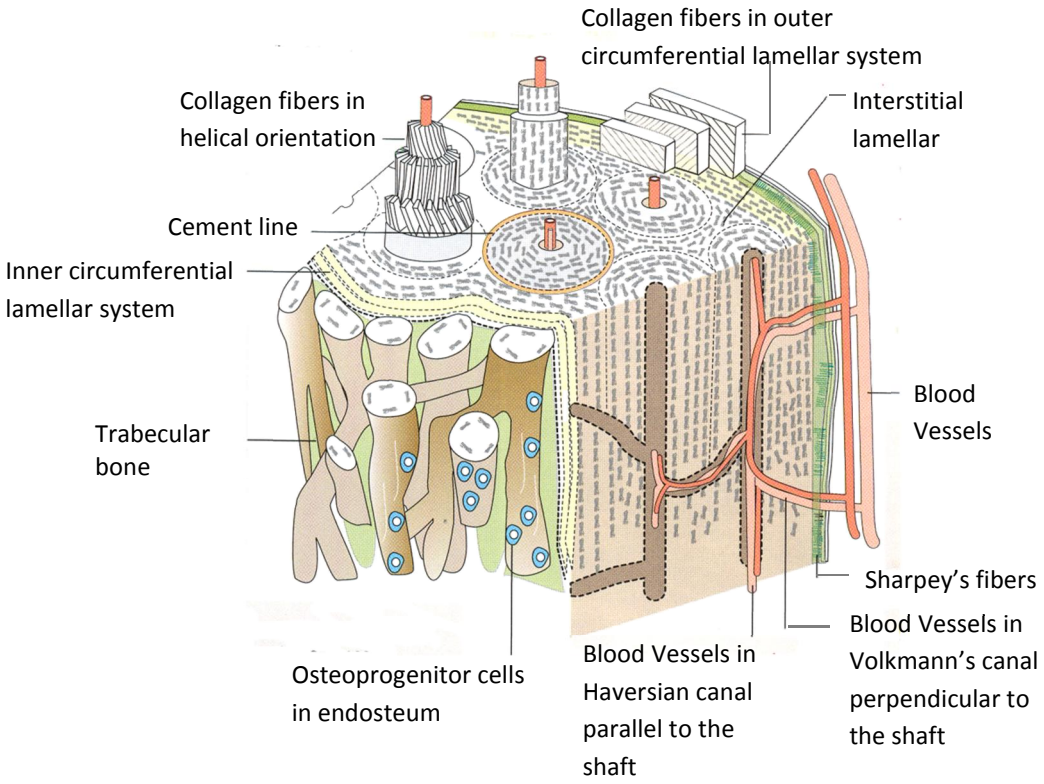


Figure 1.3: The Haversian system. The arrangement of the collagen fibers, lamellar and blood vessels are illustrated. An adaptation from Kierszenbaum and Tres (2012).

Bone remodeling

Imbalances and disturbances in bone remodeling could play a role in the etiology of the STA (Mays, 2008). Bone remodeling occurs through bone resorption and formation and is required to sustain skeletal size, shape, and biomechanical reliability (Raggatt and Partridge, 2010). Remodeling occurs continuously in life and it takes place at sites of micro-damage. The process involves replacement of old with newly formed bone in a resorption-production sequence by osteoclasts and osteoblasts (Crockett et al., 2011). Bone remodeling maintains calcium homeostasis and optimum bone strength by repairing microscopic damage known as microcracking. The hormonal control of bone remodeling is through

calcitonin, PTH, vitamin D_3 and oestrogen. With bone serving as a store for minerals, calcitonin, PTH, vitamin D_3 are important for the control of calcium levels (Amft et al., 2013). Calcitonin inhibits osteoclastic resorption (Binkley et al., 2014) whereas PTH stimulates osteoclastic bone resorption and also stimulates vitamin D_3 production (Ho et al., 2014), which in turn facilitates calcium absorption from the gastrointestinal tract and kidneys (Crockett et al., 2011). The bone remodeling cycle is divisible into five stages: activation, resorption, reversal, formation and quiescence (Fig. 1.4).

(i) Activation

The activation stage is stimulated by microdamage to localized areas of the bone (Lee et al., 2002). In STA bones, the articulation of the humerus and ulnar may potentially initiate the activation stage. During this stage, unmineralized osteoid is exposed following withdrawal and swelling of bone lining cells in response to parathyroid hormone, calcitriol, cytokines or physical damage. Osteoclast precursor cells rush to the site and fuse to form differentiated multinucleated osteoclasts (Amft et al., 2013).

(i) Resorption

Mature osteoclasts secrete hydrochloric acid and proteolytic enzymes to undertake bone resorption by removal of bone mineral leaving a pit (Amft et al., 2013). It is thought that resorption may be excessive in STA bones. The resorption pit is known as the cutting cone, and as it advances in the longitudinal axis new osteoclasts are activated while those behind the cutting cone undergo apoptosis (Raggatt and Partridge, 2010).

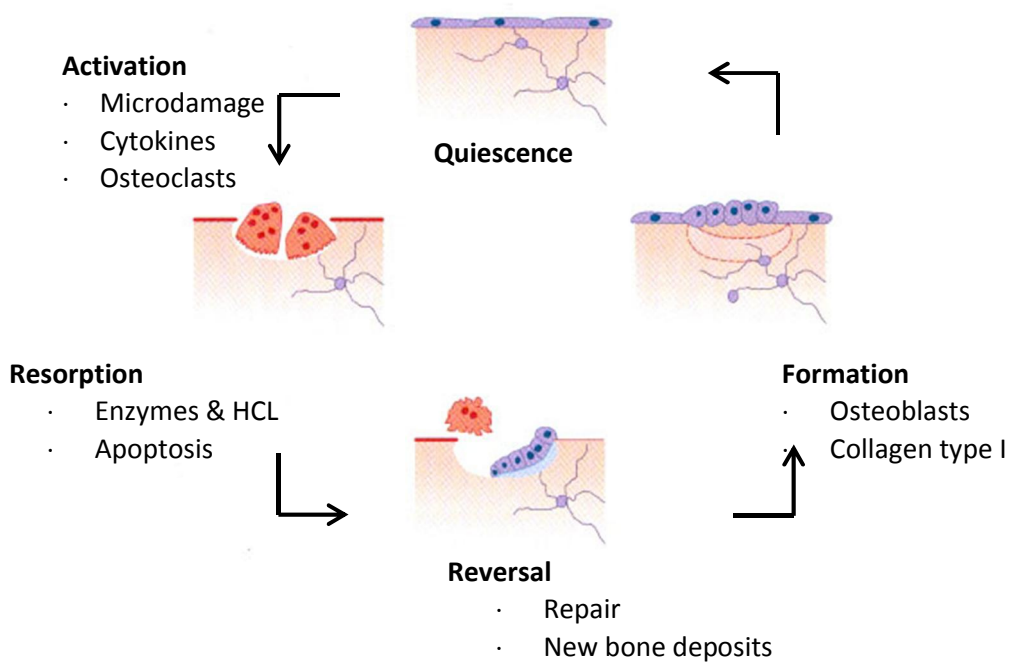


Figure 1.4: Bone remodeling phases (an adaptation from Amft et al., 2013)

(ii) Reversal

The reversal phase is the beginning of the repair process as osteoclasts withdraw and undergo apoptosis to be replaced by macrophage like cells that deposits a binding layer to cement newly deposited bone to the surface (Amft et al., 2013). The repair process may be too slow or inadequate in STA bones.

(iii) Formation

Once osteoblast progenitors have reverted to the resorption lacunae, they differentiate and secrete molecules that will form new bone. These molecules include Collagen type I, which is the principal organic component of bone. Non-collagenous proteins, such as proteoglycans, glycosylated proteins and lipids, make up the remainder of the organic material. Subsequently, hydroxyapatite is incorporated (the process of mineralization) into this new osteoid (Crockett et al., 2011; Raggatt and

Partridge, 2010). Since the STA is expressed as a deficiency in the body septum of the humerus, it is possible that bone formation in the region may be inadequate.

(iv) Quiescence

The quiescence or termination phase is the final stage of remodeling that is characterized by cessation of the remodeling cycle. At this stage, an approximately equal amount of resorbed bone has been replenished. Once mineralization has occurred, mature osteoblasts may either undergo apoptosis, or get incorporated in the mineralized matrix before differentiation into osteocytes. The microenvironment is maintained while awaiting the subsequent remodeling cycle (Amft et al., 2013; Raggatt and Partridge, 2010).

1.4 THE ELBOW JOINT – Skeletal components

The elbow joint is multifaceted and includes the humerus, radius, and ulna that articulate to form four joints: (i) the humer-oulnar joint, (ii) the humeroradial joint, (iii) the proximal radioulnar joint, (iv) and the distal radioulnar joint (Fig 1.5). The humeroulnar joint allows flexion and extension in the sagittal plane around a coronal axis. It also allows small amounts of internal and external rotation in the extreme end ranges of flexion and extension (Wilk and Andrews, 2001).

The distal end of the humerus contains features known as the capitulum and trochlea. The trochlea interlocks with the ulna of the forearm to form half of the elbow joint. The capitulum forms a loose connection with the concave head of the radius. The shape of the joint between the capitulum

and radius allows the forearm and hand to rotate and bend at the elbow while the ulna forms a tight hinge with the trochlea. Two fossae are found on either side of the corresponding articular surfaces of the humerus. Anteriorly, is the coronoid fossa which articulates with the coronoid process of the ulna during flexion. Posteriorly, the olecranon fossa receives the olecranon process of the ulna, which serves to limit extension (Moore et al., 2014; Wilk and Andrews, 2001).

The humeroradial joint is a diarthrodial, uniaxial joint that allows elbow flexion and extension along with the humeroulnar joint. The humeroradial joint swivels around the longitudinal axis to allow rotational movements in synchrony with the proximal radioulnar joint.

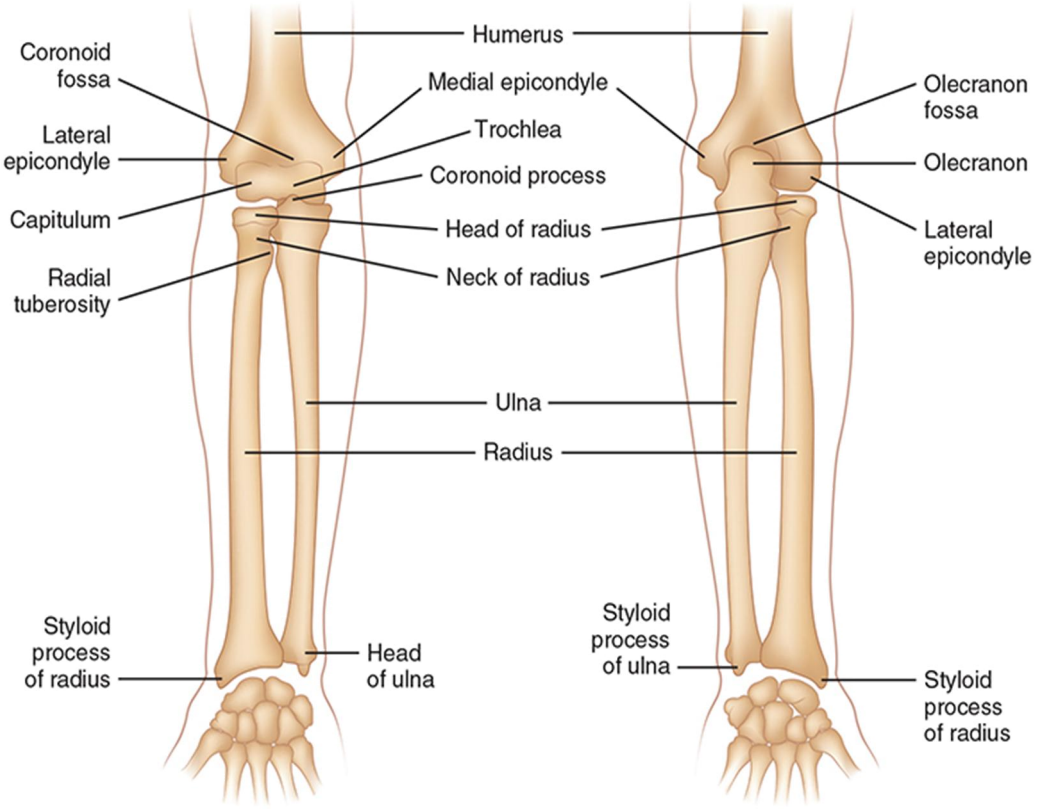


Figure 1.5: Skeletal components of the elbow joint and their articulation (Wilk and Andrews, 2001).

The articular surfaces of the humeroradial joint include the concave radial head and the spherical convex capitellum at the distal end of the humerus. The capitulotro-chlear groove separates the capitellum and trochlea of the humerus. This groove stabilizes the radial head in elbow flexion and extension. Immediately proximal to the capitellum on the anterior aspect of the humerus is the radial fossa that articulates with the radial head when the elbow is in a maximally flexed position (Moore et al., 2014).

The proximal and distal radioulnar joints permit one degree of freedom in the transverse plane around the longitudinal axis, for supination and pronation. In both movements the head of the radius rotates inside the annular ligament and the radial notch of the ulna. Little motion actually occurs in the ulna. In pronation, the radius and ulna lie parallel to each other whereas the radius crosses over the ulna in supination. The interosseous membrane connects the shafts of both bones (Wilk and Andrews, 2001).

1.5 BIOMECHANICS OF BONE

The biomechanics of bone is usually understood on the basis of ‘‘Wolff’s law’’. The premise is that mechanical strain applied to bone influences bone structure. This concept is termed ‘bone functional adaptation’ in recent literature, as reviewed by Ruff et al. (2006). Their review emphasises two general principles: (i) organisms are able to adapt their structure to changing environmental conditions, and (ii) bone has the ability to respond to localized mechanical strain. High levels of strain result in increased bone deposition thereby reducing the strain. Conversely, low

strain levels result in bone resorption, which in turn reverts to more strain. The humerus is a non-weight bearing bone, and is subjected to relatively low strain levels. A possibility exist that the low strain levels result in bone resorption and subsequent STA formation.

Other findings appear to contradict Wolff's Law. They suggest that environmental strains are often unsuccessful in effecting changes in bone mass or structure (Rubin et al., 2002). These researchers propose that bone may endure mechanical strain without resorting to remodelling. This means that if the strain threshold is not reached, there may be no remodelling response as the osteocytes may adapt to such strain.The osteocyte is thought to be capable of adapting to strain by modifying cytoskeletal structure and the way it attaches to the matrix (Rubin et al., 2002).

1.6 AIM OF THE STUDY

Researchers have had interest in the STA for more than a century, yet the etiology and features of bones that have this aperture are not well or fully described in any particular study. Proposals that individuals with STA differ in their gracility, the length of their ulnar olecranon processes, or their humeral cortical bone thickness have not been addressed together in one study using the same population group to reduce biases. Furthermore, while it is known that in life tissue covers the STA, the composition of this tissue remains subject to investigation (Nayak et al., 2009). The features of this tissue are expected to exhibit an ability to withstand the pressure of the ulnar process in elbow flexion The aim of the present study was to

investigate the characteristics of humeri that have a septal aperture and their corresponding ulnae.

1.6.1 Objectives

The objectives of the study were to:

A. Report the prevalence of the septal aperture in a South African sample.
B. Test the hypothesis that the lengths of the olecranon and coronoid processes vary relative to STA status, and if they could impinge on the septum, possibly resulting in formation of the aperture.
C. Test the hypothesis that less robust bones are more prone to aperture formation.
D. Investigate the dimensions of the medullary canal and cortical bone thickness with respect to the STA to test the hypothesis that these dimensions are smaller in STA humeri.
E. Test the hypothesis that limbs with the septal aperture may be able to hyperextend.
F. Characterize the microstructure of the septal membrane using histochemical techniques to test the hypothesis that this tissue has sufficient structural composition and strength to withstand the pressures of elbow motion

CHAPTER 2

The Supratrochlear Aperture of the Humerus among South Africans

Published in Clinical Anatomy, 2013 as:

***Robert Ndou**, Petunia Smith, Ryan Gemell and Ofentse Mohatla. The Supratrochlear Foramen of the Humerus in a South African Dry Bone Sample. Clinical Anatomy 2013; 26(7):870-874.*

Table of Contents

2.0 ABSTRACT 22
2.1 INTRODUCTION 23
2.2 MATERIALS AND METHODS 26
2.2.1 Sample of dry humeri 26
2.2.2 Procedure 27
2.2.3 Statistics 28
2.3 RESULTS 29
2.3.1 Overall prevalence of STA 29
2.3.2 Shapes of the STA 31
2.4 DISCUSSION 34
2.5 CONCLUSIONS 36

2.0 ABSTRACT

The supratrochlear aperture (STA) of the humerus is the aperture that forms when the septum separating the coronoid and olecranon fossa is perforated. Ndou et al. (2013) were first to document the prevalence of the STA among various South African ethnic groups. The presence and shapes of the STA were established by visual observation from a sample of 538 skeletonized individuals with paired humeri (1076) and of equal numbers between the sexes. Measurements of the transverse (TD) and vertical (VD) diameter of the STA were obtained using extended jaw calipers. An osteometric board was used to measure the epicondylar breadth (EB). Sliding calipers were used to measure the distance of the medial epicondyle to medial aspect of the STA (MB) and that of the lateral epicondyle to lateral border of the STA (LB) in a transverse plane.

The prevalence of STA in the South African population was 32.5% and predominantly on the left with the highest frequency among the Sotho population (41%) and the lowest frequency in Whites (16%). Females (19.5%) had a higher frequency of the STA compared to males (13%). The STA occurred in oval (136), round (77), triangular (9) and irregular (34) shapes. The average EB in the present study was 56.1 mm whereas the average MB and LB were 25.4 mm and 26.3 mm, respectively. The average TD was 6.3 mm and average VD was 4.3 mm. These findings may be of clinical significance to surgeons and osteologists and may have anthropological or forensic importance.

2.1 INTRODUCTION

The supratrochlear aperture (STA) of the humerus is the aperture that forms when the bony septum separating the coronoid and olecranon fossa is perforated (Hirsch, 1928; Lamb, 1980). Although it may have an irregular shape, the STA predominantly occurs in three shapes: oval, triangular and round, with oval being the most common shape (Nayak et al., 2009; Singhal and Rao, 2007). This aperture may occur either unilaterally or bilaterally. In unilateral cases, some researchers have found the STA predominantly on the left humerus (Ming-Tzu, 1935; Singhal and Rao, 2007; Trotter, 1934), whereas others found it predominantly on the right (Nayak et al., 2009).The formation of the STA has been debated among researchers for several decades. The two proposed etiologies for theories regarding the formation of the STA have been proposed as the mechanical theory and the genetic theory (Glanville, 1967). The mechanical explanation proposes that the STA is formed as a consequence of the perforation of the septum by the olecranon and coronoid processes of the ulna during extension and flexion (Mays, 2008; Singhal and Rao, 2007). In contrast, the genetic theory proposes that the STA is an inherited characteristic that is expressed in adolescent and adult life.

Verification of the presence of STA is helpful for successful surgical correction of diaphyseal fractures of the humerus (Akpinar et al., 2003). For example, corrective surgery of a fracture may involve intramedullary fixation, involving the insertion of a nail/rod into the vertical length of the humerus to stabilize the fracture site (Akpinar et al., 2003).

In humeri with an STA, the medullary canal tends to be shorter and have a narrower diameter than those without an STA. This shorter medullary canal and narrowing may pose difficulties in intramedullary fixation (Akpinar et al., 2003; Singhal and Rao, 2007).

Prevalence of the STA varies among different population groups worldwide. The prevalence ranges from 0.3% to 58% worldwide (Christos et al., 2011; Nayak et al., 2009). In the Chinese population, the overall frequency is 17.5% with significant differences, 6.9 % and 27.3% between males and females, respectively (Ming-Tzu, 1935). Similarly, the prevalence in Japanese populations has been found to be 18.1% (Singhal and Rao, 2007) with a higher frequency of 20.6% observed in females and a lower frequency of 13.5% observed in males in the Kyusu district (Akabori, 1934). Among Indians, a prevalence of 32% was found in Central India whereas a lower prevalence was found among the South (28%), North (27.5%), and East Indian (27.4%) population groups of mixed sexes as reviewed by Singhal and Rao, (2007).

Although the prevalence of the STA is known in various populations around the world, no such studies of South African populations are available in the literature in the literature. Therefore, the aim of this study was to determine the prevalence of the STA in South African populations. Radiologists should be aware of the occurrence of this aperture since it may be misinterpreted as an osteolytic lesion (De Wilde et al., 2004). Awareness of the various shapes and dimensions such as the transverse and vertical diameters in which this aperture occurs may help avoid misinterpretation of radiographs. Therefore, the shapes in which the STA

occurs will be noted together with the dimensions of the aperture. Measurements of the epicondylar breadth will be noted to shed some light on the gracility of these bones as the STA is known to be more prevalent in gracile bones than in robust ones (Benfer and McKern, 1966; Mays, 2008). The results of this study may be useful to orthopedic surgeons, anthropologists and radiologists working in South Africa.

2.2 MATERIALS AND METHODS

2.2.1 Sample of dry humeri

A sample of 538 skeletonized adult individuals with paired humeri (1076) and of equal numbers between the sexes was obtained from the Raymond A Dart collection of the School of Anatomical Sciences at the University of the Witwatersrand (Dayal et al., 2009). All humeri studied were free of pathology and antemortem or postmortem trauma. Features of bone healing, such as callus formation were used to identify antemortem trauma. Postmortem trauma was identified by the observation of sharp surfaces or edges of the aperture and visible trabeculae. The humeri studied belonged to individuals of six South African ethnic groups namely; White, Mixed group (Mixed), Xhosa, Sotho, Zulu, Tswana. White referred to individuals of European descent whereas the Mixed ethnicity group referred to people who have descended from Whites and indigenous Africans. The Xhosa, Sotho, Zulu, Tswana are indigenous South African ethnic groups.

For the White, Zulu, Sotho and Xhosa population groups, 100 individuals were obtained (Table 2.1) for each population (50 males and 50 females). The sample sizes for the Mixed and Tswana populations were restricted to samples of 64 and 74 individuals, respectively, since they were the only individuals in the Raymond A Dart collection that met the selection criteria (Table 2.1).

Table 2.1: Total number of skeletonized individuals studied in each ethnic group

Ethnicity	Males	Females	Total	Humeri
White	50	50	100	200
Mixed	37	37	74	148
Sotho	50	50	100	200
Tswana	32	32	64	128
Xhosa	50	50	100	200
Zulu	50	50	100	200
Total	269	269	538	1076

2.2.2 Procedure

Two observers established the presence of the STA by visual observation in each ethnic group, exercising care to differentiate between a true STA and postmortem damage. When present, the STA was categorized into one of the following shapes: round, oval and triangular. In cases where the shape of the STA could not be classified as any of the three abovementioned shapes, then such shapes were classified as irregular. All the measurements taken and the instruments used are given in table 2.2. Measurements of the maximum width and height, herein referred to as the transverse (TD) and vertical (VD) diameter of the STA respectively were obtained using extended jaw calipers (Fig 2.1). An osteometric board was used to measure the epicondylar breadth (EB). Sliding calipers were used to measure the distance of the medial epicondyle to the medial aspect of the STA (MB) and that of the lateral epicondyle to lateral border of the STA (LB). The two observers took each measurement three times and the mean per parameter was used.

Table 2.2: Measurements taken and instruments used

Measurement	Abbreviation	Instrument
Maximum distance from medial epicondyle to lateral epicondyle	EB	Mini Osteometric Board
Minimum distance from medial epicondyle to medial border of the STA	MB	Sliding Calipers
Minimum distance from lateral epicondyle to lateral border of the STA	LB	Sliding Calipers
Maximum width of STA (Transverse Distance)	TD	Extended Jaw Calipers
Maximum height of STA (Vertical Distance)	VD	Extended Jaw Calipers

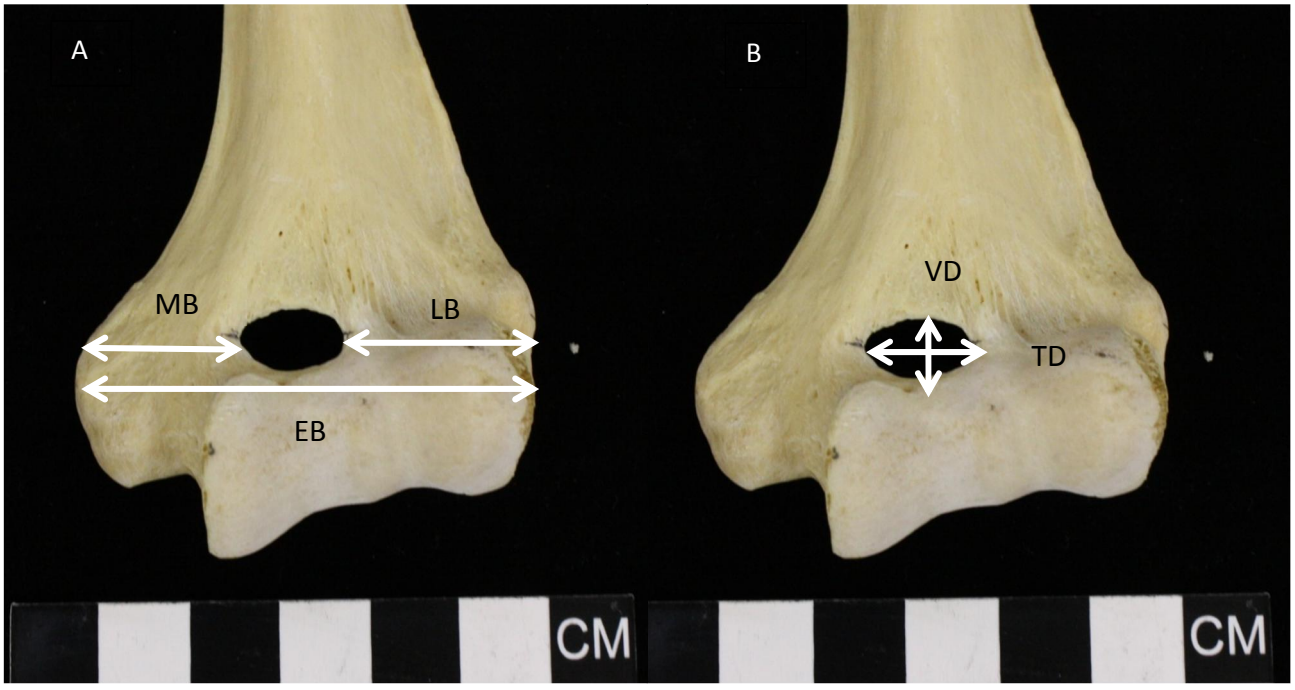


Figure 2.1 Measurements taken from the STA. A: The epicondylar breadth (EB) and minimum distance from the medial epicondyle to medial border and from lateral epicondyle to lateral border of the STA (MB and LB, respectively). B: The vertical (VD) and transverse distance (TD) of the STA.

2.2.3 Statistics

The data were managed in Microsoft Excel 2007 (Microsoft Corporation) and analyzed using STATISTICA^{R} software version 10, 2011 (StatSoft^{R}). As two observers took all the measurements, Lin's concordance correlation coefficient of repeatability was used to assess the inter-observer error. The following P_C values were obtained: EB (0.9968); MB (0.9149); LB (0.9837); TD (0.9997) and VD (0.9988). P_C values range from 0 to 1 and a value close to 1 indicates a high degree of repeatability. All the P_C values obtained were greater than 0.9 which indicates that the correlation between repeated measurements was high and thus inter-observer error was minimal. The Chi squared test was used to test for significant differences between categorical variables while the Tukey HSD post hoc analysis was applied for the continuous variables.

2.3 RESULTS

2.3.1 Overall prevalence of STA

The STA was observed either bilaterally or unilaterally in 32.5% of the 538 skeletonized individuals in this South African dry bone sample (Table 2.3). Of the overall prevalence, females (19.5%) had a significantly higher frequency of the STA than males who had 13% frequency (p=0.001). The STA occurred bilaterally in 15.1% of the sample, with twice as many females as males (p=0.04). In unilateral cases, the prevalence was higher on the left (13.9%) compared to the right (3.5%).

Whites (16%) exhibited the lowest prevalence of STA followed by the Mixed ethnic (31%) group (Table 2.4). Of the South African indigenous

groups, the Sotho (41%) had the highest prevalence followed by the Tswana (39%), Zulu (33%) and the Xhosa (33%) ethnic group (Table 2.4)

Table 2.3: The prevalence and laterality of STA in males and females
Counts and percentages of the occurrence of STA on the left or right (unilateral) as well as bilateral cases are given. The overall counts and percentages are also included.

Sex		Unilateral		Bilateral	Overall
		Left	Right		
Males	Counts (N)	35	8	27	70
	Percentage	**6.5**	**1.5**	**5.0**	**13.0**
Females	Counts (N)	40	11	54	105
	Percentage	**7.4**	**2.0**	**10.1**	**19.5**
Total	Counts (N)	75	19	81	175
	Percentage	**13.9**	**3.5**	**15.1**	**32.5**

Table 2.4: The prevalence of STA in each of the six ethnic groups studied

Ethnicity	Frequency (N)	%
White	16/100	16.00
Mixed	23/74	31.08
Sotho	41/100	41.00
Tswana	25/64	39.06
Xhosa	33/100	33.00
Zulu	37/100	37.00
Total	175/538	**32.50**

2.3.2 Shapes of the STA

The STA occurred in oval (n=136), round (n=77), triangular (n=9) and irregular (n=34) shapes (Table 2.5 and Figs. 2.2 A-D). The irregular shape presented most frequently in the Zulu group (n=13) and least in the Xhosa ethnic group (n=2). The oval shape occurred most frequently across all the ethnic groups in the study, with the highest count seen in the Sotho (n=30) and the lowest count in Whites (n=14). The Sotho also showed a high prevalence of the round shape (n=24). The triangular shape was only observed in the Mixed ethnicity group (n=1) and Sotho (n=8).

Table 2.5: Shapes of the STA in the six ethnic groups studied
The numbers are actual counts of humeri bearing the STA.

	Shape				
Population	**Irregular** (N)	**Oval** (N)	**Round** (N)	**Triangular** (N)	**Total**
White	4	14	6	0	**24**
Mixed	5	20	5	1	**31**
Sotho	6	30	24	8	**68**
Tswana	4	21	9	0	**34**
Zulu	13	22	16	0	**51**
Xhosa	2	29	17	0	**48**
Total N	**34**	**136**	**77**	**9**	**256**

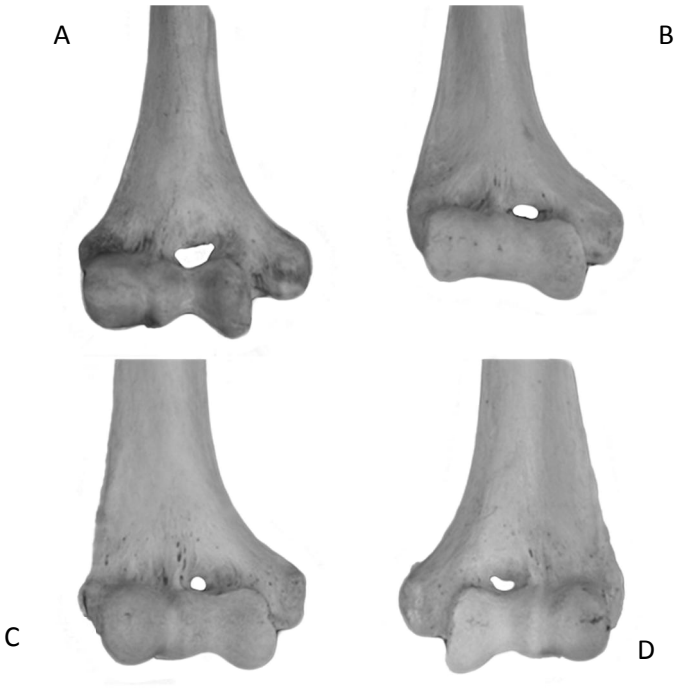


Figure 2.2: Various shapes of the STA. A-Triangular, B-Oval, C-Round and D-Irregular

The average values obtained on the various dimensions taken are given in Table 2.6. The average EB in the present study was 56.1 mm whereas the average MB and LB were 25.4 mm and 26.3 mm respectively. The average TD was 6.3 mm and average VD was 4.3 mm. The Mixed ethnicity group had a significantly smaller EB of 54.1 mm ($p=0.01$). Similarly, both the MB (23.8 mm) and LB (24.6 mm) were statistically significantly smaller compared to other groups ($p<0.001$ for both MB and LB). In contrast, this group (Mixed) had the largest TD (7.6 mm) although a statistically significant difference was not found ($p=0.07$). The EB (Table 2.7) was significantly larger in males (60.5 mm) than in females (53.4 mm) across all the ethnic groups studied ($p<0.001$). In contrast, there was no significant difference in TD and VD between males and females ($p=0.6$ for both TD and VD).

Table 2.6: The mean ($\bar{x}$) dimensions of the STA and the distal humerus in the six ethnic groups studied

The dimensions are as follows: Epicondylar breadth (EB), distance from medial epicondyle to medial border of the STA (MB), distance from lateral epicondyle to lateral border of the STA (LB), transverse distance (TD) and vertical distance (VD). All the measurements are in mm (millimeters) and the values are means and standard deviation (SD).

	EB		**MB**		**LB**		**TD**		**VD**	
Population	$\bar{x}$	SD	Mean	SD	$\bar{x}$	SD	$\bar{x}$	SD	$\bar{x}$	SD
All Groups	**56.1**	5.5	**25.4**	3.3	**26.3**	2.9	**6.3**	2.9	**4.1**	1.7
White	**57.7**	5.7	**27.1**	4.9	**28**	2.8	**5.8**	2.5	**4**	1.4
Mixed	**54.1**	5.6	**23.8**	2.7	**24.6**	2.4	**7.6**	2.7	**5.1**	1.8
Tswana	**56.5**	5.2	**25.9**	3.8	**26.5**	3.4	**6.1**	2.9	**4.3**	1.8
Zulu	**57.1**	5	**26.1**	2.2	**26.7**	2.6	**6.3**	2.9	**4.3**	1.7
Sotho	**55.7**	6.7	**25**	3.5	**26**	3.1	**6**	3	**3.4**	1.6
Xhosa	**56.1**	3.8	**25**	2.6	**26.1**	2.2	**6.3**	3	**4**	1.7

Table 2.7: Dimensions of the STA and the distal humerus in males and females

The dimensions are as follows: Epicondylar breadth (EB), distance from medial epicondyle to medial border of the STA (MB), distance from lateral epicondyle to lateral border of the STA (LB), transverse distance (TD) and vertical distance (VD). All the measurements are in mm (millimeters) and the values are means.

	Males	**Females**
EB	60.5	53.4
MB	27.6	24.0
LB	28.1	25.1
TD	6.2	6.3
VD	4.0	4.11

2.4 DISCUSSION

To our knowledge, the prevalence of the STA was determined in a relatively large sample (1076 humeri) of six South African ethnic groups for the first time, and the overall prevalence was found to be 32.5%. Additionally, the STA was studied among the Mixed ethnicity group for the first time. Use of a mini osteometric board to measure EB improved consistency as the exact same dimensions of each bone were measured, thereby reducing error.

In unilateral cases, the prevalence of STA was higher among females and on the left. While these findings are consistent with recent reports (Krishnamurthy et al., 2011; Mahajan, 2011), they differ from Nayak et al (2009) who found the STA predominantly on the right. It is not mentioned in the study (Nayak et al., 2009) whether the 220 left and 164 right humeri used belonged to the same individuals.

The prevalence of STA among indigenous South African groups was lower than that of other Africans. For example, a prevalence rate of 47% was found in Mali (Glanville, 1967). Inclusion of specimens of Whites, with 16% prevalence rate in the present study further lowered the overall prevalence rate obtained. It remains to be determined why the prevalence of STA among the native South African groups is lower than that of the West and East Africans.

Conversely, Whites in this South African sample had a marginally higher frequency of the STA compared to that recorded for Whites in other parts of the world, which is below 10% (Nayak et al., 2009). The Australians with a prevalence of 46.5% as previously reviewed (Krishnamurthy et al., 2011;

Mahajan, 2011) are an exception. It is not clear as to whether this higher prevalence found in the present study may be attributed to evolutionary adaptations to the environment that Whites may have developed when settling in South Africa. Notwithstanding the above, it is unknown whether such adaptations to the environment exist. This could be a basis for future studies to determine whether migration of Whites to South Africa resulted in genetic and phenotypic changes.

The oval shape was the most common shape observed in all populations studied. These findings are consistent with observations in previous studies (Nayak et al., 2009; Singhal and Rao, 2007). In the present study, the STA occurred in oval, round, irregular and triangular shapes. The later shape was found only among the Sotho and the Mixed ethnic groups. Factors that influence the shape of the STA remain to be determined. Future studies may be needed to establish the relationship of the shape of the olecranon process of the corresponding ulna and that of the STA.

The Mixed ethnic group had the largest TD (7.6 mm) and VD (5.1 mm), although this difference was not statistically significant when compared to the rest of the population groups studied. The lack of statistical significance in the TD and VD could be a result of the relatively smaller sample size for the Mixed ethnic group. To the contrary, this group also had the smallest EB, which may suggest that the bones belonging to this group were relatively less robust. This finding coincides with the phenomenon that the STA was more prevalent on the left and among females than males. These observations support previous suggestions that the STA is more prevalent in gracile bones such as those of females

(Benfer and McKern, 1966; Mays, 2008; Trotter, 1934). Similarly, the high prevalence of STA among females could be attributed to the small size of their bones compared to those of their male counterparts as the females had a narrower EB when compared to males.

2.5 CONCLUSIONS

The present study has, for the first time, determined the prevalence of the STA in six South African ethnic groups and was found to be 32.5%. This aperture occurred predominantly on the left and more in females (19.5%) than in males (13%). However, in the ethnic groups studied, the Sotho (41%) had the highest prevalence whereas Whites (16%) had the lowest. Additionally, the shapes in which the STA presents were identified and the most common was the oval (n=136) whereas the triangular (n=9) was the least common shape. In spite of the above findings, the etiology of the STA remains to be determined.

CHAPTER 3

Morphometric characteristics of the humerus and ulna in limbs bearing the supratrochlear aperture (STA)

Conference presentation:

The 2nd International Conference on Forensic Research & Technology 7 - 9 October 2013, Las Vegas, Nevada, USA

Contents

3.0 ABSTRACT 39
3.1 INTRODUCTION 40
3.2 MATERIALS AND METHODS 43
3.2.1 Sample 43
3.2.2 Measurement procedures 44
3.2.3 Statistics 47
3.3 RESULTS 48
3.3.1 Characteristics of the humerus 48
3.3.2 Characteristics of the ulna 58
3.3.3 Humeral and ulnar parameters contributing to population variation 67
3.3.4 Determinants of STA status 70
3.4 DISCUSSION 82
3.4.1 Robusticity 82
3.4.2 Aspects of the elbow joint 83
3.4.3 Population specific aspects of STA status 85
3.5 CONCLUSIONS 87
3.6 ACKNOWLEDGEMENTS 88

3.0 ABSTRACT

The supratrochlear aperture (STA) is a perforation of the septum found between the olecranon and coronoid fossae of the humerus. Its prevalence is population-specific and varies by sex. There is no consensus on the etiology of this feature despite decades of investigation. Two aspects of the mechanical theory, which states that the STA is formed when the ulnar olecranon and coronoid processes impinge upon the septum separating the olecranon and coronoid fossae, were investigated. First, osteometric measures of bone size were used to test the proposition that robust humeri are less prone to STA formation. We compared the dimensions of STA bearing humeri with those lacking STAs and investigated which skeletal features discriminate among South African populations. To specifically evaluate the mechanical theory that articulation with the olecranon and coronoid fossae may result in STA formation, dimensions of the olecranon and coronoid processes were compared.

Our results verified that more gracile individuals are prone to STA formation and that a significantly longer olecranon process is associated with the aperture. The olecranon process length and olecranon-coronoid distance were the main contributors to STA status using the discriminant function analysis. Variables that contributed the most towards discrimination among the South African populations were the olecranon fossa depth and right humeral head circumference. An inverse relationship between the olecranon process length and olecranon fossa depth is also associated with presence of the STA.

3.1 INTRODUCTION

The aperture that is formed when the olecranon fossa is perforated is known as the supratrochlear aperture (STA). The frequency of this feature differs in populations across the world, ranging from as low as 0.3% among Greeks (Christos et al., 2011) to 58% in Arkansas Indians (Hirsh, 1927). A recent study found an overall prevalence of 32.5% in South Africa (Ndou et al., 2013). Females have a higher STA prevalence and the left side is more likely to have the feature than the right. The size and shape of the STA differs among South African populations and is highly variable (Ndou et al., 2013).

Sahajpal and Pichora (2006), in their discussion of the STA, stated that it may be of clinical or surgical importance as fracture patterns of the distal humerus and their subsequent treatment may be influenced by the presence of an aperture. They further emphasized that radiologists might misinterpret it as an osteolytic lesion (see also De Wilde et al., 2004). The presence of the STA is also viewed as a risk factor for low energy fractures of the distal aspect of the humerus (Sahajpal and Pichora, 2006).

The etiology of the STA is currently not known, although researchers have suggested some plausible explanations. For example, Mays (2008) proposed that the interaction of the ulna and distal humerus could result in impingement of the septum by the ulnar olecranon process. The variation in prevalence observed in various populations has lead other scholars to suggest that there may be a genetic component to the etiology of the STA (Glanville, 1967). Disturbances in bone development and calcium metabolism have been cited as some of the possible factors with genetic

bases (Koyun et al., 2011). The former would affect ossification while the latler may result in weak bones. Bone resorption in early adulthood is thought to be another possible explanation for the development of the STA (Mays, 2008). This resorption would be triggered by pressure from articulation of the ulna and humerus during movement of the elbow. Some researchers have found no STAs in children (Mays, 2008), while Koyun et al. (2011) reported it only in one female aged 16 years out of a sample of 709. This implies that the aperture generally forms after the epiphyseal plates have fused. Having not found signs of bone deposition around the aperture in adults, Mays (2008) proposed that, once formed, the aperture persists as new bone formation would indicate an attempt at aperture obliteration.

Among South African populations, the Mixed ethnic group has the greatest transverse and vertical diameters of the aperture in comparison with their Black and White counterparts. Interestingly, this group also has the narrowest epicondylar breadth (Ndou et al., 2013). We also found that the STA was more prevalent on the left and among females. Considered together, these results support previous arguments that the STA is more prevalent in smaller bones such as those of females (Benfer and McKern, 1966; Mays, 2008).

Previous studies on the STA had methodological and material constraints. For example, Benfer and McKern (1966) investigated the relationship between bone size and presence of the STA in American and Mexican populations. However, they employed relatively small sample sizes with

the left side missing in most instances. Skeletal determinants were used for sex assignment. Some of the measurements were minimum and maximum diameters of the humerus without specifying as to whether they were taken anteroposteriorly or mediolaterally, impacting on reproducibility. Another study by Glanville (1967) included measurements of the olecranon and coronoid processes of ulnae from the Netherlands and Tellem, Mali. Glanville (1967) was not able to associate humeri and ulnae for part of the medieval Tellem sample. The present study therefore takes these limitations into account by only including material of known population, sex, and side from paired humeri and ulnae.

To test the hypothesis that less robust bones are more prone to aperture formation, we compared the dimensions of STA humeri with those lacking STAs in South African populations. Features of the humerus and ulna that distinguish STA status were investigated for each population. To specifically evaluate the mechanical theory that articulation of the olecranon fossa with the ulnar olecranon process may result in bone resorption in the septum, dimensions of the olecranon process were compared to the depth of the olecranon fossa in bones that do and do not have the STA.

3.2 MATERIALS AND METHODS

3.2.1 Sample

A total of 1175 paired dry humeri and ulnae from 596 skeletonized individuals were analyzed. Limbs of both sides were included for 579 individuals, whereas 17 individuals had only a single side present. A case-control design was used with approximately equal numbers of individuals with and without the STA included (Table 3.1). These bones are from three South African groups: 126 Whites (individuals of European descent), 232 Mixed ethnicity (descendants of Whites, Blacks and Khoisan people (De Wit et al., 2010), and 238 Blacks (indigenous South Africans) (Table 3.1). Individuals are from the Raymond A Dart Collection of Human Skeletons housed at the University of the Witwatersrand School of Anatomical Sciences (Dayal et al., 2009), the University of Cape Town, the University of Stellenbosch and the University of Pretoria (L'Abbe et al., 2005). Bones with evidence of trauma were excluded. Features of bone healing, such as a callus, were used to identify antemortem trauma. Postmortem trauma was determined by the presence of sharp surfaces or edges and visible trabecular bone.

Table 3.1: Sample

		Individuals	Sides included		Total limbs*
			Both	Single	
STA status					
STA	Yes	293	285	8	578
	No	303	294	9	597
	Total	596	579	17	1175
Population affiliation					
Population	White	126	123	3	246
	Mixed	232	227	5	454
	Black	238	229	9	458
	Total	596	579	17	1175

*Total limbs were obtained by multiplying the both sides column by 2 and adding the single side column.

3.2.2 Measurement procedures

Humerus

The epicondylar breadth was measured using a mini osteometric board, whereas the humeral length was measured using a standard laboratory osteometric board. The circumference of the head and the shaft were measured using a cloth measuring tape. The circumference of the shaft was measured at three positions – the 25th (proximal), 50th (midshaft) and 75th (distal) percentile marks of the humeral length (Fig. 3.1). These points where determined by dividing the humeral length into quartiles.

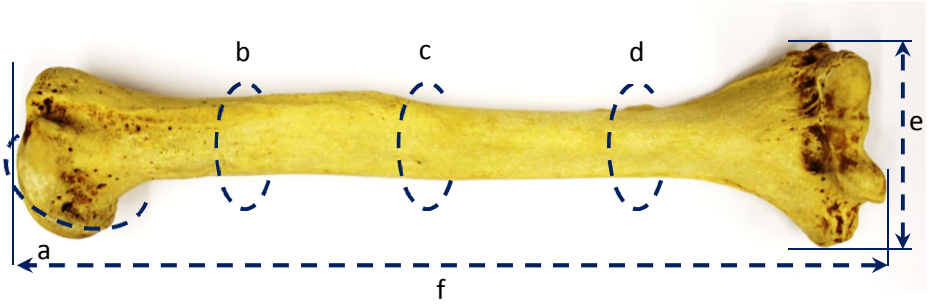


Figure 3.1: Measurements taken from the humerus
(a): Head circumference; (**b), (c)** and (**d)** respectively: Shaft circumference at the 25th, 50th and 75th percentile marks of the humerus length; (**e**): Epicondylar breadth, **(f)**; Humerus length.

Depth of the olecranon fossa

The depth of the fossa was measured using a palatometer. A pencil line joining the outermost aspect of the medial and lateral epicondyles was used to mark the points where the arms of the palatometer should be positioned when taking the depth measurement (Fig. 3.2). The medial aspect of the palatometer was in line with the top edge or brim of the fossa at the position of the pencil line. The bone was horizontal and the palatometer was vertical or perpendicular to longitudinal axis of the bone when the depth of the fossa was measured.

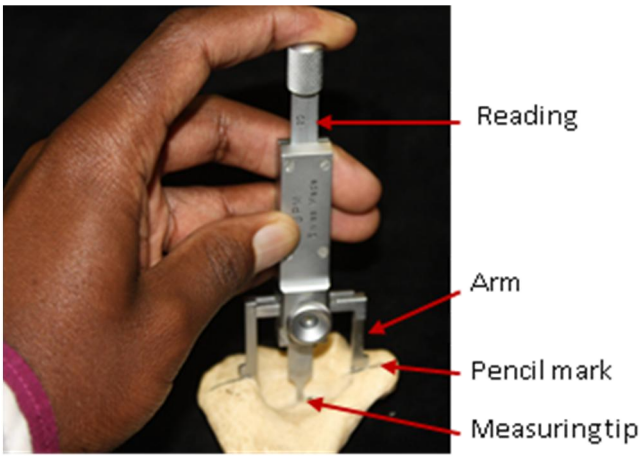


Figure 3.2: Measuring the depth of the olecranon fossa using a palatometer
The arms of the palatometer are on the pencil line that runs across the maximum epicondylar breadth. The medial border of the arms is positioned to be continuous with the edge of the fossa along the line and the measuring tip is in the deepest part of the fossa. The depth caliper is positioned perpendicular to the bone. Image courtesy of R Ndou and B Billings.

Projections of the coronoid and olecranon processes

An adaptation of a method for measuring the coronoid and olecranon length (Glanville, 1967) was applied. To determine the projections of the coronoid and olecranon processes, measurements were taken at the humero-ulnar articulation (Fig. 3.3). Lengths of the ulnar coronoid and olecranon processes were measured using sliding calipers. With the guide of a goniometer, lines A and B (Fig. 3.3) were drawn such that they were tangents to the curvature of the trochlear notch, ascertaining that a 45^{o} angle resulted where the two lines (A and B) intercept. The length of lines O and C represent the lengths of the olecranon and coronoid process as measured using sliding calipers. The depth (D) of the trochlear notch was measured using a palatometer. For consistency, the arms of the palatometer were in contact with the highest points of the olecranon and coronoid processes. The shortest distances from the highest points of the olecranon and coronoid processes were used to estimate the olecranon-coronoid distance (OC) (Fig. 3.3). The length of the ulna was taken using an osteometric board.

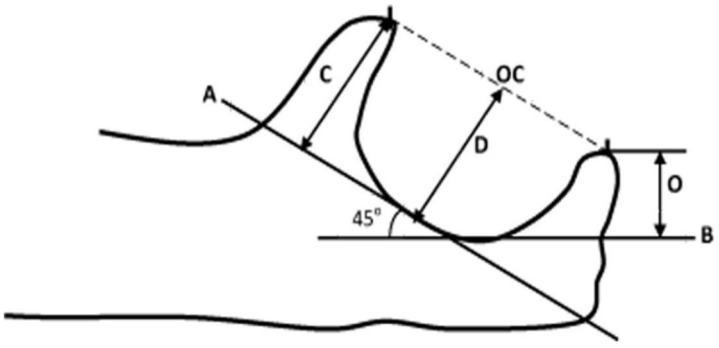


Figure 3.3: Measurements taken from the proximal aspect of the ulna
(O): olecranon process length, **(C):** coronoid process length, **(D)**: trochlear notch depth **(OC)**: olecranon-coronoid distance. Adapted from Glanville (1967).

3.2.3 Statistics

The data were managed in Microsoft Excel 2007 (Microsoft Corporation) and analyzed using STATISTICA^{R} (StatSoft^{R}) software version 12, 2014. The Kruskal-Wallis test was used as the data were not normally distributed. Discriminant function analysis was conducted with SPSS® version 22, IBM® to identify variables that distinguish among the populations and to predict STA status for each population. For the basic descriptive statistics, the left and right humeri were combined but were separated for the multivariate analysis. The significance level was considered to be $p<0.05$.

3.3 RESULTS

3.3.1 Characteristics of the humerus

Humeral head circumference (HC)

Differences in the HC among the populations were observed, with Whites having the largest HC followed by Blacks and individuals from the Mixed group ($p<0.001$ among all groups) (Table 3.2). A similar pattern was found when the STA was present and when it was absent (Fig. 3.4A), and in both sexes of each population (Fig. 3.4B). White males had a greater HC compared to their Black and Mixed group counterparts. Similarly, White females had a greater HC than Black and Mixed group females (Table 3.2; Fig. 3.4B). Although the HC was smaller when the STA was present for males and females of each population, statistically significant differences were only detected in Blacks. In this group, the mean HC was 118 mm in females without the STA compared to 116.1 mm in those with the feature ($p=0.05$) (Fig. 3.4B). Similarly, Black males had significantly greater HCs when the STA was absent than when it was present ($p=0.005$) (Fig. 3.4B).

Table 3.2: Humerus head circumference.
Means ($\overline{X}$) and standard deviations (SD) in millimeters for each population stratified by sex.

		White			Mixed			Black		
Sex	STA	N	$\overline{X}$	SD	N	$\overline{X}$	SD	N	$\overline{X}$	SD
Male	Yes	38	138.89	8.86	87	126.70	11.20	89	129.26	7.12
	No	102	140.35	7.94	160	128.61	8.31	149	131.87	6.53
	Total	140	139.96	8.19	247	127.94	9.45	238	130.9	6.86
Female	Yes	40	123.07	6.05	91	112.28	8.62	101	116.11	6.03
	No	69	126.00	7.26	121	112.78	7.96	128	117.97	6.65
	Total	109	124.92	6.96	212	112.57	8.23	229	117.15	6.44
All Groups		249	133.38	10.70	459	120.84	11.75	467	124.16	9.57

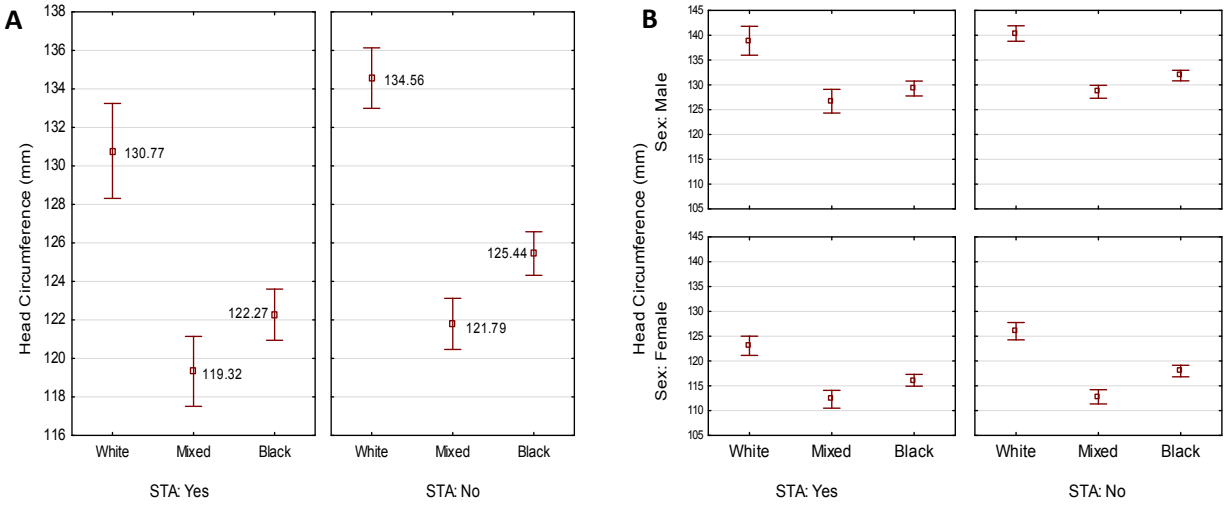


Figure 3.4: Humerus head circumference
Humeri by population with and without the STA **(A)** and further stratified by sex **(B)**.

Humerus epicondylar breadth (EB)

Population specific variation in the mean EB was documented, with Whites having significantly greater EBs than Blacks and the Mixed group ($p<0.001$ among all groups) (Table 3.3). A similar pattern was found when the STA was present and when it was absent (Fig. 3.5A). The EB was larger when the STA was absent for each population ($p=0.007$ for Whites; $p=.012$ for the Mixed group; $p<0.001$ for Blacks) (Fig. 3.5A). When populations were stratified by sex, both males and females had a greater EB when the STA was absent (Figs. 3.5A and 3.5B). However, significant differences in EB according to STA status were only found for Black and White males ($p<0.001$ and 0.05 for Blacks and Whites respectively).

Humeral length (HL)

The mean humeral length was greatest in Whites followed by Blacks and individuals of Mixed ethnicity ($p<0.001$ among all groups) (Table 3.4). This pattern characterized both STA and non STA humeri (Fig. 3.6A). However, in STA cases, there was no significant difference in humeral length between the Mixed group and Blacks. Both White males and females had a greater humeral length compared to their Black and Mixed group counterparts ($p<0.001$ among all groups). The length of the humerus was greater when the STA was absent in males and females of all groups, although a significant difference in humeral length was only found between White females with and without the STA ($p=0.017$) (Fig. 3.6B).

Table 3.3: Humerus epicondylar breadth
Means ($\bar{X}$) and standard deviations (SD) in millimetres for each population stratified by sex.

		White			Mixed			Black		
Sex	STA	N	$\bar{X}$	SD	N	$\bar{X}$	SD	N	$\bar{X}$	SD
Male	Yes	38	62.59	4.56	87	59.93	5.19	89	61.55	3.44
	No	102	64.39	3.56	160	61.09	4.42	149	63.20	3.37
	Total	140	63.90	3.92	247	60.68	4.73	238	62.58	3.48
Female	Yes	40	57.06	3.05	91	53.43	3.81	101	55.29	3.16
	No	69	57.69	3.48	121	54.06	3.32	128	55.68	4.58
	Total	109	57.46	3.33	212	53.79	3.54	229	55.50	4.01
All Groups		249	61.08	4.87	459	57.50	5.44	467	59.11	5.16

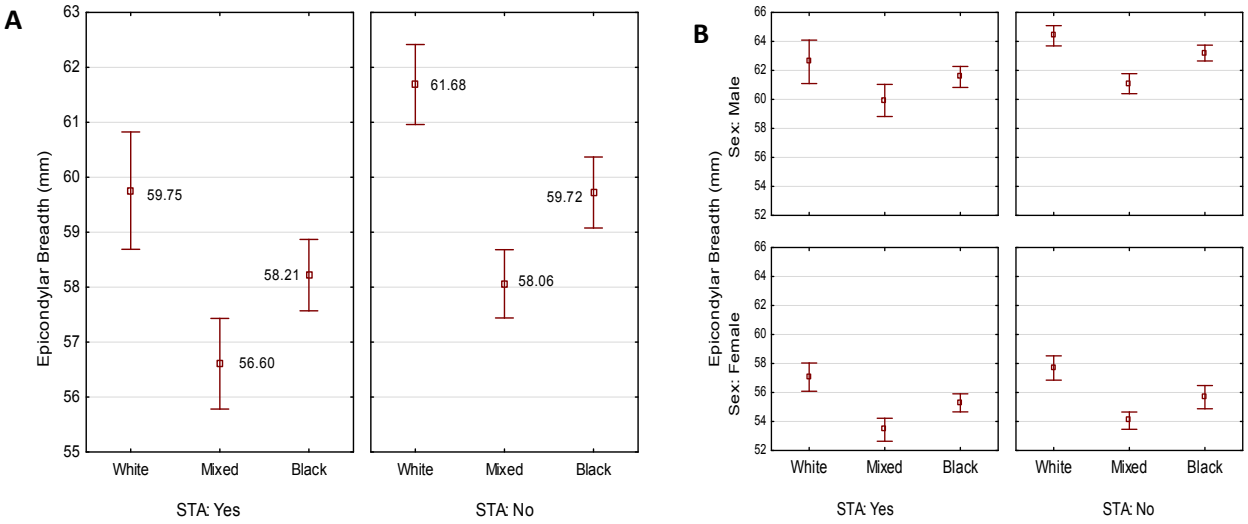


Figure 3.5: Epicondylar breadth (EB)
Humeri by population with and without the STA **(A)** and further stratified by sex **(B)**.

Table 3.4: Humeral length
Means ($\overline{X}$) and standard deviation (SD) in millimeters for each population stratified by sex.

Sex	STA	White			Mixed			Black		
		N	$\overline{X}$	SD	N	$\overline{X}$	SD	N	$\overline{X}$	SD
Male	Yes	38	333.00	18.24	87	316.81	24.29	89	320.15	18.26
	No	102	333.53	16.38	160	312.66	20.31	149	321.58	19.3
	Total	140	333.39	16.84	247	314.12	21.84	238	321.04	18.89
Female	Yes	40	311.93	13.36	91	291.75	18.43	101	296.14	15.49
	No	69	319.04	14.70	121	292.94	18.05	128	298.33	15.00
	Total	109	316.43	14.58	212	292.43	18.18	229	297.37	15.22
All Groups		249	325.96	17.96	459	304.10	22.92	467	309.43	20.86

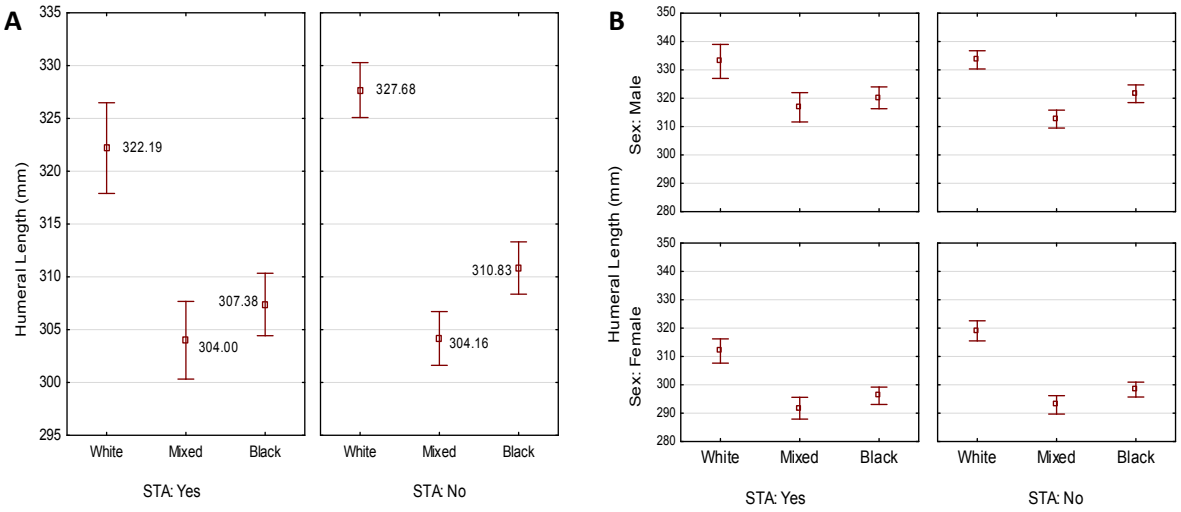


Figure 3.6: Humeral length
Humeri by population with and without the STA **(A)** and further stratified by sex **(B)**.

Humerus shaft circumferences

The greatest mean humeral shaft circumference in all populations was the distal circumference. The proximal and midshaft regions were characterized by similar dimensions (Table 3.5). In all three segments of the shaft, a larger circumference was found when the STA was absent than when it was present. These differences were statistically significant ($p=0.001$, $p=0.037$ and $p=0.007$ for the proximal, midshaft and distal aspects respectively). Males had a significantly greater shaft circumference than females for all the segments ($p<0.001$ for all three segments). The same pattern was observed whether the STA was present or absent.

Blacks had the greatest mean circumference for the proximal portion whereas the smallest value characterized the Mixed group ($p<0.001$ for all groups) (Fig. 3.7A). In the midshaft and distal regions, Whites had the greatest mean circumferences, followed by Blacks then the Mixed group ($p<0.001$ in both regions for Mixed group vs. Whites or Blacks (Fig. 3.7B). There were no significant differences between Whites and Blacks in the midshaft and distal regions ($p=0.72$). Shaft circumferences were greater when the STA was absent than when it was present in males and females, with the exception of the Black females. This group exhibited no significant differences in the circumference at all three areas when the STA was absent compared to when it was present ($p=0.10$, $p=0.17$ and $p=0.26$ for the proximal, midshaft and distal aspect respectively) (Fig. 3.7A-C).

Table 3.5: Proximal, midshaft, and distal humeral circumferences
Means ($\overline{X}$) and standard deviation (SD) in millimeters for each population stratified by sex.

Shaft Region	Sex	STA	White			Mixed			Black		
			N	$\overline{X}$	SD	N	$\overline{X}$	SD	N	$\overline{X}$	SD
Proximal	Male	Yes	38	61.46	4.80	87	60.15	6.33	89	64.63	4.53
		No	102	64.17	5.32	160	62.78	5.74	149	66.62	4.72
		Total	140	63.44	5.31	247	61.86	6.07	238	65.87	4.74
	Female	Yes	40	54.74	4.39	91	53.08	4.52	101	58.45	4.13
		No	69	56.97	4.52	121	55.28	4.61	128	59.73	5.06
		Total	109	56.15	4.58	212	54.34	4.69	229	59.16	4.70
	All Groups		249	60.25	6.17	459	58.38	6.64	467	62.58	5.79
Midshaft	Male	Yes	38	63.03	5.27	87	60.44	5.80	89	62.48	4.14
		No	102	65.20	5.03	160	62.32	5.25	149	65.33	5.39
		Total	140	64.61	5.17	247	61.65	5.52	238	64.26	5.14
	Female	Yes	40	56.18	3.81	91	53.78	5.15	101	57.05	4.03
		No	69	58.66	4.83	121	55.74	5.35	128	58.16	4.62
		Total	109	57.75	4.62	212	54.90	5.34	229	57.67	4.40
	All Groups		249	61.61	5.99	459	58.53	6.39	467	61.03	5.81
Distal	Male	Yes	38	67.39	6.42	87	63.08	7.32	89	65.79	4.78
		No	102	70.51	5.46	160	66.55	6.05	149	68.36	5.1
		Total	140	69.66	5.88	247	65.33	6.72	238	67.4	5.13
	Female	Yes	40	59.24	4.61	91	55.08	5.29	101	58.65	4.49
		No	69	61.99	6.32	121	57.80	6.46	128	59.64	5.23
		Total	109	60.98	5.88	212	56.63	6.12	229	59.20	4.93
	All Groups		249	65.86	7.28	459	61.31	7.77	467	63.38	6.49

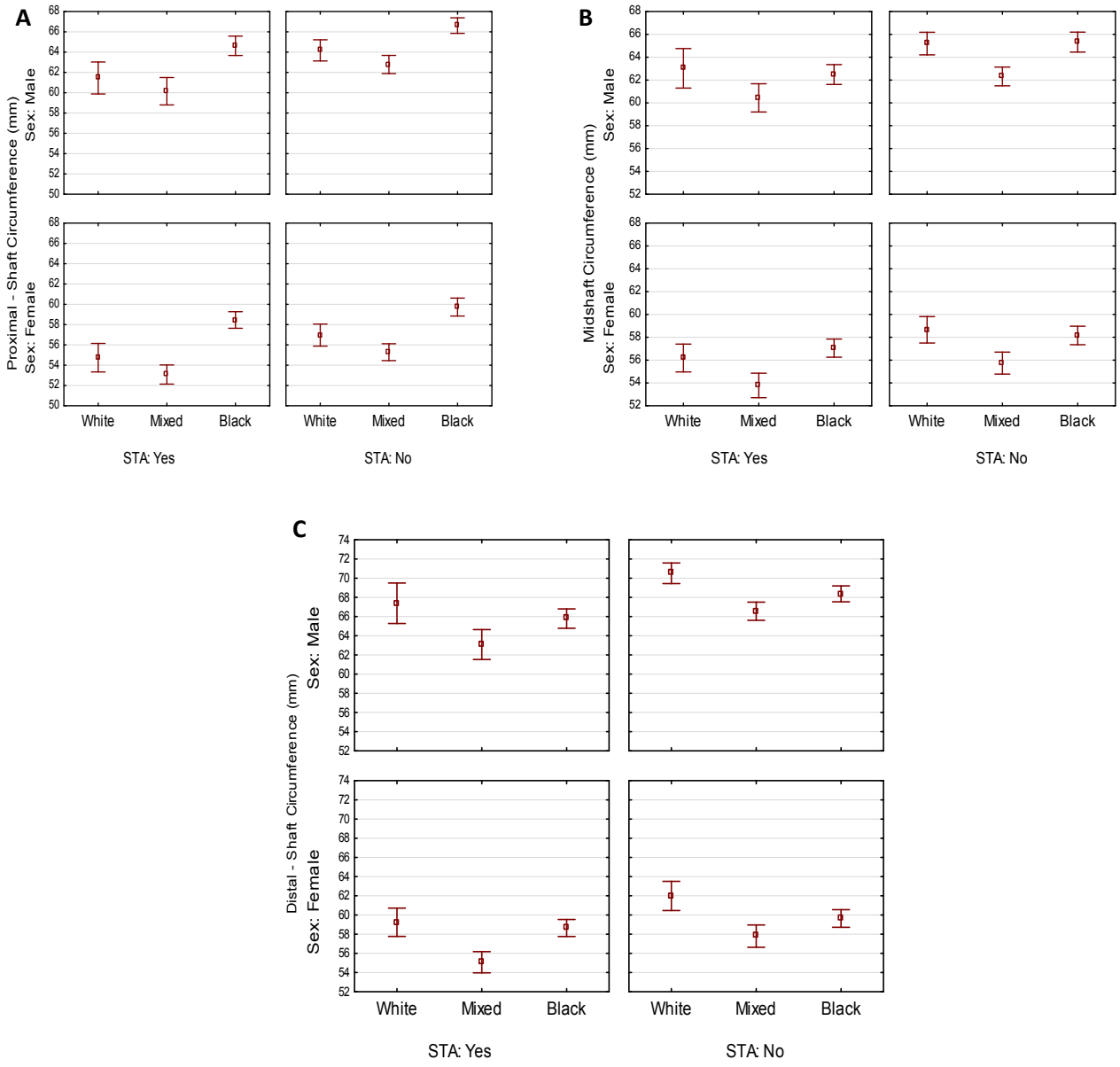


Figure 3.7: Humerus shaft circumferences - Proximal, midshaft and distal
Males and females of each population are shown stratified by STA status.

Olecranon fossa depth

Whites had significantly deeper olecranon fossae than both Blacks and individuals of Mixed ethnicity (p<001). The latter two groups had the same mean fossa depth (Table 3.6). The olecranon fossa depth was also greater in Whites regardless of whether the STA was present or absent (p<0.001 for both STA and no STA cases) (Fig. 3.8A). For both males and females, the humeral length was greater in Whites compared to their Black and Mixed group counterparts (p<0.001 for Whites vs Black or Mixed group). In male and female Whites, there was no significant difference in the depth of the fossa when the STA was absent or present (p=0.09 and p=0.24, for males and females, respectively) (Fig. 3.8B). In contrast, Black females and males showed significant differences in the fossa depth depending on the STA status, with greater depths characterizing bones with the STA (p=0.003 and p<0.001 for females and males, respectively) (Fig. 3.8B).

Table 3.6: Olecranon fossa depth
Means ($\bar{X}$) and standard deviations (SD) in millimeters for each population stratified by sex.

Sex	STA	White			Mixed			Black		
		N	$\bar{X}$	SD	N	$\bar{X}$	SD	N	$\bar{X}$	SD
Male	Yes	38	13.96	1.33	87	12.52	1.26	89	12.28	1.47
	No	102	14.18	1.20	160	12.95	1.51	149	12.94	1.45
	Total	140	14.12	1.23	247	12.80	1.44	238	12.7	1.49
Female	Yes	40	13.30	1.11	91	12.42	1.27	101	12.17	1.41
	No	69	13.67	1.10	121	12.31	1.34	128	12.75	1.23
	Total	109	13.54	1.11	212	12.36	1.31	229	12.49	1.34
All Groups		249	13.86	1.21	459	12.60	1.40	467	12.60	1.42

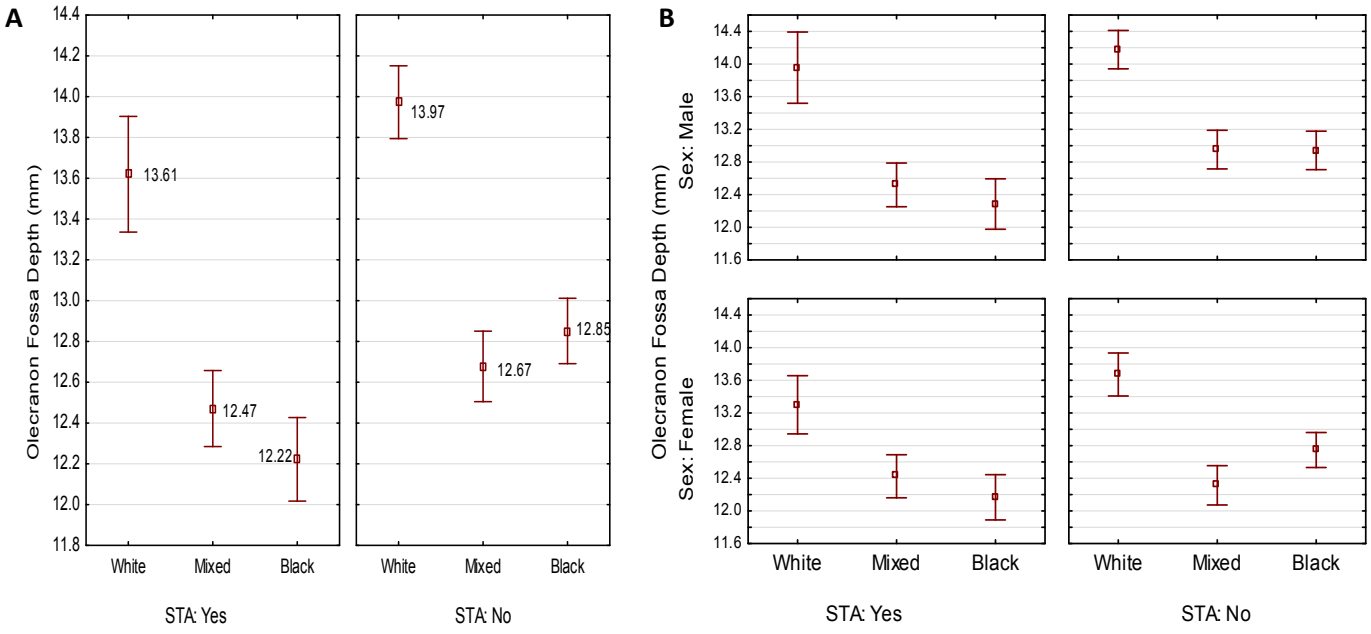


Figure 3.8: Olecranon fossa depth
Each population studied is shown with and without the STA **(A)** and further stratified by sex **(B).**

3.3.2 Characteristics of the ulna

Olecranon process length (O)

Minor but significant population variability was found for the olecranon process length. Blacks had the longest olecranon processes whereas Whites and Mixed ethnicity individuals exhibited marginally shorter processes (Table 3.7). Significant differences were found when comparing the Mixed group with Whites ($p=0.002$) and Blacks ($p<0.001$). When the STA was present, Blacks had a greater olecranon process length than Whites or the Mixed group although significant differences were only found between Blacks and the Mixed group ($p<0.001$). In contrast, olecranon process length was greater in Whites when the STA was absent ($p<0.001$ for all groups) (Fig. 3.9A). For both males and females, the length was significantly greater when the STA was present in all three populations ($p<0.001$ for all groups) (Fig. 3.9B).

Coronoid process length (C)

The coronoid process length was marginally greater in Blacks followed by the Mixed group and then Whites and these population differences were not statistically significant ($p=0.47$) (Table 3.8). For all three populations, the coronoid process length did not vary according to the STA status ($p=0.36$) (Fig. 3.10A). This similarity occurred across all the sexes in all groups except for Black females, who had significantly greater coronoid process lengths when the STA was present ($p=0.001$).

Table 3.7: Olecranon process length (O)
Means ($\bar{X}$) and standard deviation (SD) in millimeters for each population stratified by sex.

Sex	STA	White			$\bar{X}$Black			Black		
		N	$\bar{X}$	SD	N	$\bar{X}$	SD	N	$\bar{X}$	SD
Male	Yes	38	10.93	1.35	87	10.54	1.44	89	10.64	1.49
	No	102	9.54	0.99	160	8.80	1.31	149	9.1	1.28
	Total	140	9.92	1.26	247	9.41	1.59	238	9.67	1.55
Female	Yes	40	9.55	1.27	91	9.48	1.55	101	10.71	1.56
	No	69	8.48	1.05	121	7.94	1.27	128	8.93	1.32
	Total	109	8.87	1.24	212	8.60	1.59	229	9.72	1.68
All Groups		249	9.46	1.35	459	9.04	1.64	467	9.69	1.61

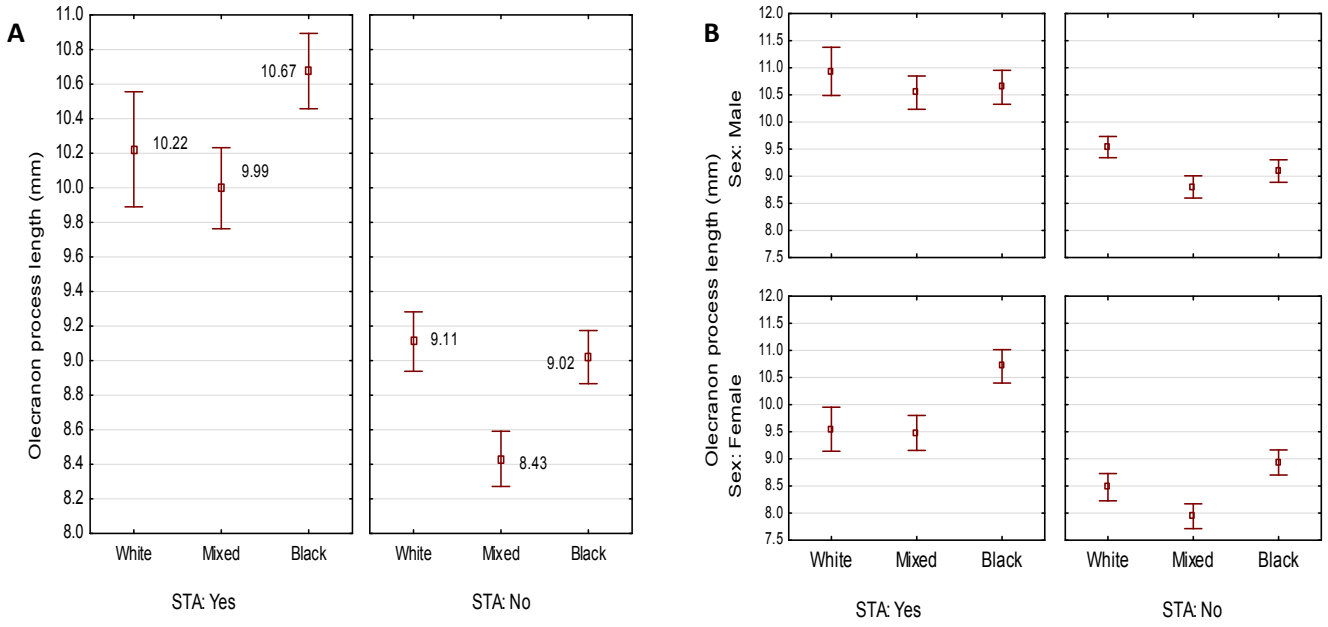


Figure 3.9: Olecranon process length (O)
Each population is shown by STA status **(A)** and further stratified by sex **(B).**

Table 3.8: Coronoid process length
Means ($\bar{X}$) and standard deviations (SD) in millimeters for each population stratified by sex.

Sex	STA	White			Mixed			Black		
		N	$\bar{X}$	SD	N	$\bar{X}$	SD	N	$\bar{X}$	SD
Male	Yes	38	6.53	1.10	87	6.98	1.89	101	6.60	1.46
	No	102	6.63	1.27	160	6.99	1.55	128	5.97	1.42
	Total	140	6.61	1.22	247	6.99	1.67	229	6.25	1.47
Female	Yes	40	5.73	0.98	91	5.62	1.25	89	6.39	1.24
	No	69	5.63	1.08	121	5.59	1.33	149	6.50	1.44
	Total	109	5.67	1.04	212	5.60	1.29	238	6.46	1.37
All Groups		249	6.20	1.23	459	6.35	1.66	467	6.36	1.42

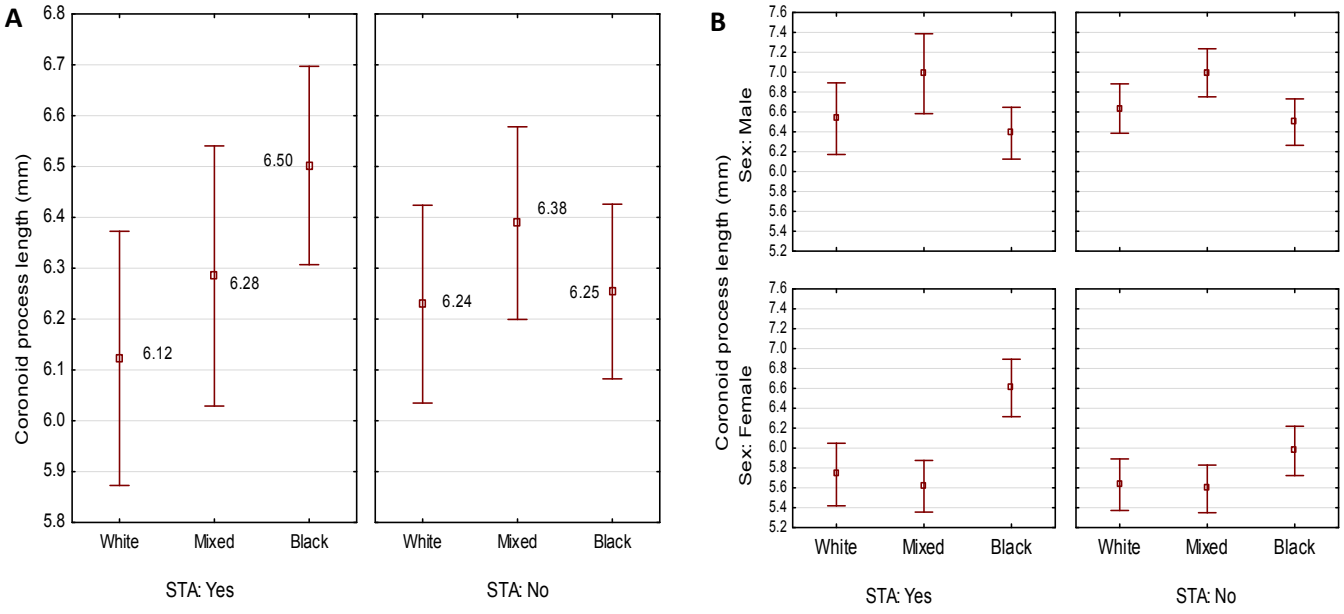


Figure 3.10: Coronoid process length
Each population studied is shown with and without the STA **(A)** and further stratified by sex **(B).**

Olecranon-coronoid distance (O-C)

Blacks and Whites had similar mean olecranon-coronoid distances that were marginally greater than the values for the Mixed group (Table 3.9). Although small, these differences were statistically significant ($p<0.001$ for Mixed vs. Blacks or Whites). The olecranon-coronoid distance was also similar when the STA was present for all three groups ($p<0.41$) (Fig. 3.11A). In contrast, when the STA was absent, the olecranon-coronoid distance was smaller in the Mixed group than in Whites ($p=0.001$) or Blacks ($p<0.001$) (Fig. 3.11A). Among males, the olecranon-coronoid distance was smallest in the Mixed group ($p<0.001$ for Mixed group vs Blacks or Whites). It was also smallest in females of the Mixed group although significant difference were only found between females of the Mixed group and their Black counterparts. When stratified according to STA status, only White males and Mixed females did not show statistically significant differences in the olecranon-coronoid distance (White males, $p=0.06$; Mixed group females $p=0.24$).

Table 3.9: Olecranon-coronoid distance (O-C)
Means ($\bar{X}$) and standard deviation (SD) in millimeters each population stratified by sex.

		White			Mixed			Black		
Sex	STA	N	$\bar{X}$	SD	N	$\bar{X}$	SD	N	$\bar{X}$	SD
Male	Yes	38	24.05	2.03	87	23.37	2.29	89	23.3	1.75
	No	102	24.83	2.07	160	24.14	2.07	149	24.9	1.68
	Total	140	24.62	2.08	247	23.87	2.18	238	24.3	1.87
Female	Yes	40	21.46	1.85	91	21.62	1.92	101	21.53	1.65
	No	69	22.65	1.46	121	21.95	1.69	128	23.07	2.33
	Total	109	22.21	1.71	212	21.81	1.79	229	22.39	2.20
All Groups		249	23.57	2.27	459	22.92	2.26	467	23.36	2.25

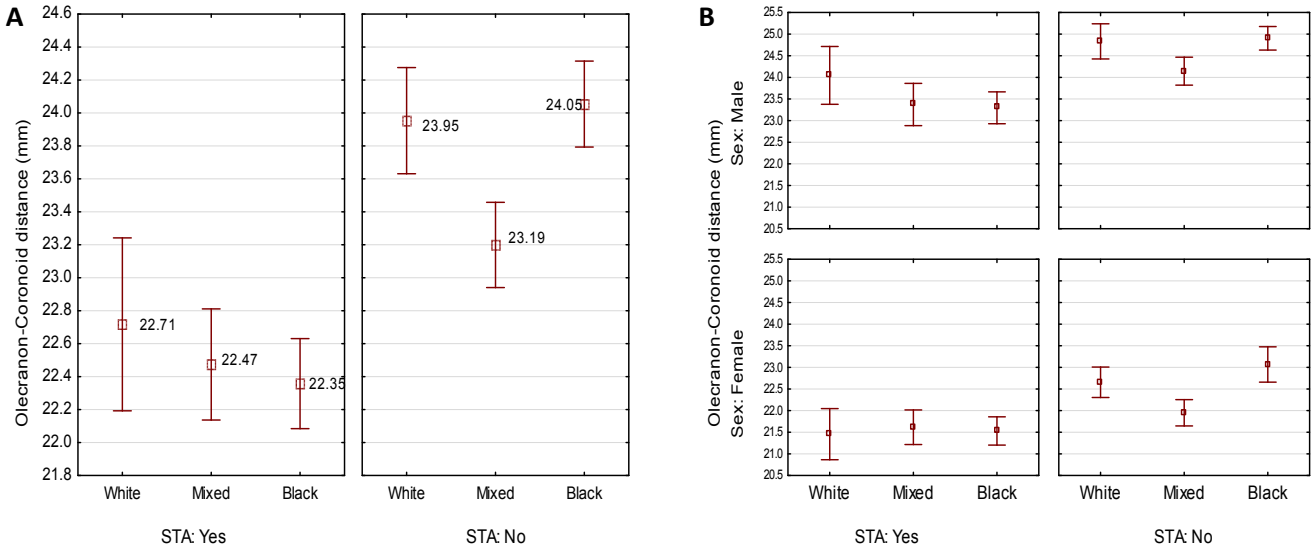


Figure 3.11: Olecranon-coronoid distance (O-C)
Each population studied is shown with and without the STA **(A)** and further stratified by sex **(B).**

Trochlear notch depth (D)

The mean trochlear notch depth was marginally greater in Blacks followed by Whites, and then the Mixed group. Although small, these population differences in trochlear notch depth were statistically significant ($p<0.001$ for Blacks vs the Mixed group and $p=0.015$ Blacks vs Whites). When the STA was present, Blacks had a significantly greater trochlear notch depth $p<0,001$ for Blacks vs Mixed or Whites). Similarly, when the STA was absent Blacks had a significantly greater trochlear notch depth although significant differences were only found between Blacks and individuals of the Mixed group ($p<0.001$).

When stratified by sex, Black females had marginally deeper trochlear notches than their White and Mixed ethnicity counterparts ($p<0.001$ for Blacks vs Whites or Mixed group) (Table 3.10). In males, the depth of the notch was similar for Blacks and Whites compared to the Mixed group that had shallower trochlear notches. However, significant differences in trochlear notch depth among males were only detected between Blacks and the Mixed group ($p<0.001$). In females, it was greatest in Blacks followed by Whites, then the Mixed group and only the latter two groups did not show significant differences ($p=0.99$). When stratified by sex, both Black males and females had greater trochlear notch depths followed by Whites and the Mixed group although significant differences were only observed in Blacks and the Mixed group ($p<0.001$ for both sexes) (Fig. 3.12B).

Table 3.10: Trochlear notch depth (D)
Means ($\overline{X}$) and standard deviation (SD) in millimeters for each population stratified by sex.

Sex	STA	White			Mixed			Black		
		N	$\overline{X}$	SD	N	$\overline{X}$	SD	N	$\overline{X}$	SD
Male	Yes	38	11.95	1.27	87	11.60	1.61	89	12.28	1.13
	No	102	12.17	1.22	160	11.94	1.39	149	12.56	1.35
	Total	140	12.11	1.24	247	11.82	1.47	238	12.46	1.28
Female	Yes	40	10.31	1.18	91	10.25	1.43	101	11.12	1.19
	No	69	10.77	1.36	121	10.56	1.34	128	11.05	1.28
	Total	109	10.60	1.31	212	10.42	1.39	229	11.08	1.24
All Groups		249	11.45	1.47	459	11.18	1.59	467	11.78	1.43

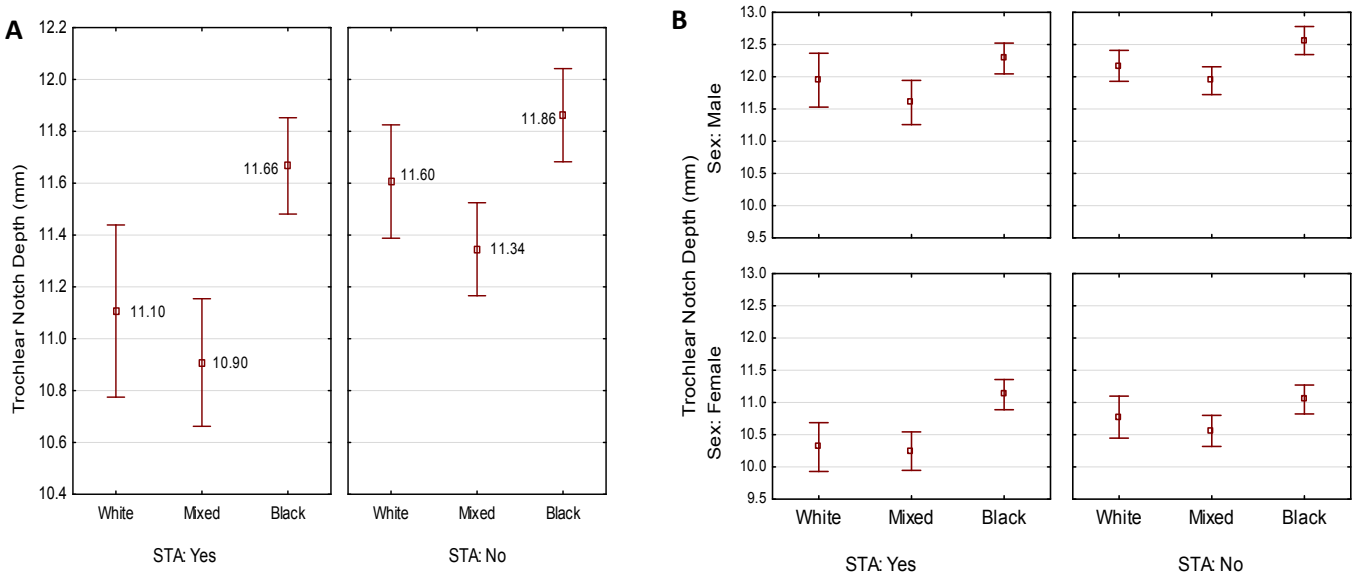


Figure 3.12: Trochlear notch depth (D)
Each population studied is shown with and without the STA **(A)** and further stratified by sex **(B).**

Ulnar length

The ulnar length was greatest in Blacks, followed by Whites and the Mixed group. It was not significantly different in Blacks and Whites compared to their counterparts in the Mixed group ($p=0.58$ for Blacks vs. Whites; $p<0.001$ for the Mixed group vs. Blacks or Whites (Table 3.11). The Mixed group had the shortest ulnar both when the STA was present ($p<0.001$ Mixed group vs Black) and absent ($p<0.001$ Mixed group vs Black or White). In both sexes, Blacks had the greatest ulnar length while the Mixed group had the shortest ulnae when the STA was absent ($p<0.001$ among all groups) or present (Table 3.11; Figs 3.13A and B). No significant differences in ulnar length between Blacks and Whites of both sexes were detected when the STA was present ($p=0.36$).

Table 3.11: Ulnar length

Means ($\bar{X}$) and standard deviation (SD) in millimeters for each population stratified by sex.

Sex	STA	White			Mixed			Black		
		N	$\bar{X}$	SD	N	$\bar{X}$	SD	N	$\bar{X}$	SD
Male	Yes	38	265.05	15.94	87	259.51	18.88	89	271.93	15.46
	No	102	267.54	15.67	160	257.08	17.55	149	272.49	15.62
	Total	140	266.87	15.72	247	257.93	18.03	238	272.28	15.53
Female	Yes	40	245.88	12.92	91	240.36	19.43	101	248.16	13.93
	No	69	248.82	12.69	121	238.13	15.76	128	250.20	14.25
	Total	109	247.74	12.79	212	239.08	17.42	229	249.30	14.12
All Groups		249	258.49	17.33	459	249.23	20.07	467	261.01	18.77

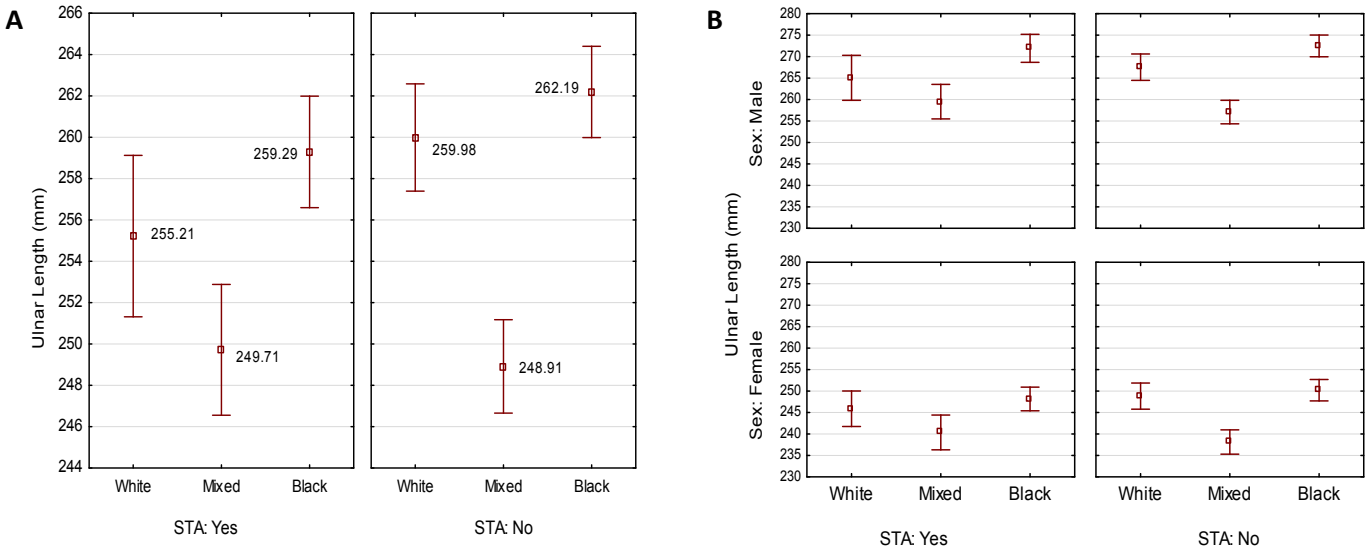


Figure 3.13: Ulnar length. Each population studied is shown with and without the STA **(A)** and further stratified by sex **(B)**

3.3.3 Humeral and ulnar parameters contributing to population variation

A discriminant function analysis was conducted to determine the upper limb skeletal parameters that contribute to population variation. All the humeral and ulnar variables in this study had a role in discriminating among the populations (Table 3.12). The discriminant analysis yielded 2 functions, and the Wilk's lambda showed a good fit for the functions (Wilk's lambda 0.337 and 0.720, for Functions 1 and 2 respectively; $p<0.001$ for both functions). Function 1 accounted for 74.5% of the total population variability whereas Function 2 accounted for only 24.5%. Other factors not in the analysis accounted for the remaining 1% of the variability among the populations.

The structure matrix showed that both the humeral and ulna variables made major contributions to population variability (Table 3.12). Olecranon fossa depth and the right humeral head circumference contributed the most to population variability. The cross-validated classification showed that overall 74.1% of individuals were correctly classified according to their population affiliation. The model correctly classified 78.9% of the individuals as White, 68% as Mixed and 79% as Black (Table 3.13). Therefore, each population was clearly distinguished from the others (Fig. 3.14).

Table 3.12: Structure matrix showing correlations between variables distinguishing populations and standardized canonical discriminant functions

The contributing variables are arranged in descending order according to Function 1, with major contributors in bold (above .3).

Structure Matrix		
Contributing variables	**Function**	
	1	**2**
Olecranon fossa depth (Right)	**.350**	.236
Head circumference (Right)	**.331**	.495
Olecranon fossa depth (Left)	**.309**	.266
Humeral length (Left)	.297	.380
Head circumference (Left)	.292	.468
Humeral length (Right)	.267	.434
Epicondylar breadth (Right)	.143	.373
Proximal shaft circumference (Left)	.136	.440
Epicondylar breadth (Left)	.135	.325
Distal shaft circumference (Left)	.133	.341
Proximal shaft circumference (Right)	.122	.436
Distal shaft circumference (Right)	.118	.313
Coronoid Length (Right)	.097	.216
Trochlear notch depth (Left)	.077	.284
Trochlear notch depth (Right)	.070	.231
Olecranon Length (Left)	.055	.241
Olecranon length (Left)	.050	.341
Olecranon-coronoid Length (Left)	.050	.195
Midshaft circumference (Right)	.046	.354
Ulnar length (Left)	.039	.451
Ulnar length (Right)	.038	.453
Midshaft circumference (Left)	.024	.360
Olecranon-coronoid Length (Right)	.020	.163
Coronoid Length (Left)	.018	.273
Function loading	74.5%	24.5%

Table 3.13: Population classification

Classification Results[a,c]						
		Population	Predicted Group Membership			Total
			White	Mixed	Black	
Original	Count	White	97	16	10	123
		Mixed	20	165	42	227
		Black	2	41	186	229
	%	White	78.9	13.0	8.1	100
		Mixed	8.8	72.7	18.5	100
		Black	.9	17.9	81.2	100
Cross-validated[b]	Count	White	97	15	11	123
		Mixed	22	156	49	227
		Black	4	49	176	229
	%	White	**78.9**	12.2	8.9	100
		Mixed	9.7	**68.7**	21.6	100
		Black	1.7	21.4	**76.9**	100

a. 77.4% of original grouped cases correctly classified.

b. Each case is classified by the functions derived from all cases other than that case.

c. 74.1% of cross-validated grouped cases correctly classified.

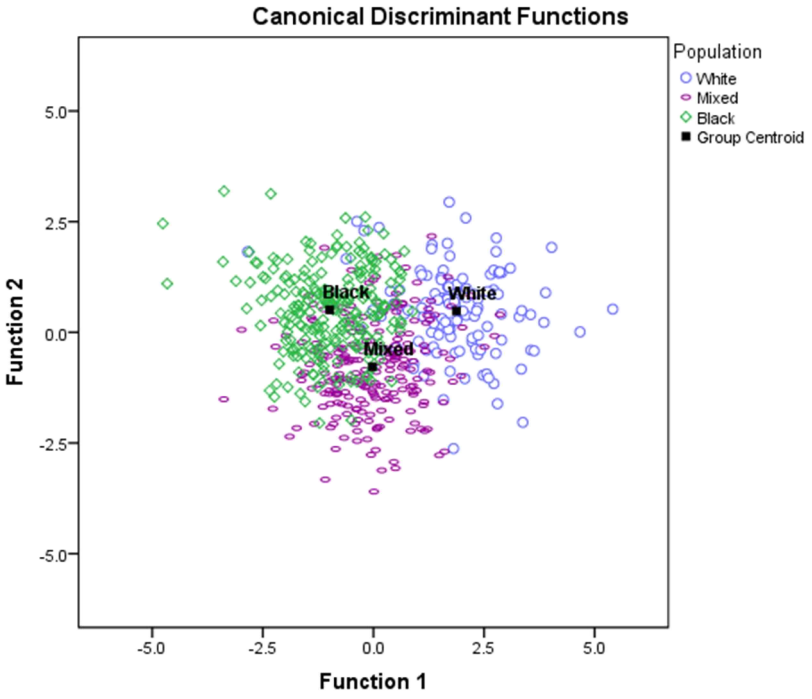


Figure 3.14: Population discrimination

3.3.4 Determinants of STA status

Factors influencing the presence of the STA in the combined sample

Discriminant function analysis was conducted to determine the variables that contribute to STA status. The structure matrix showed that the humeral contributing variables were epicondylar breadth, head circumference, the three shaft circumferences (proximal, midshaft and distal) and olecranon fossa depth. The olecranon length, olecranon-coronoid distance, and notch depth were the ulnar contributors (Table 3.14).

The discriminant analysis yielded 3 functions, although the Wilk's lambda results indicate a good fit for only Functions 1 and 2 [Wilk's lambda = 0.425, 0.722 for Functions 1 and 2 ($p<0.001$)]. Function 3 was not significant ($p=0.53$). Function 1 accounted for 64.9% of the variability, and Function 2 accounted for 31.5%. However, only olecranon length and olecranon-coronoid distance were major contributors to STA status (Table 3.14). For the cross-validated classification, 67.7% of humeri were correctly classified according to their STA status. The model correctly classified 86.3% of the humeri as lacking the STA, and 66.2% as having bilateral occurrences. However, for unilateral cases the model could not reliably predict whether the aperture was on the left (39.8%) or right (7.3%) (Table 3.14 and Fig. 3.15)

Table 3.14: Structure matrix showing correlations between STA status discriminating variables and standardized canonical discriminant functions in the combined sample

The contributing variables are arranged in descending order according to Function 1, with major contributors in bold (above .3).

Structure Matrix			
Contributing variables	**Function**		
	1	**2**	**3**
Olecranon length (Right)	**.602**	.339	.129
Olecranon length (Left)	**.586**	.402	.210
Olecranon-coronoid Length (Left)	**.369**	.060	.021
Olecranon-coronoid Length (Right)	**.339**	.066	.093
Distal shaft circumference (Left)	.278	.050	.334
Distal shaft circumference (Right)	.267	.051	.367
Midshaft circumference (Right)	.260	.051	.450
Midshaft circumference (Left)	.241	.046	.483
Proximal shaft circumference (Right)	.234	.066	.482
Proximal shaft circumference (Left)	.232	.065	.437
Fossa depth (Left)	.184	.050	.063
Head circumference (Right)	.181	.050	.173
Epicondylar breadth (Right)	.177	.010	.105
Fossa depth (Right)	.177	.191	.135
Head circumference (Left)	.175	.079	.143
Trochlear notch depth (Right)	.164	.032	.246
Epicondylar breadth (Left)	.154	.013	.137
Trochlear notch depth (Left)	.130	.075	.101
Function loading	64.9%	31.5%	3.6%

Table 3.15: Classification by STA status

Classification Results[a,c]							
		STA	Predicted Group Membership				Total
			No	Left	Right	Bilateral	
Original	Count	No	260	16	3	20	299
		Left	44	47	0	12	103
		Right	25	1	7	8	41
		Bilateral	33	9	1	93	136
	%	No	87	5.4	1	6.7	100
		Left	42.7	45.6	0	11.7	100
		Right	61	2.4	17.1	19.5	100
		Bilateral	24.3	6.6	0.7	68.4	100
Cross-validated[b]	Count	No	258	16	3	22	299
		Left	47	41	0	15	103
		Right	28	1	3	9	41
		Bilateral	36	9	1	90	136
	%	No	86.3	5.4	1	7.4	100
		Left	45.6	39.8	0	14.6	100
		Right	68.3	2.4	7.3	22	100
		Bilateral	26.5	6.6	0.7	66.2	100

a. 70.3% of original grouped cases correctly classified.

b. Each case is classified by the functions derived from all cases other than that case.

c. 67.7% of cross-validated grouped cases correctly classified.

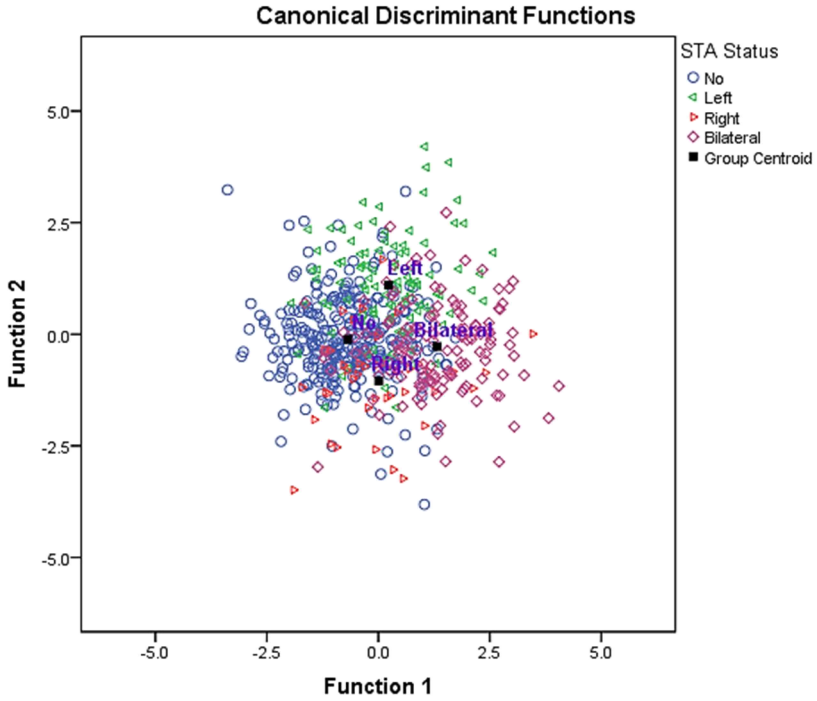


Figure 3.15: Segregation by STA status

Factors influencing the presence of the STA among Whites

Discriminant analysis was conducted to predict the presence of the STA and the side on which it occurred in Whites. The structure matrix indicated that the humeral shaft circumferences (proximal, midshaft and distal) and the olecranon process length, olecranon-coronoid distance and left trochlear notch depth were contributors to STA status and side (Table 3.16).

The discriminant analysis yielded three functions, although the Wilk's lambda results indicate a good fit for Functions 1 and 2 [Wilk's lambda = 0.425, 0.741 for Function 1 ($p<0.001$) and Function 2 ($p=0.04$)]. Function 3 was not significant ($p=0.62$). Function 1 accounted for 69.2% of the total variability, while Function 2 accounted for 24%. Olecranon length and olecranon-coronoid distance were main contributors to STA status in Whites (Table 3.16). The cross-validated classification found that overall 61.8% of humeri were correctly classified according to their STA status. The model correctly classified 80.3% of humeri as lacking the STA, yet when the STA was present it could not reliably predict whether the STA was on the left or right (Table 3.17 and Fig. 3.16).

Table 3.16: Structure matrix showing correlations between variables distinguishing STA status and standardized canonical discriminant functions in Whites

The contributing variables are arranged in descending order according to Function 1, with major contributors in bold (above .3).

Structure Matrix			
Contributing variables	**Function**		
	1	**2**	**3**
Olecranon process length (Right)	**.561**	.222	.173
Olecranon process length (Left)	**.369**	.323	.067
Olecranon-coronoid distance (Right)	**.347**	.268	.374
Olecranon-coronoid distance (Left)	**.337**	.368	.266
Humeral proximal shaft circumference (Right)	**.318**	.231	.143
Trochlear notch depth (Left)	**.306**	.064	.331
Humeral proximal shaft circumference (Left)	.292	.269	.241
Trochlear notch depth (Right)	.289	.164	.367
Humeral midshaft circumference (Right)	.280	.283	.102
Humeral distal shaft circumference (Left)	.279	.293	.155
Humeral distal shaft circumference (Right)	.269	.274	.045
Humeral midshaft circumference (Left)	.255	.297	.255
Function loading	69.2%	24%	6.8%

Table 3.17: Classification of limbs by STA status in Whites

Classification Results[a,c]							
		STA	Predicted Group Membership				Total
			No	Left	Right	Bilateral	
Original	Count	No	64	4	1	2	71
		Left	14	9	0	0	23
		Right	5	1	0	1	7
		Bilateral	4	4	0	14	22
	%	No	90.1	5.6	1.4	2.8	100
		Left	60.9	39.1	0	0	100
		Right	71.4	14.3	0	14.3	100
		Bilateral	18.2	18.2	0	63.6	100
Cross-validated[b]	Count	No	57	8	1	5	71
		Left	16	5	1	1	23
		Right	5	1	0	1	7
		Bilateral	4	4	0	14	22
	%	No	**80.3**	11.3	1.4	7	100
		Left	69.6	**21.7**	4.3	4.3	100
		Right	71.4	14.3	**0**	14.3	100
		Bilateral	18.2	18.2	0	**63.6**	100

a. 70.7% of original grouped cases correctly classified.
b. Each case is classified by the functions derived from all cases other than that case.
c. 61.8% of cross-validated grouped cases correctly classified.

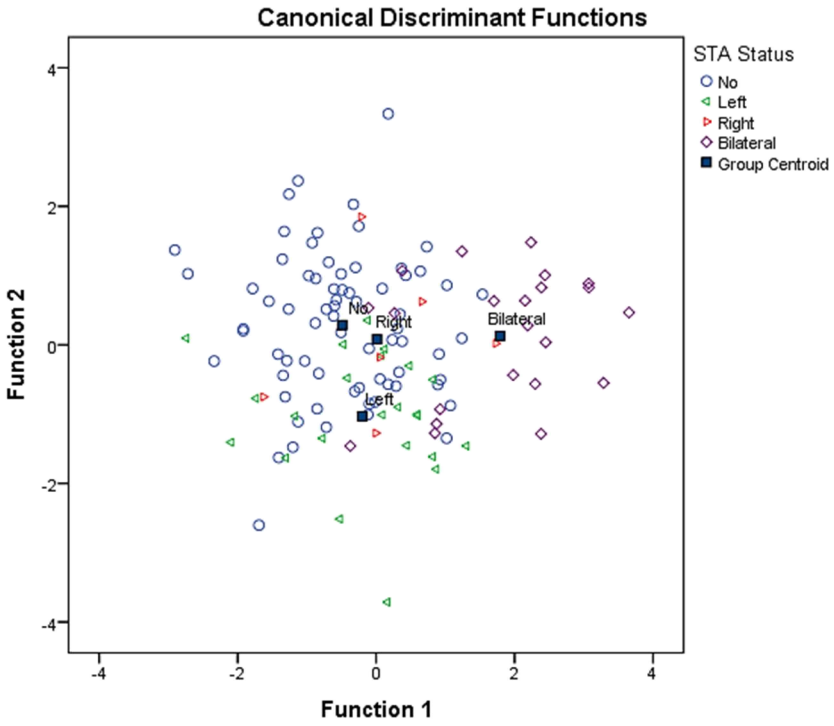


Figure 3.16: Classification of limbs by STA status in Whites.

Factors influencing the presence of the STA in the Mixed group

Discriminant analysis was then conducted to predict presence of the STA and the side on which it occurred in individuals of the Mixed group. The structure matrix indicated that only the olecranon process length was the main contributor to STA status in this group (Table 3.18).

The discriminant analysis yielded three functions, although the Wilk's lambda results indicate a good fit for Functions 1 and 2 [Wilk's lambda = 0.371, 0.632 for Functions 1 and 2 ($p<0.001$)]. Function 3 was not significant ($p=0.08$). Function 1 accounted for 56.4% of the total variability, while Function 2 accounted for 38.8%. Olecranon process length was the single major contributor to STA status for the Mixed group (Table 3.18). The cross-validated classification showed that overall 66.1% of humeri were correctly classified according to their STA status. The model correctly classified 85.6% of the humeri as lacking the STA, yet when the STA was present it could not reliably predict whether the STA was on the left or right, although the group centroids were clearly separated (Table 3.19 and Fig. 3.17).

Table 3.18: Structure matrix showing correlations between variables discriminating STA status and standardized canonical discriminant functions in the Mixed group

The contributing variables are arranged in descending order according to Function 1, with major contributors in bold (above .3).

Structure Matrix			
Contributing variables	Function		
	1	2	3
Olecranon process length (Right)	**.710**	.003	.066
Olecranon process length (Left)	**.369**	.571	.263
Humeral distal shaft circumference (Left)	.297	.115	.173
Humeral distal shaft circumference (Right)	.289	.138	.299
Humeral proximal shaft circumference (Left)	.278	.110	.155
Humeral proximal shaft circumference (Right)	.253	.145	.399
Humeral midshaft circumference (Left)	.248	.056	.200
Olecranon-coronoid distance (Right)	.244	.036	.345
Humeral midshaft circumference (Right)	.230	.054	.256
Function loading	56.4%	38.8%	4.7%.

Table 3.19: Classification of STA status in the Mixed group

Classification Results[a,c]							
		STA	Predicted Group Membership				Total
			No	Left	Right	Bilateral	
Original	Count	No	96	8	1	6	111
		Left	13	19	0	5	37
		Right	11	0	8	7	26
		Bilateral	15	2	1	35	53
	%	No	86.5	7.2	0.9	5.4	100
		Left	35.1	51.4	0	13.5	100
		Right	42.3	0	30.8	26.9	100
		Bilateral	28.3	3.8	1.9	66	100
Cross-validated[b]	Count	No	95	8	2	6	111
		Left	12	17	1	7	37
		Right	12	0	7	7	26
		Bilateral	17	2	3	31	53
	%	No	**85.6**	7.2	1.8	5.4	100
		Left	32.4	**45.9**	2.7	18.9	100
		Right	46.2	0	**26.9**	26.9	100
		Bilateral	32.1	3.8	5.7	**58.5**	100

a. 69.6% of original grouped cases correctly classified.

b. Each case is classified by the functions derived from all cases other than that case.

c. 66.1% of cross-validated grouped cases correctly classified.

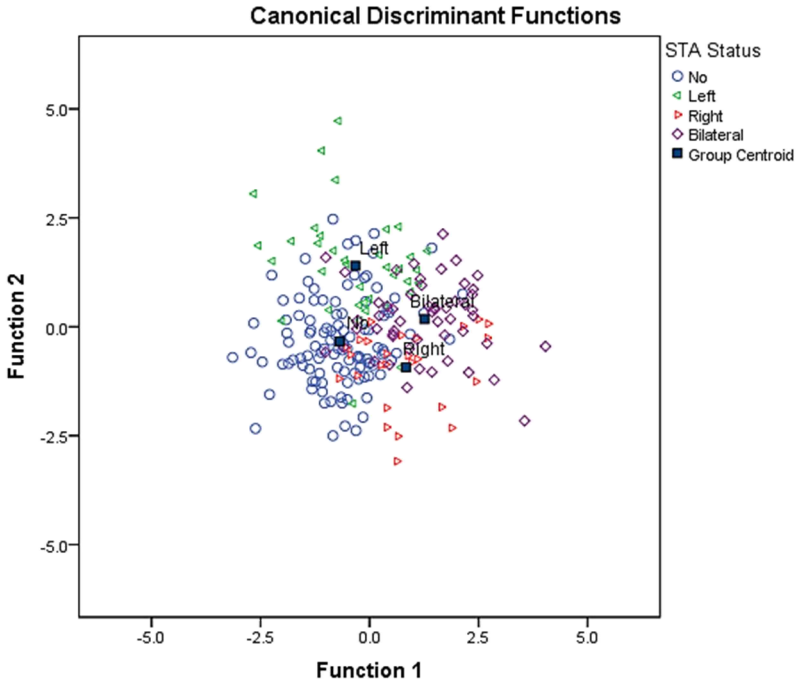


Figure 3.17: Classification of limbs by STA status in the Mixed group

Factors influencing the presence of the STA among Blacks

Another discriminant function analysis was conducted to predict the presence of the STA and the side on which it occurred in Blacks. The structure matrix indicated that the olecranon process length was the main variable contributing to STA status in this group (Table 3.20).

The discriminant analysis yielded 3 functions, although the Wilk's lambda results indicate a good fit for Functions 1 and 2 [Wilk's lambda = 0.461, 0.780 for Functions 1 and 2 ($p<0.001$) ($p=0.04$)]. Function 3 was not significant ($p=0.72$). The two functions accounted for the most variability with Function 1 accounting for 71.4%, and Function 2 accounting for 27.6%. Olecranon length was the sole main contributor to STA status. The cross-validated classification showed that overall 73.8% of humeri were correctly classified according to their STA status. The model correctly classified 91.5% of the humeri as lacking the STA. However, when the STA was present, it could not reliably predict whether it was on the left or right, although the group centroids were far apart (Table 3.21 and Fig. 3.18).

Table 3.20: Structure matrix showing correlations between variables discriminating STA status and standardized canonical discriminant functions in Blacks

The contributing variables are arranged in descending order according to Function 1, with major contributors in bold (above .3).

Structure Matrix			
Contributing variables	Function		
	1	2	3
Olecranon process length (Left)	**.801**	.275	.122
Olecranon process length (Right)	**.538**	.524	.215
Olecranon fossa depth (Left)	.243	.183	.314
Humeral midshaft circumference (Right)	.240	.089	.576
Coronoid process length (Left)	.222	.174	.643
Olecranon fossa depth (Right)	.194	.376	.485
Function loading	71.4%,	27.6%	0.1%

Table 3.21: Classification of STA by presence and STA side in Blacks

Classification Results[a,c]							
		STA	Predicted Group Membership				Total
			No	Left	Right	Bilateral	
Original	Count	No	107	2	0	8	117
		Left	13	25	0	5	43
		Right	7	0	0	1	8
		Bilateral	15	7	0	39	61
	%	No	91.5	1.7	0	6.8	100
		Left	30.2	58.1	0	11.6	100
		Right	87.5	0	0	12.5	100
		Bilateral	24.6	11.5	0	63.9	100
Cross-validated[b]	Count	No	107	2	0	8	117
		Left	14	23	0	6	43
		Right	7	0	0	1	8
		Bilateral	15	7	0	39	61
	%	No	**91.5**	1.7	0	6.8	100
		Left	32.6	**53.5**	0	14	100
		Right	87.5	0	**0**	12.5	100
		Bilateral	24.6	11.5	0	**63.9**	100

a. 74.7% of original grouped cases correctly classified.

b. Each case is classified by the functions derived from all cases other than that case.

c. 73.8% of cross-validated grouped cases correctly classified.

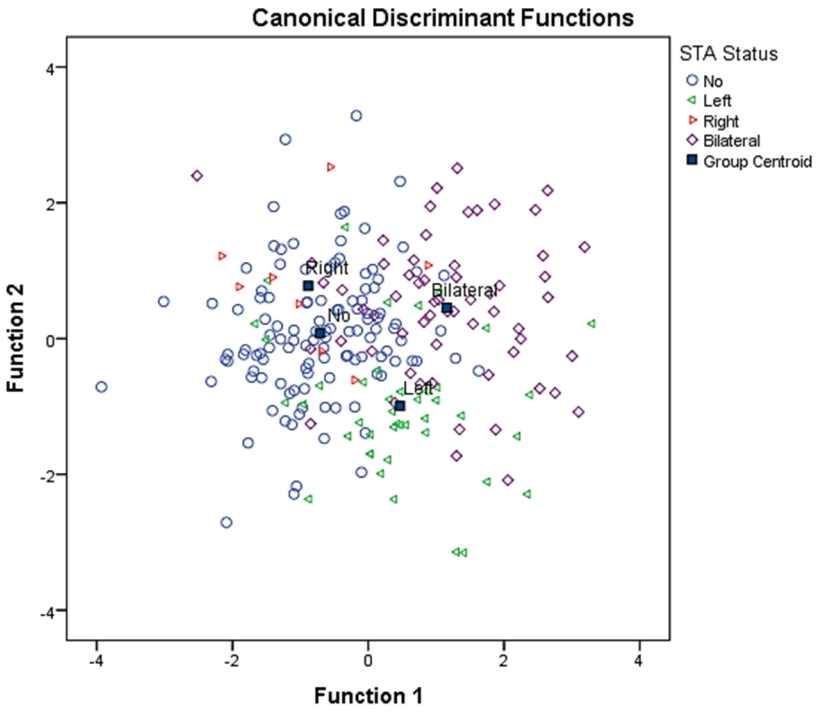


Figure 3.18: Classification of limbs by STA presence and absence in Blacks

3.4 DISCUSSION

Two aspects of the mechanical theory of STA etiology were investigated. First, osteometric measures of overall bone size were used to test whether STA status was correlated with bone dimensions. Then the olecranon and coronoid processes were compared to evaluate whether differences in their dimensions were associated with the STA. Additionally, we investigated the parameters that distinguish the three populations and those that predict STA status in each group. Our results support the proposition that smaller individuals are prone to STA formation. Furthermore, we established that a significantly longer olecranon process, but not a longer coronoid process, was associated with the STA. Finally, we found that the parameters that distinguish STA status are not common to all the groups, but are population specific.

3.4.1 Bone size

Benfer and McKern (1966) found an increase in the humeral midshaft diameter to be associated with a lessened likelihood of STA presence. Silveira et al. (2007) more recently reported corroborating findings of smaller humeral midshaft circumferences in bones with the STA in a Brazilian sample. We had similar results for the current study. For all the populations, humeral shaft circumferences in all three regions (proximal, midshaft and distal) were smaller when the STA was present. This supports the proposition that larger bone size is inversely correlated with STA formation. As a major contributor to population overall bone size is sexual dimorphism, a greater association between STAs and females is commonly observed (Benfer and McKern, 1966). In the present study,

females in all populations had smaller shaft circumferences (in all three shaft regions), and higher prevalence of the STA.

Glanville (1967) hypothesized that gracile individuals could have a genetic basis for the STA development. As bone size differences appear to be specifically correlated with STA formation, we propose that genes for a larger body frame might result in a phenotype that has lesser propensity for STA formation. Volkman et al. (2003) found 14 genetic markers in mice associated with bone size and cortical bone thickness, indicating that there is complex genetic control over bone morphology. It remains subject to future investigation whether such mechanisms play a role in STA formation.

3.4.2 Aspects of the elbow joint

Ulnar process lengths

Glanville (1967) and Mays (2008) found the length of both the olecranon and coronoid processes to be greater when the STA is present, signifying that both ulnar processes may be implicated in the etiology of the septal aperture. In the present study, only the olecranon process was longer in STA cases. This implies that the olecranon process alone may have a role in the etiology of the aperture in the current sample. Our findings are consistent with clinical observations that the coronoid process may not be locked in the coronoid fossae during elbow flexion due to the development of muscles and soft tissues in the anterior aspect of the limb. These muscles, such as the brachialis biceps brachi, brachioradialis and flexor carpi radialis together with soft tissues such as skin and adipose tissue would likely restrict the range of flexion (Rouleau et al., 2012). To the

contrary, the olecranon process occupies the olecranon fossa in full extension (Mays, 2008) thereby limiting hyperextension (see also chapter 6).

Mays (2008) indicated that longer ulnar processes could impinge upon the septum separating the olecranon and coronoid fossae causing bone resorption that is observed as an STA. In the present study, we found the olecranon process, but not the coronoid process is longer in STA cases. In support of this theory of STA etiology, Mays (2008) cited an example in which Ortner (2003) noted that an aneurism exerting pressure on a bone caused osseous resorption. Mays (2008) independently found a depression on the surgical neck of the humerus of an individual who had an upward shoulder joint displacement in which the humerus impinged upon the lower border to the glenoid cavity. This depression was considered to be a consequence of the bone resorption resulting from contact between the humerus and the lower border of the glenoid cavity. Therefore, in conjunction with these observations, our findings lend support to the idea that pressure from a long olecranon could result in an STA.

Fossa depth

The mean olecranon fossa depth was greater in males of all three populations. It was also greater when the STA was absent. However, when the STA was present, the olecranon fossa depth was significantly shallower in both sexes. At the same time, the olecranon process was significantly longer in STA cases. These observations demonstrate that a shallow fossa may be implicated in septal perforation as the shallowness

of the fossa might restrict room for the olecranon process during elbow extension. This lends support to the idea that a combination of a shallow fossa and longer olecranon process could result in impingement of the septum and the subsequent septal perforation.

Joint space

Mays (2008) suggested that reduced joint space may increase propensity for STA occurrence. In the present study, all three populations had smaller mean olecranon-coronoid distance when the STA was present and in females. A smaller olecranon-coronoid distance may constrain the room for the ulnar processes in flexion and extension. This restrained space may result in impingement of the septum between the olecranon and coronoid fossae which may subsequently resorb to form the STA. However, to test this hypothesis requires *in situ* joints, and so it remains untested.

3.4.3 Population specific aspects of STA status

Although all the humeral and ulnar parameters in this study had a role in distinguishing population affiliation, the right humeral head circumference and the olecranon fossa depth made the most contribution to population discrimination. Both of these variables differed in all three populations and they were significantly smaller in the Mixed group compared to Whites or Blacks.

In our initial study of a relatively small sample (Ndou et al., 2013), individuals belonging to the Mixed group had the smallest epicondylar breadth. In the present study, a larger sample size was used and more

osteometric measurements of the humerus were included. Although Blacks had smaller dimensions than Whites (Steyn and Iscan, 1999) for most of the humeral and ulnar dimensions, the Mixed group had smaller values irrespective of the STA status. A considerable component (32–43%) of the Mixed group's ancestry is from the Khoisan, who are people of small stature (De Wit et al., 2010). Therefore, the possibility exists that the smaller skeletal dimensions in this group could be attributed to their ancestry.

Our results showed that determinants of STA status are population specific. Whites, with a lower prevalence of STA, require more parameters for STA prediction compared to the Mixed group or Blacks. These additional parameters were proximal humeral shaft circumference (right) and trochlear notch depth (left). The lower prevalence may make the determination more difficult for this group. The involvement of more skeletal parameters contributing to STA status in Whites might also indicate that this sample may be diverse; they originated from various parts of Europe. Various studies detected the existence of genetic differences among Europeans (Nayak et al., 2009; Sajantila et al., 1995), therefore it is possible that the Whites in our sample may be of diverse genetic makeup that may impact on their skeletal characteristics.

In contrast, among Blacks and the Mixed group, only the olecranon process length was the main contributor to STA status. Lower loadings occur in the Mixed group. Therefore, this variable can more reliably predict

STA status in Blacks compared to the Mixed group. These findings indicate that factors influencing STA status are population specific.

The differences in the loadings for the left and right humeral variables in the population and STA status predictions using discriminant analysis could be a result of handedness or predominant utilization of a particular arm. Occupation and other behaviors are some of the determinants of extensive usage of one arm that may result in bilateral humeral asymmetry and body size. These differences in loading between the left and right sides further indicate that the features associated with the determinants of STA may be population specific as physical activities are very different.

3.5 CONCLUSIONS

Most parameters of overall humeral size were significantly larger when the STA was absent. This supports the proposition that small bodied individuals are prone to septal perforation. The olecranon process was longer in ulnae from individuals with septal apertures, whereas the coronoid process was similar irrespective of septal perforation. Therefore, the olecranon process appears to play a more key role in septal perforation. This is further supported by the discriminant function analysis that found the olecranon process was a major factor in discriminating STA status irrespective of population affiliation. Among Whites, the right proximal humeral shaft circumference and left trochlear notch depth were the additional parameters required for distinguishing STA status. Although the olecranon fossa depth did not play a major role in stratification of humeri by STA status, it was significantly shallower in the STA group in

this sample. Therefore, it appears that a long olecranon process, coupled with a shallow olecranon fossa, is associated with the presence of the STA. These findings support the mechanical STA etiology that proposes that a longer olecranon process may impinge upon the septum separating the olecranon from the coronoid fossae, causing bone resorption and ultimate perforation.

3.6 ACKNOWLEDGEMENTS

We are very grateful to the following people for granting us permission to use the skeletal material: Brendon Billings for access to the Raymond A Dart Collection, Mandi Alblas for use of the University of Stellenbosch bone collection, Professor Alan Morris for use the University of Cape Town bone collection, and Professor Ericka L'Abbé and Marius Loots for use of the Pretoria Bone Collection. We thank Dr T Esan for advice on statistical methods. The funds for the project came from the National Research Council (South Africa), University of the Witwatersrand Faculty Research Council, the Wits WHC dividend, and the JJJ Smieszek Fellowship.

CHAPTER 4

A radiographic investigation of the relationships between humeral cortical bone thickness, medullary canal width and the supratrochlear aperture (STA)

Table of Contents

4.0 ABSTRACT 91
4.1 INTRODUCTION 93
4.2 MATERIALS AND METHODS 97
4.2.1 Sample 97
4.2.2 Radiography and measurement procedures 98
4.2.3 Statistics 99
4.3 RESULTS 101
4.3.1 Humeral width 101
4.3.2 Medullary canal width 104
4.3.3 Medullary canal width differences stratified by age STA status 107
4.3.4 Standardized comparisons of medullary canal width 112
4.3.5 Correlation of humeral medullary canal width and cortical thickness 117
4.4 DISCUSSION 124
4.4.1 Medullary canal width 124
4.4.2 Medullary canal width standardized by bone width or length 126
4.4.3 Correlation of medullary canal width and cortical bone thinness by age & sex 127
4.5 CONCLUSIONS 128
4.6 ACKNOWLEDGMENTS 128

4.0 ABSTRACT

The osteological variant that occurs in the humerus, exhibited as a perforation of the septum between the olecranon and coronoid fossae, is known as the supratrochlear aperture (STA). Individuals with the STA are prone to diaphyseal fractures of the humerus and unusual fracture patterns tend to occur. Bones with this feature are thought to have a narrower medullary canal. Our aim was to explore the relationship of the STA with medullary canal width. To do that, the relationship of STA status with medullary canal width and cortical bone thickness, as well as population variation in medullary canal width by STA status and age, was investigated.

The study employed a case-control research design with approximately equal numbers of individuals with and without the STA. The humeri were from South African Whites, Blacks, and the Mixed ethnic group. Radiographs were taken anteroposteriorly using a Lodox Statscan. The image processing software Image J® was used to acquire measurements from the radiographs.

Humeri with the STA appeared to have narrower medullary canal dimensions. However, this was not the case after standardizing for bone size. The smaller medullary canal width, reported in the orthopedic literature for STA-bearing humeri, is therefore due to the overall bone size differences rather than the presence of the STA. We propose that bone size, and not STA presence, is the major factor to consider when making choices of a rod for intramedullary fixation. The medullary canal width increased as cortical bone thickness decreased. However, there was no

correlation between medullary canal width and cortical bone thickness among individuals after the age of 75 years, which suggests that the bone remodeling cycle is different for individuals of this age cohort.

4.1 INTRODUCTION

Bone forms the basic structure that supports the entire body and facilitates movement. Population differences in bone strength and density have been documented. For example, in the US population, denser and stronger bones characterize Blacks compared to Whites (Leonard et al., 2010). Similarly, Black adult females in South Africa have a lower risk of fractures than their White counterparts (Cauley et al., 2005), and Black teenagers are less prone to fractures than their White age mates (Thandrayen et al., 2009). Differences in bone response to mechanical loading exist among South African children, with Blacks having a slower response to bone loading compared to Whites (Meiring et al., 2013). Additionally, Black children have greater bone mineral content at the femoral neck and mid-radius compared to their White counterparts (Vidulich et al., 2006).

In non-weight bearing bones such as in the upper limb, muscle attachments can affect cortical bone thickness. Consequently, localized variation in cortical bone may occur, with muscle attachment sites being associated with bone thickening (Niinimaki et al., 2013). This suggests that muscle attachment may exert a localized form of mechanical loading to the bone that then responds by increasing the cortical thickness.

Miyamoto et al. (2005) found that in dental surgery, cortical bone thickness has more influence on the stability of an implant than the actual depth of the implant. These researchers noticed that implants in thinner cortical areas were unstable and took longer to heal than when the bone was thicker. There are no comparable studies on limbs, possibly because these skeletal components are repaired by surgical means that adequately

compensate for implant instability. For example, intramedullary devices may be stabilized by interlocking screws (Keating, 2013).

Cortical bone density is known to decrease faster in elderly females (Parfitt, 1984). This loss of cortical bone would result in an increase in relative medullary canal width with age. Rapid bone loss due to excessive resorption leads to increased size of medullary canal. On the other hand, slow bone loss results from incomplete refilling of resorption cavities leading to bone thinning (Pearson and Lieberman, 2004).

Bone cortical thickness may only be studied by radiation imaging such as is commonly used for diagnostic purposes in hospitals. Although computed tomography may be employed, X ray is the fastest and least expensive imagining modality. There is the conventional method (cone beam) and a low dose X ray system (Lodox) that is also faster than the conventional method. Distortion and magnification errors are not a major concern when using imaging for diagnostic purposes, but these factors are undesirable in scientific research, which requires that the former be minimized and the latter be accounted for. Scatter is greater in all directions with the cone beam (Fig. 4.1 a). In contrast, Lodox radiography has hardly any scatter in the y axis, while scatter mainly affects peripherally positioned objects along the x axis (Fig. 4.1b). Therefore, the Lodox system yields images with minimal distortion in both the x and y axes (Stull et al., 2013).

The osteological variant that occurs in the distal humerus, exhibited as a perforation of the septum between the olecranon and coronoid fossae, is

known as the supratrochlear aperture (STA). Despite over a century of study pertaining to this feature, there are no satisfactory answers about characteristics of humeri that have the aperture. The main shortcoming of research in this area is that no single study has taken an integrated approach using large samples of known age, sex and population history.

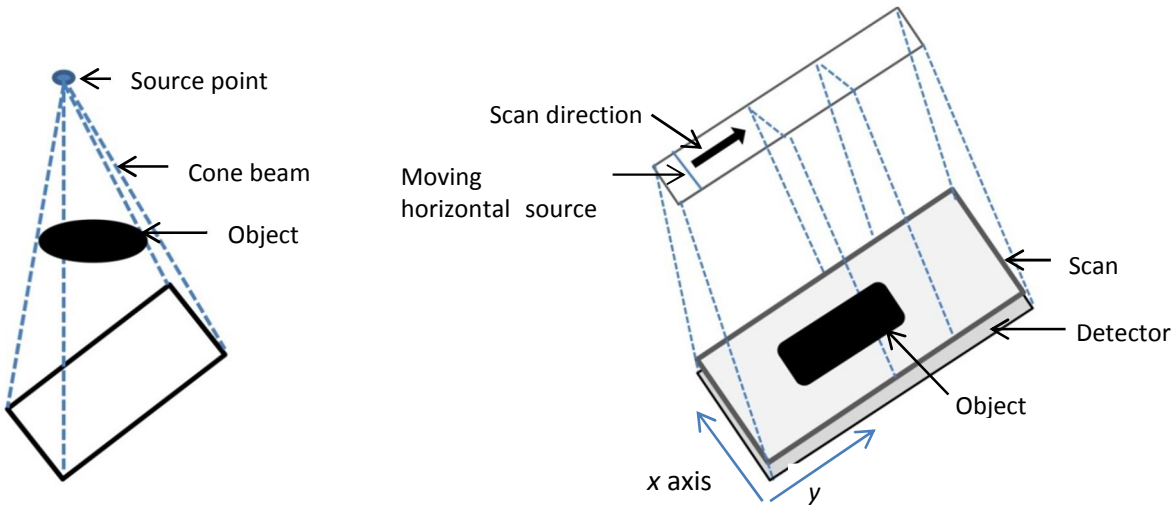


Figure 4.1: Representation of cone bean (a) and Lodox Statscan (b) configurations
In the cone beam, scatter is equal in all directions whereas the Lodox has minimum scatter in the y axis and x axis.

According to the clinical literature, individuals with the STA are prone to fractures of the humerus and unusual fracture patterns tend to occur (Sahajpal and Pichora, 2006). Bones with septal perforation are thought to have a narrower and shorter medullary canal (Paraskevas et al., 2010). This may pose a risk for secondary fractures in intramedullary fixation,

which requires insertion of a rod or nail bridging the fracture site to enhance stability (Keating, 2013).

The present study tested the hypothesis that the medullary canal width is smaller in STA humeri. We explored the association of the STA status with medullary canal width. To account for the effect of bone size, we investigated whether differences exist with respect to the STA status in the medullary canal proportion to the humeral width, and also when standardized by humeral length. Further, we investigated population and sex-based variability in the relationship of STA presence and medullary canal width as a proportion of cortical bone widths after stratifying by age. Cortical bone quality deteriorates after 60 years and does so differently for males and females (Laval-Jeantet et al., 1983).

4.2 MATERIALS AND METHODS

4.2.1 Sample

A total of 1097 dry humeri from 552 skeletonized individuals was used for a case-control study where 242 individuals had STA and 312 lacked the aperture. A limited portion of the total sample did not have both humeri present (Table 4.1). The sample includes bones from Whites (individuals of European descent, n=113), the Mixed population (descendants of Whites, Blacks and Khoisan, n=221) (Akagi et al., 2010), and Blacks (indigenous South Africans, n=218). The age range was from 18 – 100 years and the humeri were grouped by age cohorts (Table 4.2). Only bones with epiphyseal fusion were included. Individuals are from the Raymond A Dart Collection of Human Skeletons housed at the University of the Witwatersrand School of Anatomical Sciences (Dayal et al., 2009), the University of Cape Town, the University of Stellenbosch and the University of Pretoria (L'Abbe et al., 2005). The bones were free of pathology and pre- or postmortem damage. Features of bone healing, such as a callus, were used to identify premorterm damage, whereas visible trabeculae indicated postmorterm trauma.

Table: 4.1. STA status of the sample

STA status					
		Individuals	Humeri		Total humeri*
			Both sides	Single side	
STA	No	312	308	4	620
	Yes	240	237	3	477
	Total	552	547	7	1097
Population affiliation					
Population	White	113	112	1	225
	Mixed	221	216	5	437
	Black	218	217	1	435
	Total	552	547	7	1097

*Total humeri was obtained by multiplying the both sides column by 2 and adding the single side column.

Table 4.2: Age profile by population, sex and STA status

		STA					No STA				
Population	Sex	<30	30-45	46-60	61-75	>75	<30	30-45	46-60	61-75	>75
White	Male	0	1	15	15	7	2	3	29	39	13
	Female	0	0	3	20	13	0	0	9	29	27
	Total	0	1	18	35	20	2	3	38	68	40
Mixed	Male	14	30	29	10	2	14	44	41	49	6
	Female	27	27	22	5	3	15	45	32	17	9
	Total	37	57	51	15	5	29	89	73	66	15
Black	Male	16	20	24	25	3	16	38	43	45	5
	Female	7	35	18	22	1	13	35	26	38	5
	Total	23	55	42	47	4	29	73	69	83	10

4.2.2 Radiography and measurement procedures

A Lodox Statscan was used to produce the images. The radiographs were taken anteroposteriorly (AP) with the humeri positioned on the platform in pairs belonging to the same individual. A list with the sequence of identification numbers (codes) was used for the sequential positioning to simplify the referencing and bone identification. Each radiograph contained 16 humeri belonging to 8 individuals. In cases where a bone

was missing, a space for that humerus was left in order to prevent mismatches when referring to the list of identification numbers. South African 10 cent coins were placed distal to the pairs of humeri for calibration with the image processing software (Image J®) prior to taking measurements. The metric value of the diameter of the coin was used to set the scale. In this way, the diameter of the coin represented a standardized distance when measuring the radiographed humeri. The humeral measurements taken are given in Table 4.3. The medullary canal width was standardized by bone length as follows: $\frac{\text{medullary canal width/}}{\text{humeral length}} * 100$.

4.2.3 Statistics

The data were managed in Microsoft Excel 2007 (Microsoft Corporation) and analyzed using SPSS® version 22 (IBM®). Parametric tests (student t-test and ANOVA) were used for normally distributed variables. Post hoc (Tukey) tests were used for multiple comparisons of means. The Kruskal Wallis test was used for non-parametric variables. The significance level was $p<0.05$.

Table 4.3: Measurements taken from the radiographs

Variable	Description
Humeral length	Maximum length from the most superior point of the humeral head to the most distal point of trochlea
Humeral shaft diameter: (25th percentile mark) - Proximal	Maximum diameter at the 25th percentile mark of the shaft.
Humeral shaft diameter: (50th percentile mark) - Midshaft	Diameter at the shaft midpoint.
Humeral shaft diameter: (75th percentile mark) - Distal	Diameter at the 75th percentile mark of the shaft.
Medullary canal width (25th percentile mark) - Proximal	Diameter of the canal at the 25th percentile shaft mark.
Medullary canal width: (50th percentile mark) - Midshaft	Maximum diameter of the canal at the shaft midpoint.
Width of medullary canal: (75th percentile mark) - Distal	Maximum diameter of the canal at the 75th percentile shaft mark
Shaft cortical thickness: (25th percentile mark) - Proximal	Maximum distance from medial/lateral border of shaft to medial/lateral border of canal at the 25th percentile mark.
Shaft cortical thickness: (50th percentile mark) - Midshaft	Maximum distance from medial/lateral border of shaft to medial/lateral border of canal at the midpoint of canal.
Shaft cortical thickness: (75th percentile mark) - Distal	Maximum distance from medial/lateral border of shaft to medial/lateral border of canal at the 75th percentile mark.
Medullary canal width proportion: (25th percentile mark) - Proximal	(Medullary canal width/ humeral width)*100 at the 25th percentile mark of the shaft.
Medullary canal width proportion: (50th percentile mark) - Midshaft	(Medullary canal width/ humeral width)*100 at the midshaft
Medullary canal width proportion (75th percentile mark) - Distal	(Medullary canal width/ humeral width)*100 at the 75th percentile mark of the shaft.

4.3 RESULTS

4.3.1 Humeral width

In the proximal shaft region, the greatest humeral width was observed among White males and females when the STA was present or absent ($p<0.001$ for all groups) (Fig. 4.2A).

Whites also had greater humeral widths for the midshaft ($p<0.001$) (Table 4.4). Among males, the midshaft diameter was greatest in Whites whether the STA was present or absent ($p<0.01$ for Whites vs. Black or the Mixed group) (Table 4.4; Fig. 4.2). Among females, Blacks had the greatest midshaft diameter when the STA was present, although significant differences were only detected between the Mixed and Blacks ($p=0.02$). In contrast, the midshaft diameter was greatest in Whites when the STA was absent ($p<0.001$ for Whites vs. Black or the Mixed group) (Fig. 4.2B).

In the distal humerus, Blacks had a significantly greater width than Whites or the Mixed population irrespective of sex or STA status ($p<0.001$) (Table 4.4; Fig. 4.2C). Notably, there were no significant differences in the distal region humeral width between Whites and the Mixed population ($p=0.99$).

Table 4.4: Proximal, midshaft, and distal humeral width

Mean ($\bar{X}$) and standard deviation (SD) in millimeters for each population stratified by sex and STA status.

Shaft Region	Sex	STA	White			Mixed			Black		
			N	$\bar{X}$	SD	N	$\bar{X}$	SD	N	$\bar{X}$	SD
Proximal	Male	Yes	38	22.49	2.28	85	20.94	2.25	88	21.76	2.01
		No	86	23.34	1.99	154	21.94	2.46	147	22.78	2.02
		Total	124	23.08	2.11	239	21.59	2.43	235	22.40	2.07
	Female	Yes	36	19.49	1.58	84	18.64	2.24	83	19.11	1.69
		No	65	20.77	2.22	118	19.39	2.43	117	19.57	2.04
		Total	101	20.31	2.10	202	19.07	2.38	200	19.38	1.91
	All Groups		225	21.84	2.52	441	20.44	2.71	435	21.01	2.50
Midshaft	Male	Yes	38	21.77	2.41	83	20.52	2.70	88	20.70	1.92
		No	86	22.58	2.37	154	20.74	2.12	147	21.96	2.10
		Total	124	22.33	2.40	239	20.66	2.34	235	21.49	2.12
	Female	Yes	36	18.28	1.46	82	17.76	2.18	83	18.47	1.77
		No	65	20.05	2.39	118	18.32	2.23	117	18.85	2.16
		Total	101	19.42	2.27	202	18.09	2.22	200	18.70	2.01
	All Groups		225	21.03	2.75	441	19.48	2.62	435	20.20	2.49
Distal	Male	Yes	38	21.81	2.81	85	22.03	3.18	88	23.89	2.50
		No	86	23.50	3.06	154	23.40	3.42	147	24.65	2.66
		Total	124	22.98	3.08	239	22.91	3.39	235	24.37	2.62
	Female	Yes	36	18.89	2.08	84	19.31	2.66	83	20.35	1.99
		No	65	19.94	2.64	118	20.09	2.66	117	21.28	2.77
		Total	101	19.56	2.50	202	19.77	2.68	200	20.89	2.52
	All Groups		225	21.45	3.30	441	21.47	3.46	435	22.77	3.10

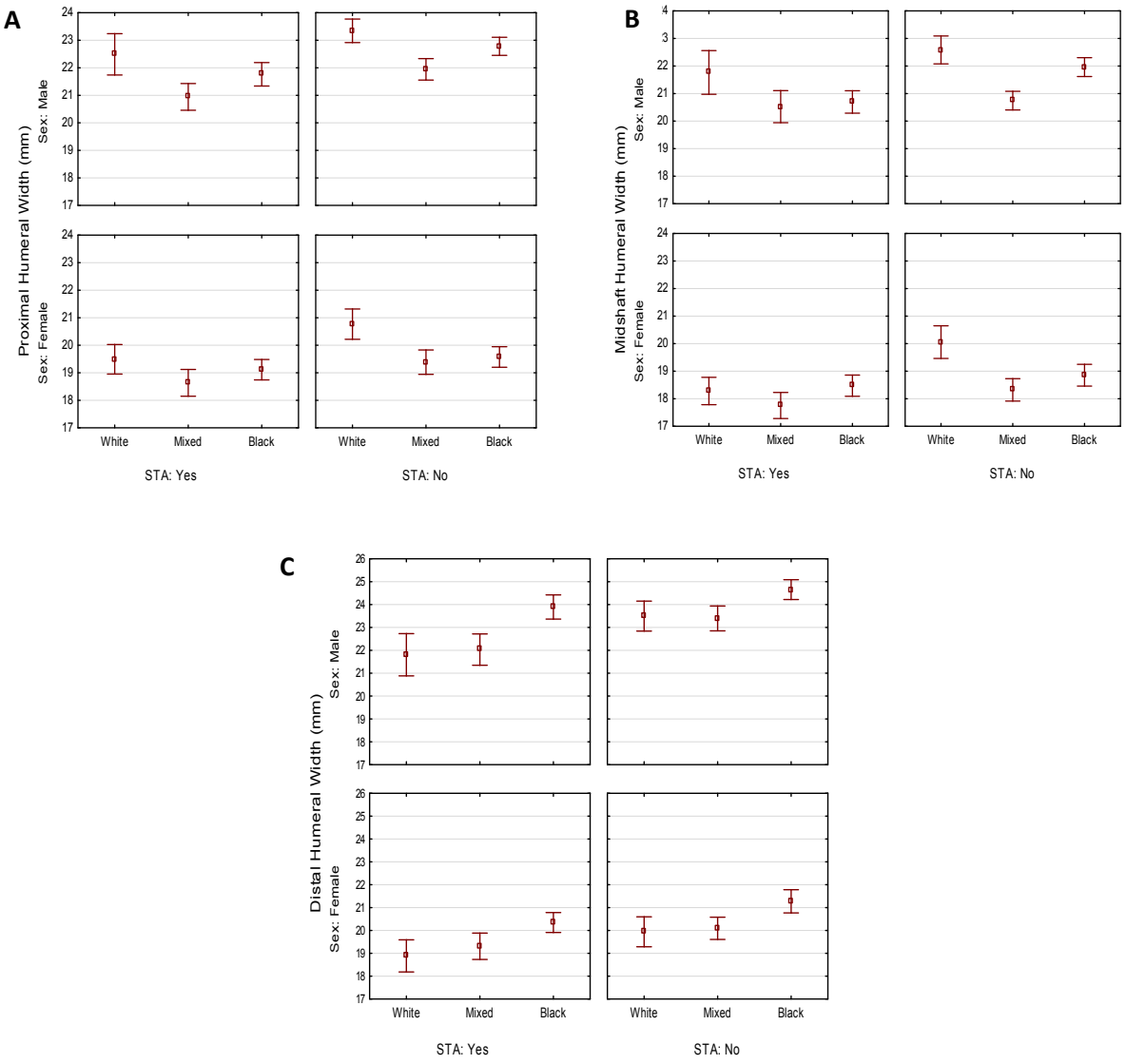


Figure 4.2: Width of the humerus
The mean and 95% confidence interval in the proximal (A), midshaft (B) and distal (C) regions in males and females for each population with and without the STA.

4.3.2 Medullary canal width

In the proximal shaft, the medullary canal width was smaller when the STA was present in all three populations ($p<0.001$). In both males and females, the canal width was greater for Whites than for Blacks or the Mixed group in the proximal segment irrespective of STA status (Table 4.5; Fig. 4.3A). However, no significant differences were found among males when the STA was present (p=.0.54).

In the midshaft, the medullary canal width was smaller when the STA was present although significance was only detected in the Mixed group and Blacks ($p<0.001$ for both groups). However, both male and female Whites had greater medullary canal widths than their Black or the Mixed group counterparts irrespective of STA status although no significant differences were found among males when the STA was present (p=.0.07) (Table 4.5; Fig. 4.3B).

In the distal shaft, the medullary canal width was smaller when the STA was present although significance was only detected in the Mixed group and Blacks ($p=0.001$ and $p=0.01$, respectively). In this region, the canal width was greatest in Black males whether the STA was present or absent. However significance was only detected in the Mixed group vs. Blacks ($p=0.02$). When the STA was present and when it was absent, only the Black vs. Whites did not show significant differences ($p=0.98$ for both) (Table 4.5; Fig. 4.3C).

Table 4.5: Proximal, midshaft, and distal medullary canal width
Means ($\bar{X}$) and standard deviations (SD) in millimeters for each population stratified by sex and STA status.

Shaft Region	Sex	STA	White			Mixed			Black		
			N	$\bar{X}$	SD	N	$\bar{X}$	SD	N	$\bar{X}$	SD
Proximal	Male	Yes	38	15.23	2.73	85	13.94	2.55	88	14.63	2.41
		No	86	16.66	2.48	154	15.19	2.69	147	15.71	2.34
		Total	124	16.22	2.63	239	14.75	2.70	235	15.31	2.42
	Female	Yes	36	13.83	2.10	84	11.99	2.31	83	12.88	2.06
		No	65	14.58	2.65	118	12.83	2.53	117	13.41	2.33
		Total	101	14.31	2.48	202	12.48	2.47	200	13.19	2.23
	All Groups		225	15.36	2.73	441	13.71	2.83	435	14.34	2.56
Midshaft	Male	Yes	38	11.36	2.08	83	10.44	2.51	88	10.55	1.88
		No	86	11.86	2.34	154	10.68	2.21	147	11.31	2.10
		Total	124	11.71	2.27	239	10.59	2.32	235	11.03	2.05
	Female	Yes	36	10.87	1.68	82	8.90	2.08	83	10.11	2.02
		No	65	11.46	2.76	118	9.76	2.19	117	10.44	2.29
		Total	101	11.25	2.44	202	9.40	2.19	200	10.30	2.18
	All Groups		225	11.50	2.35	441	10.05	2.33	435	10.69	2.14
Distal	Male	Yes	38	10.33	1.95	85	9.90	2.19	88	10.74	1.83
		No	86	11.19	2.14	154	10.56	2.47	147	11.26	1.96
		Total	124	10.92	2.11	239	10.32	2.39	235	11.06	1.93
	Female	Yes	36	10.51	1.50	84	8.89	1.94	83	10.30	2.10
		No	65	10.40	1.96	118	9.60	1.97	117	10.68	2.30
		Total	101	10.44	1.80	202	9.30	1.98	200	10.52	2.22
	All Groups		225	10.71	1.99	441	9.86	2.27	435	10.81	2.08

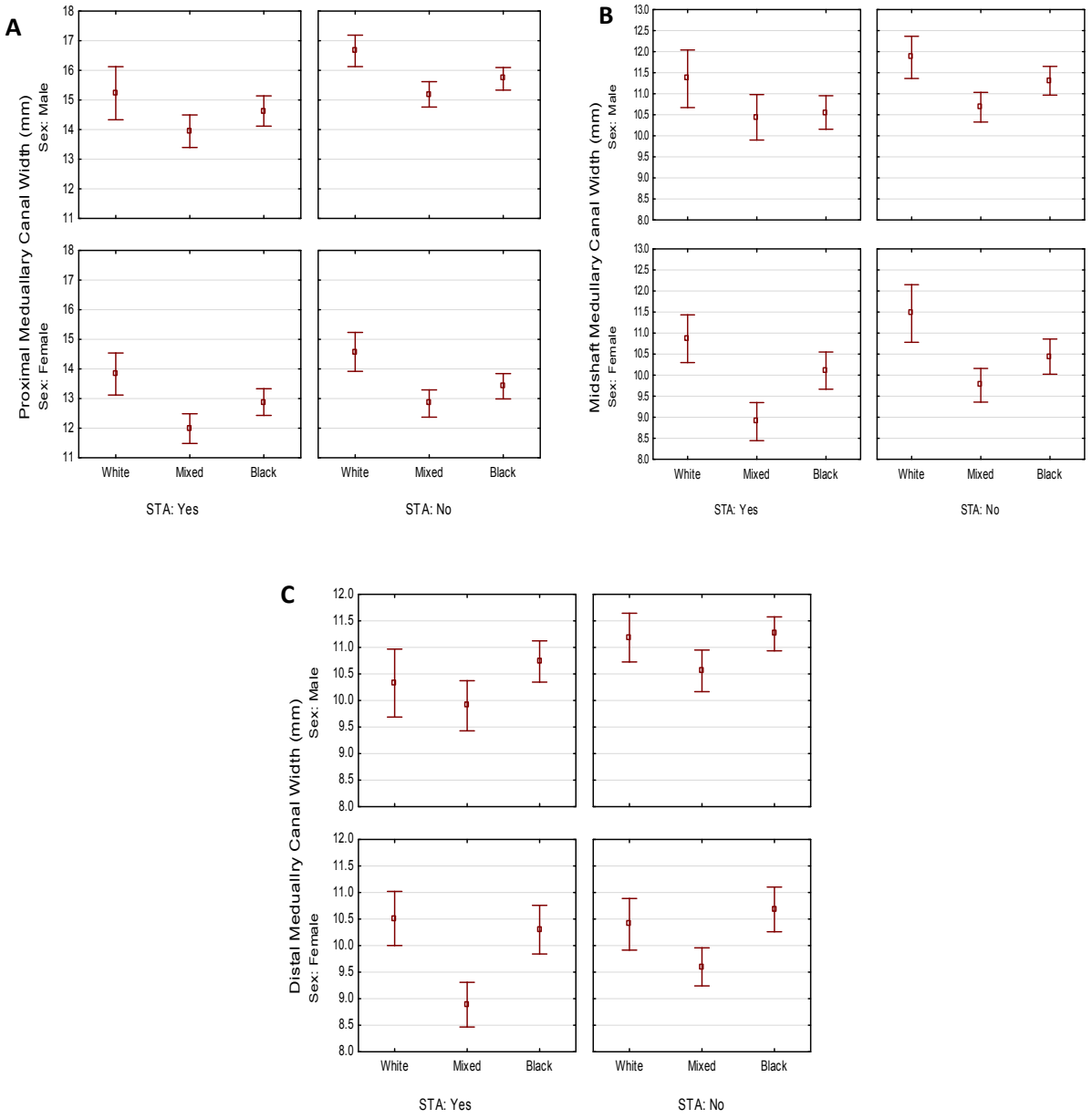


Figure 4.3: The medullary canal
The mean and 95% confidence interval in the proximal (A), midshaft (B) and distal (C) regions in males and females for each population group with and without the STA are given.

4.3.3 Medullary canal width differences stratified by age and STA status

Whites

White individuals below the age of 45 were not included in this analysis as they were too few in number (Table 4.2). Among White males the medullary canal width was smaller when the STA was present in all age cohorts. However, significant differences were only detected in the proximal shaft region for individuals aged 46-60 years (p=0.03) and in the proximal (p=0.01) and midshaft regions (p=0.03) for those older than 75 years (Fig. 4.4). No significant differences were found in medullary canal width in individuals aged 61-75 years stratified by STA status and sex. In females aged 46-60, the medullary canal width was greater for STA cases in the distal shaft segment (p=0.002). It was also significantly greater in the proximal region when the STA was present among females over 75 years of age (p=0.002). In the midshaft and distal regions, it was also significantly greater when the STA was absent (p=0.02; p=0.04, respectively) (Fig. 4.4).

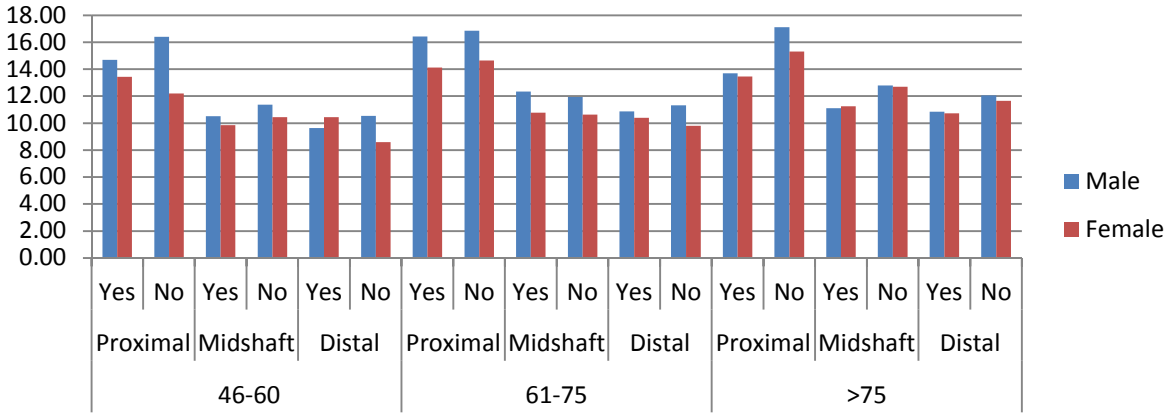


Figure 4.4: Differences in mean medullary canal width in Whites by humeral shaft region, stratified by STA status and age

Mixed ethnic group

Mixed ethnicity males below 46 years of age had similar medullary canal widths when the STA was present or absent in all three shaft regions. The medullary canal width in males was smaller when the STA was absent for individuals over 45 years but not exceeding 75 years (Fig. 4.5). However, statistical significance was only detected in the proximal region for males aged 46-60 and in the proximal and midshaft regions for individuals aged 61-75 years ($p=0.01$; $p=0.001$; $p=0.03$, respectively). No significant differences were detected for males before age 45 or over 75 ($p=>0.05$ for all regions). No significant differences in female medullary canal widths were detected in all shaft regions for all age cohorts when the STA was present or absent ($p>0.05$) (Fig. 4.5).

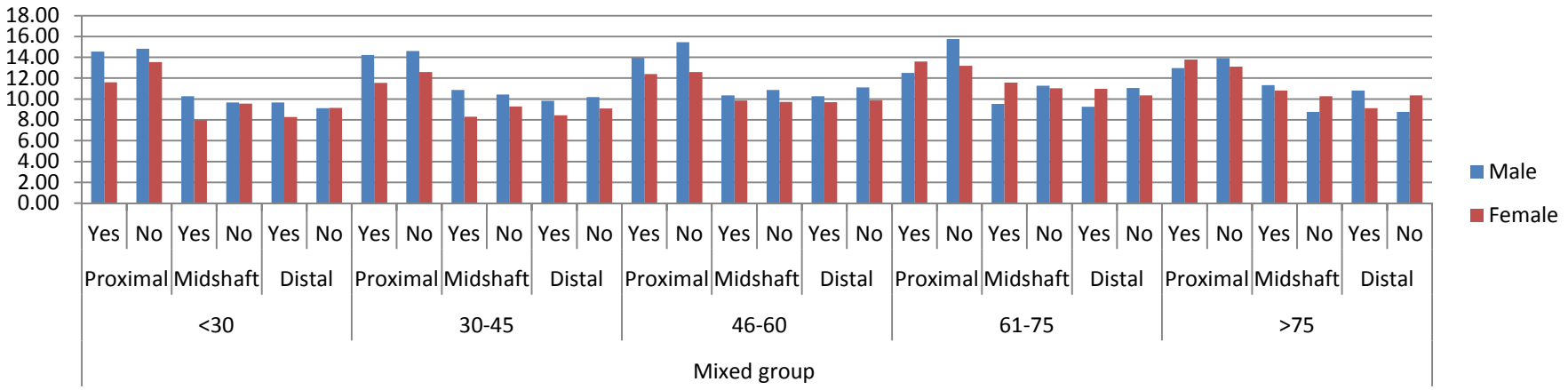


Figure 4.5: Differences in mean medullary canal width in the Mixed group by humeral shaft region, stratified by STA status and age.

Blacks

For Black males below age 30, the medullary canal width was smaller when the STA was present although significance was only found for the proximal and midshaft regions (p=0.02 and p=0.03, respectively) (Fig. 4.6). No significant differences were detected in the medullary canal width by STA status among individuals aged 30-45 years. For individuals aged 46-60, the medullary canal width was smaller when the STA was present although significance was only detected in the proximal and midshaft regions (p=0.02 and p=0.03, respectively). Among individuals aged 61-65 years, significance was only found for the proximal region (p=0.03), whereas no significant differences were detected in the medullary canal width by STA status among individuals over 75. The females had no significant differences in medullary canal widths according to STA status in all shaft regions for all age groups (p>0.05) (Fig. 4.6).

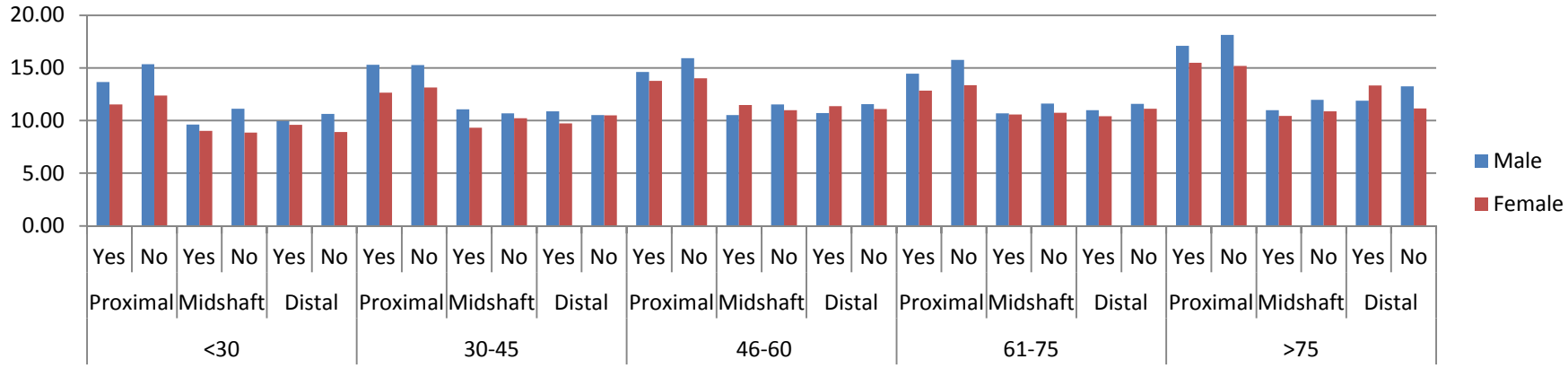


Figure 4.6: Differences in mean medullary canal width in Blacks by humeral shaft region, stratified by STA status and age

4.3.4 Standardized comparisons of medullary canal width

The medullary canal width was standardized using two humeral variables to control for size effects. These included using the canal width as a proportion of the humeral width in the different shaft regions and using a canal width to total humeral length index.

Medullary canal width as a proportion of humeral width

In the proximal shaft region, the medullary canal width proportion was significantly greater when the STA was absent among males of all groups (White, $p=0.01$; Mixed, $p<0.001$; Blacks, $p=0.03$) (Table 4.6). Among females, the medullary canal width proportion for the proximal and midshaft regions was significantly smaller when the STA was present for only the Mixed group ($p<0.04$; $p=.0.01$, respectively). In the distal aspect, no significant differences were detected in both males and females among all three groups.

Table 4.6: Proportion of the medullary canal width to cortical bone thickness by population, and further stratified by sex and STA status

Medullary canal proportion	STA	N	Whites								
			Males					Females			
			$\bar{X}$	SD	t	p value	N	$\bar{X}$	SD	t	p value
Proximal	Yes	38	67.44	8.01	2.81	0.01	36	70.72	6.90	-0.53	0.60
	No	86	71.07	5.94			65	69.87	7.98		
Midshaft	Yes	38	52.31	8.44	0.03	0.97	36	59.29	6.90	-1.21	0.23
	No	86	52.37	7.84			65	56.95	10.44		
Distal	Yes	38	47.59	8.54	0.08	0.94	36	55.84	7.42	-1.89	0.06
	No	86	47.71	7.60			65	52.47	9.18		
			Mixed								
Proximal	Yes	83	66.21	7.14	2.92	<0.001	82	63.91	6.67	2.02	0.04
	No	154	68.92	6.72			118	65.95	7.32		
Midshaft	Yes	83	50.49	7.90	0.67	0.50	82	49.89	8.92	2.54	0.01
	No	154	51.18	7.45			118	52.96	8.14		
Distal	Yes	83	44.80	7.09	0.21	0.83	82	46.09	8.43	1.46	0.14
	No	154	45.01	7.36			118	47.75	7.56		
			Blacks								
Proximal	Yes	88	66.90	6.41	2.23	0.03	83	67.12	6.31	1.14	0.25
	No	147	68.76	6.03			117	68.19	6.68		
Midshaft	Yes	88	50.85	6.60	0.54	0.59	83	54.58	8.89	0.42	0.67
	No	147	51.36	7.24			117	55.11	8.79		
Distal	Yes	88	44.92	5.82	0.94	0.35	83	50.49	8.15	-0.38	0.70
	No	147	45.72	6.69			117	50.07	7.55		

Medullary canal width as a proportion of humeral width by age and population affiliation

Whites males had a smaller medullary canal width proportion when the STA was present for individuals aged 46-60 (p=0.04 for the proximal region) (Fig. 4.7). No significant differences were detected for age ranges greater than 60 years in all three shaft regions. In White females, significant differences were only detected in the proximal shaft region for individuals aged 46-60 years (p=0.03).

Among Blacks and individuals of the Mixed group, the medullary canal width did not differ according to STA status in all age ranges for both males and females (p>0.05 for all) (Figs. 4.8 and 4.9).

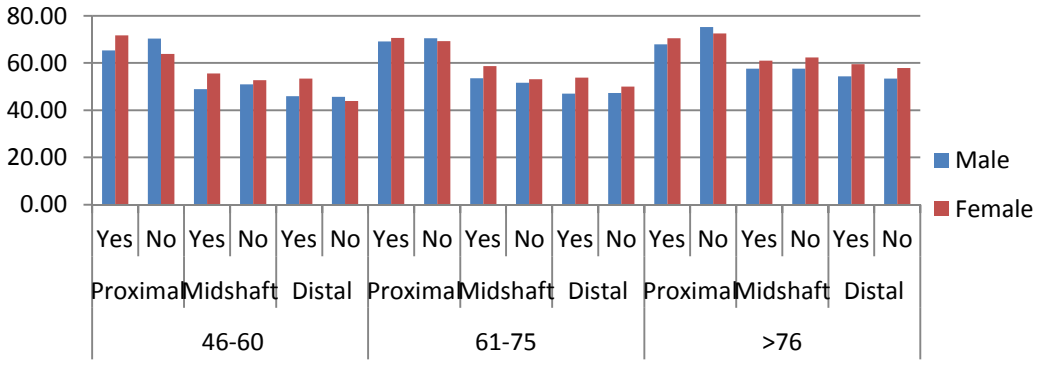


Figure 4.7: Differences in mean medullary canal proportion in Whites by humeral shaft region, stratified by STA status and age

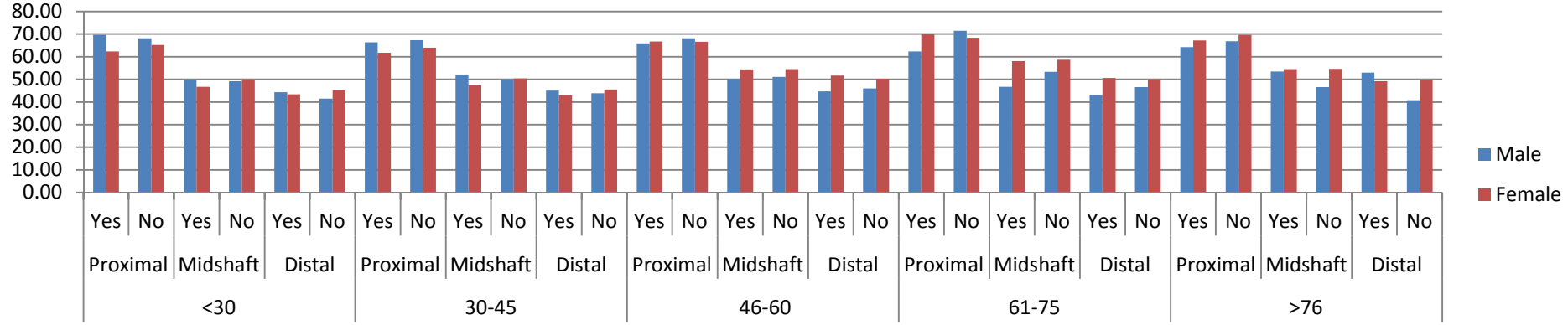


Figure 4.8: Mean differences in medullary canal width proportion in the Mixed group by humeral shaft region, stratified by STA status and age

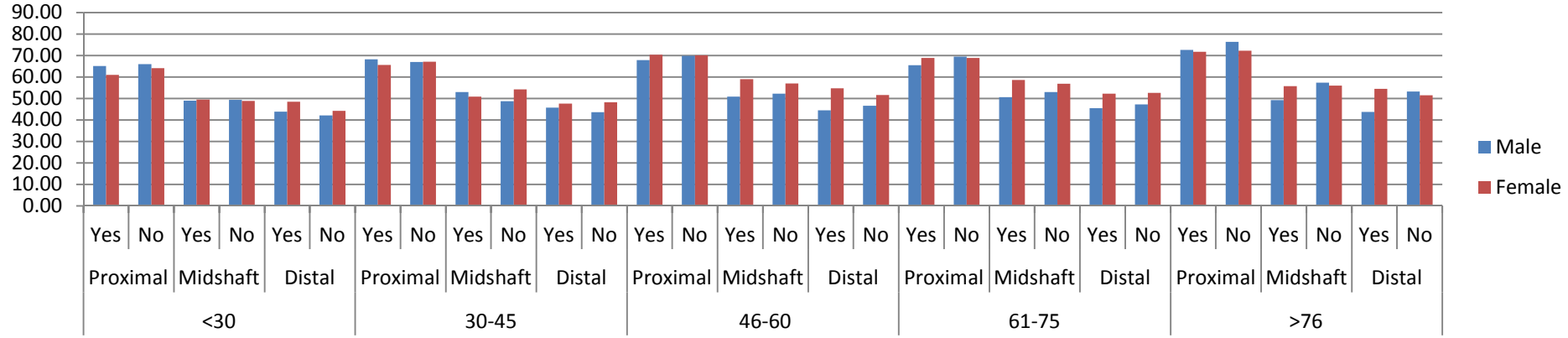


Figure 4.9: Mean differences in medullary canal width proportion in Blacks by humeral shaft region, stratified by STA status and age

Medullary canal width standardized by humeral length

When the medullary canal width was standardized by humeral length in individuals aged 46-60, there were no population differences irrespective of STA status among the males. For females, the medullary canal width was significantly smaller in Whites when the STA was absent (p=0.02 White vs. Mixed; and p=0.003 Whites vs. Blacks).

Among males, the standardized medullary canal width for both the proximal and distal regions was smaller when the STA was present. However, significance was only detected for the Mixed group in the proximal (p=0.03) and distal regions (p=0.02). In females, only Whites showed significantly smaller standardized medullary canal widths in the distal region (p=0.04) (Fig. 4.10).

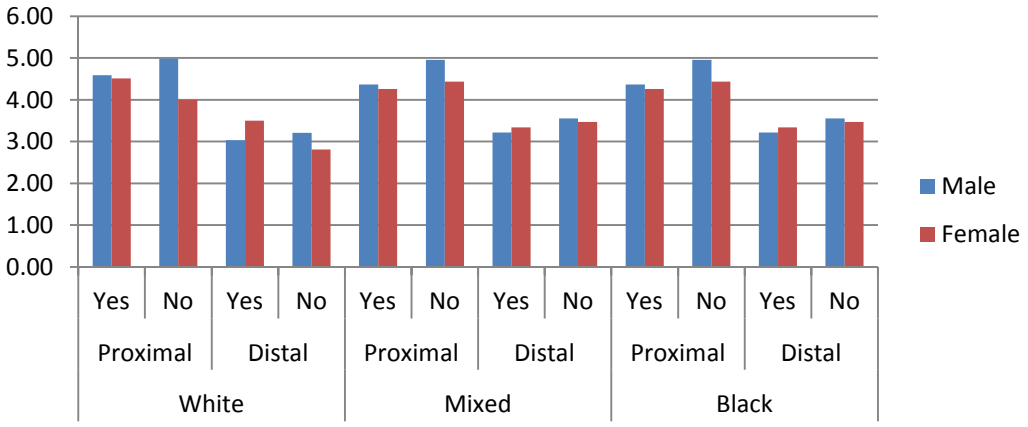


Figure 4.10: Standardized mean medullary canal width proportion in the proximal and distal shaft regions for combined age cohorts 46-60, stratified by population and STA status

4.3.5 Correlation of humeral medullary canal width and cortical thickness

Whites

White males and females aged below 46 years with the STA were excluded from this analysis due to sample size limitations (Table 4.2).

In the proximal shaft region, males with the STA showed a strong negative correlation between the medullary canal width and cortical bone thickness. When the STA was absent, significant differences were not detected for males aged 30-45 years and those over 75 ($p=0.66$ and $p=0.43$, respectively). White females with the STA also had a strong negative correlation between the variables, although significance was only detected for individuals aged 61-75 ($p<0.001$) (Table 4.7). In contrast, when the STA was absent, only females greater than 75 years of age did not have a correlation between the medullary canal width and the cortical bone thickness ($p=0.66$).

In the midshaft a strong negative correlation was also observed, although significance was only detected for individuals aged 61-75 when the STA was present or absent ($p=0.04$ and $p=0.002$, respectively). Similarly, in females with and without the STA, significance was only found for individuals aged 61-75 ($p=0.016$ and $p=0.011$, respectively). In contrast, no significant differences were detected in the distal region for the correlation of the medullary canal width and the cortical bone thickness among all age ranges in both sexes with or without the STA (Table 4.7).

Table 4.7: Spearman's correlation for the cortical thickness (CT) and medullary canal width (MCW) by age cohorts and further stratified by STA status in Whites

		White												
		Male							Female					
		Cortical thickness (CT)							Cortical thickness (CT)					
		STA			No STA				STA			No STA		
		46-60	61-75	>75	30-45	46-60	61-75	>75	46-60	61-75	>75	46-60	61-75	>75
MCW Proximal	Correlation	-.817	-.577	-.793	-.500	-.571	-.728	-.236	.500	-.809	-.224	-.840	-.662	.087
	p value	.000	.024	.033	.667	.001	<.001	.438	.667	<.001	.461	.005	<.001	.665
	N	15	15	7	3	29	39	13	3	20	13	9	29	27
MCW Midshaft	Correlation	-.460	-.521	.455	.500	-.551	-.185	-.083	-1.000	-.532	-.023	-.617	-.464	-.322
	p value	.084	.046	.305	.667	.002	.260	.786		.016	.939	.077	.011	.101
	N	15	15	7	3	29	39	13	3	20	13	9	29	27
MCW Distal	Correlation	-.418	-.325	-.357	-.866	-.124	.114	-.246	-.500	-.178	.065	-.395	-.182	.041
	p value	.121	.237	.432	.333	.520	.491	.418	.667	.452	.833	.293	.346	.840
	N	15	15	7	3	29	39	13	3	20	13	9	29	27

Mixed

Mixed group individuals older than 75 were excluded from the analysis as they were too few in number (Table 4.2).

In the proximal shaft region, Mixed males showed a negative correlation between the medullary canal width and cortical bone thickness for all age ranges when the STA was present or absent. These correlations were only significant for males aged 46-60 and those aged 61-75 when the STA was present or absent ($p<0.05$) (Table 4.8). Mixed females with the STA only showed significant differences for individuals aged 30-45 years. In contrast, when the STA was absent, only females aged 61-75 did not show significance ($p=0.81$).

In the midshaft region, there was no significant correlation between medullary canal width and cortical bone thickness when the STA was present. However, when the STA was present significance was detected for individuals aged 61-75 years and those over 75 ($p=0.001$ and $p=0.008$ respectively. Among females with the STA, significance was only detected for those aged 46-60 ($p=0.001$). When the STA was absent, only individuals aged 30-45 years and 46-60 years showed a significant correlation between the variables ($p=0.024$ and $p=0.009$, respectively). In the distal shaft region, no significant differences were detected except for males aged 46-60 with the STA ($p=0.01$) (Table 4.8).

Table 4.8: Spearman's correlation for the cortical thickness (CT) and medullary canal width (MCW) by age cohorts and further stratified by STA status among individuals of the Mixed group

Mixed group

		Male									Female									
		Cortical thickness (CT)									Cortical thickness (CT)									
		STA				No STA					STA					No STA				
		<30	30-45	46-60	61-75	<30	30-45	46-60	61-75	>75	<30	30-45	46-60	61-75	>75	<30	30-45	46-60	61-75	>75
MCW Proximal	Correlation	-.466	-.182	-.637	-.821	-.395	-.206	-.438	-.526	-.725	-.176	-.422	-.378	-.700	.500	-.626	-.340	-.514	-.063	-.723
	p value	.093	.335	<.001	.004	.163	.179	.004	<.001	.103	.379	.028	.083	.188	.667	.012	.022	.003	.811	.028
	N	12	30	29	10	14	44	41	49	6	25	27	22	5	3	15	45	32	17	9
MCW Midshaft	Correlation	.182	-.132	-.209	-.612	-.459	-.283	-.124	-.452	-.928	-.203	-.333	-.672	-.872	.500	.211	-.337	-.312	-.612	-.100
	p value	.534	.487	.277	.060	.099	.063	.441	.001	.008	.309	.090	.001	.054	.667	.451	.024	.082	.009	.798
	N	12	30	29	10	14	44	41	49	6	25	27	22	5	3	15	45	32	17	9
MCW Distal	Correlation	.409	.176	-.455	-.164	-.033	.283	.147	.004	-.486	.053	-.275	-.275	-.700	1.00	.057	-.224	-.189	-.196	.378
	p value	.147	.352	.013	.650	.911	.063	.361	.978	.329	.794	.166	.215	.188		.839	.138	.299	.451	.316
	N	12	30	29	10	14	44	41	49	6	25	27	22	5	3	15	45	32	17	9

Blacks

Black females over 75 with the STA were excluded from the analysis because of the small sample (Table 4.2).

In the proximal shaft region, Black males and females showed a strong negative correlation between the medullary canal width and cortical bone thickness irrespective of STA status. Only individuals younger than 30 years and those older than 75 did not show a significant correlation (Table 4.9). When the STA was absent in both sexes, only individuals over 75 did not show a significant correlation (Table 4.9).

In the midshaft, Black males younger than 30 years with the STA had no correlation between medullary canal width and cortical bone thickness. For the ages greater than 30, a negative correlation was observed. However, significance was only detected for individuals aged 30-45 years and those aged 56-60 ($p=0.034$ and $p<0.001$, respectively). When the STA was present, a significant correlation was only detected for individuals aged 61-75 ($p<0.001$). In females, the pattern of a negative correlation was observed. However, when the STA was present, significance was not detected for individuals before the age of 30 ($p=0.45$). In contrast, when the STA was absent, significance was only detected for individuals aged 45-60 years and 61-75 years ($p=0.001$ and $p=0.013$, respectively).

In the midshaft and the distal shaft regions, males less than 30 years of age had no correlation between the variables irrespective of STA status

(Table 4.9). Among individuals over 30 years, a negative correlation was observed although significance was only detected for individuals with the STA aged 46-60 ($p=0.03$). In females, a significant correlation was only detected for individuals over 46 years of age ($p<0.001$).

Table 4.9: Spearman's correlation for the cortical thickness (CT) and medullary canal width (MW) by age cohorts and further stratified by STA status in Blacks

		Blacks																		
		Male										Female								
		Cortical thickness (CT)										Cortical thickness (CT)								
		STA					No STA					STA				No STA				
		<30	30-45	46-60	61-75	>75	<30	30-45	46-60	61-75	>75	<30	30-45	46-60	61-75	<30	30-45	46-60	61-75	>75
MCW Proximal	Correlation	-.410	-.538	-.489	-.485	-.500	-.658	-.656	-.324	-.471	-.700	-.721	-.468	-.675	-.522	-.242	-.361	-.828	-.350	.500
	p value	.114	.015	.015	.014	.667	.006	<.001	.034	.001	.188	.068	.005	.002	.013	.426	.033	<.001	.031	.391
	N	16	20	24	25	3	16	38	43	45	5	7	35	18	22	13	35	26	38	5
MCW Midshaft	Correlation	.077	-.476	-.689	.302	-.500	-.176	-.298	-.273	-.505	-.667	-.342	-.373	-.709	-.502	0.000	-.534	-.482	-.310	-.667
	p value	.777	.034	<.001	.142	.667	.513	.070	.077	<.001	.219	.452	.028	.001	.017	1.000	.001	.013	.059	.219
	N	16	20	24	25	3	16	38	43	45	5	7	35	18	22	13	35	26	38	5
MCW Distal	Correlation	.030	-.202	-.437	.285	-.500	-.064	-.173	-.224	-.175	-1.000	-.739	-.069	-.740	-.745	-.131	-.099	.125	-.137	-.700
	p value	.913	.393	.033	.167	.667	.813	.299	.149	.249		.058	.695	.000	.000	.669	.570	.543	.410	.188
	N	16	20	24	25	3	16	38	43	45	5	7	35	18	22	13	35	26	38	5

4.4 DISCUSSION

The present study tested the premise that the medullary canal width is smaller in humeri with STA. To do this, we compared the humeral and medullary canal widths and cortical bone thickness at three points along the diaphysis, Comparisons were made between males and females in three SA populations, controlling for general bone size differences. In addition, as cortical bone thickness and consequently medullary canal size are known to change over the life course, the analyses involving those variables were conducted using age cohorts

The medullary canal width was narrower in STA bearing individuals of all groups. Its proportion to bone width was smaller in STA cases among males in all three shaft regions for all populations, although statistical significance was only detected in the proximal shaft region. In females, statistical significance was only detected in the Mixed group for the proximal and distal regions. When standardized by bone length, the medullary canal width was similar when the STA was present or absent in all groups. The age-adjusted relationship of cortical bone thickness and medullary canal width varied by shaft region; most significant correlations were detected in the proximal shaft and in males. Only females of the Mixed ethnic group showed significant correlations between medullary canal width and humeral width in the proximal and midshaft regions.

4.4.1 Medullary canal width

Nayak et al. (2009) reported that bones bearing the STA have a smaller medullary canal width. We had similar findings in the present study, with

STA bones having a smaller medullary canal width. We also noted that Whites generally had greater humeral and medullary canal widths and that males of all three populations had greater humeral and medullary canal widths. As bone size was greater in Whites and among males irrespective of population affiliation, this indicates that general bone size is the main determinant of medullary canal width. Therefore, we propose that the medullary canal width is smaller in STA bones because of their relatively smaller size and not as a direct influence of the STA.

In the present study, there were population differences in the medullary canal width by sex and STA status. In Whites, a greater medullary canal width was generally observed for the proximal shaft region in males and females over 45 years of age. In contrast, no age differences in medullary canal width were detected, irrespective of sex and STA status, among Blacks and individuals of the Mixed group in all the shaft regions. Cortical bone density is known to decrease faster in elderly females (Parfitt, 1984). The loss of cortical bone would result in an increase in relative medullary canal width with age. This was not the case in our study likely due to loss of cortical bone density (Mays, 1996) and not affecting the actual dimensions of the medullary canal.

Paraskevas et al. (2010) found the medullary canal width to be smaller in the distal shaft of STA humeri. These authors suggested that anterograde intramedullary fixation for repair of humeral shaft fractures may be more appropriate when the STA is present. In contrast, our results show no

significant differences in medullary canal width by STA status in the distal region. Therefore, we suggest that retrograde intramedullary fixation would be more appropriate for our sample, and by inference for SA populations.

Another point regarding medullary canal size and the implications for intramedullary fixation involves the supposition that the canal length is shorter in bones with the STA (Nayak et al., 2009). It was not possible to test this in our study due to the difficulties of establishing the superior and inferior boundaries of the canal. This is complicated by the presence of cancellous bone in those regions. Further research is needed that employs a definitive method for defining the canal, perhaps using a bone density cut point as the means for identifying the extent of the canal.

4.4.2 Medullary canal width standardized by bone width or length

When standardized by humeral length, the medullary canal width was smaller among Whites. This group also has greater humeral length, supporting our proposition that the medullary canal width is smaller in STA bones as an effect of smaller bone size. Although the proportion of the medullary canal width to humeral width was smaller when the STA was present among males in all three shaft regions for all populations, statistical significant was only detected in the proximal shaft region. In females, statistical significance was only detected in the Mixed group for the proximal and distal regions. The sex differences in the proportion of medullary canal width may be related to physiological differences in males and females. In males androgens increase bone formation whereas estrogens inhibit bone resorption in females (Bronner and Farach-Carson,

2004). It is possible that Black and White females have a balance of bone resorption and new bone formation irrespective of STA status. In order to maintain stability a collar of circumferential lamellar may be formed on the outer surface of the bone leading to increased robusticity (Pearson and Lieberman, 2004). The Mixed group females may be different due to genetic or occupational factors.

4.4.3 Correlation of medullary canal width and cortical bone thinness by age and sex

In both sexes of all three populations, a strong negative correlation of the medullary canal width with cortical bone thickness was observed for the proximal shaft region. However, this correlation was not significant for individuals after the age of 75 years in all groups. A negative correlation between the variables means that the medullary canal width increases as cortical bone thickness decreases. This is of course expected, and it would also be expected for this correlation to be stronger and more significant in the over 75 years cohort as cortical bone loss increases with age (Laval-Jeantet et al., 1983). Since our sample for individuals over 75 years was small, this may be why the expected statistical significance was not detected in this study

The relationship between cortical bone and the medullary canal varies along the length of the humerus. In the mid and distal shaft most age cohorts did not show a significant correlation between the two variables. This may be attributed to the shape of the bone in these regions and that the measurements were taken only in the mediolateral aspect. It is

possible that different results would have been obtained if it was possible to take the measurements in the anteroposterior aspect. Further studies using CT scans may be more appropriate for investigation of this relationship.

4.5 CONCLUSIONS

We did not find differences in the proportions of the medullary canal width with respect to STA status when bone size was factored in. Therefore, the smaller medullary canal width observed in STA humeri is due to bone size differences rather than the presence of the STA. Furthermore, there is no correlation between medullary canal width and cortical bone thickness among individuals after the age of 75 years, which suggests that the bone remodeling cycle is different for individuals of this age cohort. We propose that overall bone size, determined either by the humeral length or the diameter in the region where the break occurs, is the major factor to consider when choosing a rod for intramedullary fixation.

4.6 ACKNOWLEDGMENTS

We thank Nafeesah Karriem for permission to use the Lodox scanner and providing technical assistance at the University of Cape Town and Professor Wadee for permission to use the Lodox facility at the Department of Forensic Pathology, Stellenbosch University. We are very grateful to the following people for access to skeletal material: Brendon Billings for access to the Raymond A Dart Collection of Human Skeletons, Mandi Alblas for use of the University of Stellenbosch Bone Collection,

Professor Alan Morris for use the University of Cape Town Bone Collection, and Professor Ericka L'Abbé and Marius Loots for use of the Pretoria Bone Collection. Sovana Maharaj took measurements from the radiographs. We thank Dr T Esan for advice on statistical methods. Funding for the project came from the National Research Foundation (South Africa), University of the Witwatersrand Faculty Research Council, the Wits WHC dividend, and the J J J Smieszek Fellowship.

CHAPTER 5

The relationship between elbow extension angle and the supratrochlear aperture (STA)

Table of Contents

5.0 ABSTRACT 132
5.1 INTRODUCTION 133
5.2 MATERIALS AND METHODS 136
5.2.1 Sample 136
5.2.2 Procedure 137
5.2.3 Statistics 139
5.3 RESULTS 140
5.3.1 Repeatability 140
5.3.2 Extension Angle 140
5.3.3 Magnitude of Extension 142
5.3.4 Factors influencing the presence of the STA 144
5.3.5 Variables predicting the degree of elbow extension 147
5.4 DISCUSSION 149
5.5 CONCLUSIONS 152
5.6 ACKNOWLEDGEMENTS 152

5.0 ABSTRACT

Assessment of the range of motion at a joint is among the methods employed by orthopedic surgeons and physiotherapists to determine courses of therapy and joint recovery. Females tend to have a greater range of motion at the elbow joint than males. In the present case-control study, the elbow extension angle was compared between males and females with and without the supratrochlear aperture (STA). A total of 453 dry humeri and their corresponding ulnae were included in the study and elbow extension angle was measured using a goniometer. The average extension angle in this sample was 173^{o}, and it was significantly greater when the STA was present ($\bar{X}$=175.4^{o}) than when it was absent ($\bar{X}$=171^{o}). It was greater in females ($\bar{X}$=174.5^{o}) compared to males ($\bar{X}$=171.3^{o}) and was greater on the left in both sexes. Hyperextension characterized 13% of the sample whereas the majority (76%) showed hypoextension and only a few (11%) exhibited normal extension. Ulnar notch depth and olecrano-coronoid distance contributed toward predicting the presence of the STA while the transverse and vertical diameters of the STA contributed the most to the degree of extension. The functional benefits of hyperextension at the elbow joint are not fully understood. However, these results are important to orthopedic surgeons and physiotherapists in enhancing their understanding of normal elbow range of motion in the South African population.

5.1 INTRODUCTION

The range of motion at a joint is often used in clinical settings to obtain an impairment rating that aids in the determination of therapeutic, medical or surgical interventions as well as evaluating the success of those interventions (Gunal et al., 1996). At the elbow joint, motion is required for most activities of daily living such as combing hair, brushing teeth, or simply picking up a glass of water (De Groot et al., 2011; Vasen et al., 1995). Flexion and extension of the elbow are crucial to bringing the hand to a functional position (O'Neill et al., 1992). Even a seemingly simple task such as bringing a spoon from the plate to the mouth is impossible without elbow flexion (Magermans et al., 2005), and extension is required to return the spoon to the plate.

Numerous movements of upper limb joints such as scapular lateral rotation, glenohumeral elevation and pronation, and elbow flexion and extension are needed to perform daily activities (Magermans et al., 2005). A minimum elbow range of motion of 110^{o} is required for most activities (De Groot et al., 2011). For example, an elbow angle of 135.7^{o} is required for combing hair, and 131.5^{o} is needed for eating with a spoon (Magermans et al., 2005). In cases of limited joint mobility, compensatory motions are deployed to accomplish daily living tasks (De Groot et al., 2011; O'Neill et al., 1992; Vasen et al., 1995). For example, the wrist may compensate for impaired elbow motion (O'Neill et al., 1992). Correspondingly, impaired motion at the shoulder, elbow and the wrist restricts hand function (Bland et al., 2008).

Differences in elbow extension angle between the left and right side have been reported, with the left exhibiting a greater extension angle than the right (Gunal et al., 1996). Additionally, hyperextension at the elbow joint has been observed in children (Ellenbecker and Roetert, 2003) as well as in adults (Gunal et al., 1996). The normal elbow extension angle is considered to be 180^{o} and hyperextension is motion beyond this angle (Bryce and Armstrong, 2008).

Strength at the elbow joint varies with the angle of flexion and extension and therefore the torque (strength) also varies. Torque is the amount of force the muscles attached to the limbs are able to produce. The greatest strength at the elbow occurs during flexion, while weakness occurs in extension or with a decreasing (below 90^{o}) angle of flexion. Torque differences have been observed between the sexes, with males showing greater torque than females. Nevertheless, the maximum torque is obtained at 90^{o} flexion in both males and females (Provins and Salter, 1955).

Several factors may affect the range of motion at the elbow joint including the morphology of the ulna (Rouleau et al., 2012), the morphology of the humerus, or disease such as osteoarthritis (Chapleau et al., 2013). Previous studies (Glanville, 1967; Mays, 2008) suggest that the presence of the supratrochlear aperture (STA) could potentially enable an increased range of motion, particularly hyperextension, at the elbow joint.

The STA is the aperture that is formed when the olecranon and coronoid fossae of the humerus communicate via an opening. The frequency of this feature varies by population, ranging from as low as 0.3% among Greeks (Christos et al., 2011) to 58% in Arkansas Indians (Hirsh, 1927). The overall prevalence in South Africa is 32.5% although there are significant differences among the subpopulations (Ndou et al., 2013). Females are reported to have a greater prevalence and the left side is more susceptible to this feature than the right (Mays, 2008).

The STA may be of clinical or surgical importance as its presence may increase risk of fracture to the distal aspect of the humerus and influence fracture patterns and their subsequent treatment (Sahajpal and Pichora, 2006). Further, it is recommended for radiologists to be aware of its occurrence to avoid misinterpretation of images as the STA may be interpreted as an osteolytic lesion (De Wilde et al., 2004).

Mays (2008) suggested that individuals with the STA may have a potential for hyperextension at the elbow joint based on his observation that the tip of the olecranon process of the ulna goes into the STA in full elbow extension. Therefore, we sought to determine whether the presence of the STA is associated with the degree of extension at the elbow joint using articulated dry bones. We also investigated whether there are differences in the degree of elbow extension between males and females with and without the STA. In addition, the osteological parameters that contribute

the most to the presence of the STA and the degree of extension were investigated.

5.2 MATERIALS AND METHODS

5.2.1 Sample

A case-control design was used with roughly equal numbers of bones with and without the STA included. The sample consisted of 453 paired humeri and ulnae from the Raymond A Dart collection of the School of Anatomical Sciences at the University of the Witwatersrand (Dayal et al., 2009). The bones belonged to males (N=164) and females (N=289). Some of the humeri had the STA (N=227) either on the right (N=87) or the left (N=140) and some did not have it (N=226) (Table 5.1). All bones studied were free of pathology and antemortem or postmortem trauma. Features of bone healing, such as a callus, were used to identify antemortem trauma. Postmortem trauma was identified by the presence of sharp surfaces or edges of the aperture and visible trabecular bone.

Table 5.1: Number of humeri with and without STA

	STA	Male	Female	Total
STA Side	**Yes**	**83**	**144**	**227**
	Left	57	83	140
	Right	26	61	87
	No	**81**	**145**	**226**
	Total	164	289	453

5.2.2 Procedure

Parameters of the humerus

Two observers working together established the presence of the STA by visual observation, exercising care to differentiate between a true STA and post mortem damage to the septum. When the STA was present, measurements of the maximum width and height, herein referred to as the transverse (TD) and vertical (VD) diameters of the STA, respectively, were obtained using extended jaw calipers. The product of the TD and VD was used as an estimate of STA size, which was then divided into three groups (small, medium and large) based on equal divisions of the range of values. Measurements of the epicondylar breath (EB), head circumference (HC), humeral length and midshaft circumference were also taken.

Ulnar measurements

An adaptation of a method for measuring the coronoid and olecranon length (Glanville, 1967) was applied. To determine the projections of the coronoid and olecranon processes, measurements were taken at the humero-ulnar articulation (Fig. 5.1). Lengths of the ulnar coronoid and olecranon processes were measured using sliding calipers. With the guide of a goniometer, lines A and B (Fig. 5.1) were drawn such that they were tangents to the curvature of the trochlear notch, ascertaining that a 45^{o} angle resulted where the two lines (A and B) intercept. The length of lines O and C represent the lengths of the olecranon and coronoid process as measured using sliding calipers. The depth (D) of the olecranon notch was measured using a palatometer. For consistency, the arms of the

palatometer were in contact with the highest points of the olecranon and coronoid processes. The shortest distances from the highest points of the olecranon and coronoid processes were used to estimate the olecrano-coronoid distance (OC) (Fig. 5.1). The length of the ulna was taken using an osteometric board.

Measuring the extension angle

For measurement of extension angle, the medial epicondyle was positioned at the center of the goniometer and the humerus was aligned with one arm of a goniometer and stabilized with a hand (Fig. 5.2). The ulna was articulated and positioned to be aligned with the other arm of the goniometer. Both arms of the goniometer were placed with their longitudinal axis matching the corresponding axis along each bone in question (humerus and ulna). The angle of extension was categorized as follows: Normal (180^o), Hypoextension ($<180^o$) and Hyperextension ($>180^o$).

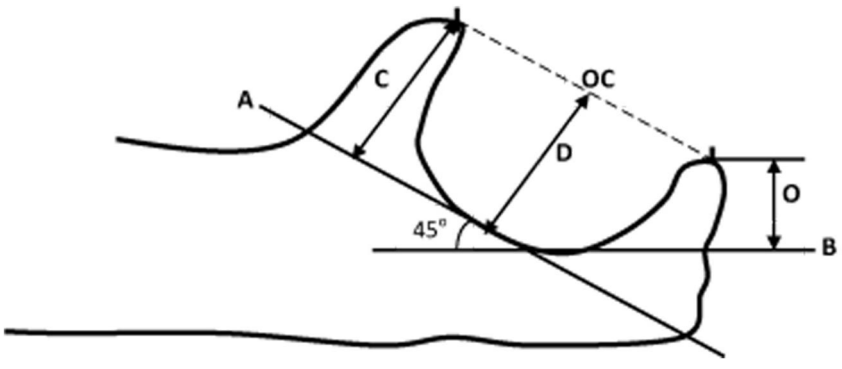


Figure 5.1: Measurements taken from the ulna
(O): olecranon process length, **(C):** coronoid process length, **(D)** ulnar notch depth **(OC)**: olecranon-coronoid distance. Adaptation of Glanville (1967).

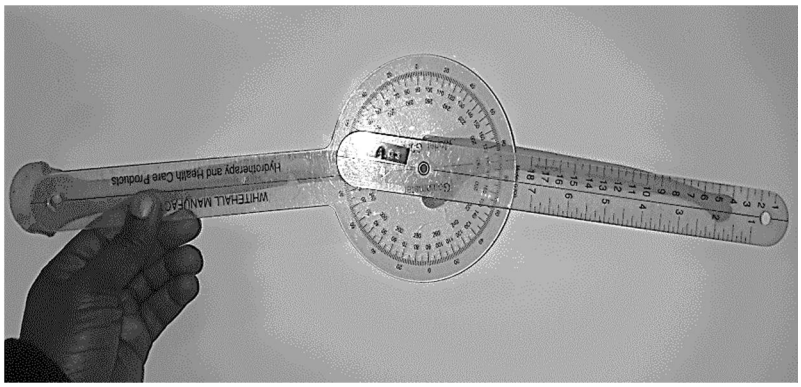


Figure 5.2: Measuring the extension angle

5.2.3 Statistics

The data were managed in Microsoft Excel 2010 (Microsoft Corporation) and analyzed using STATISTICA® software version 12, 2013 (StatSoft®). As two observers took the measurements, Lin's concordance correlation coefficient of repeatability was used to assess the inter-observer error. The Chi-squared (X^2) test was used for the categorical variables whereas the Kruskal-Wallis test was used for the continuous variables as the data were not normally distributed. To identify the variables that contribute the most to the presence of the STA and the degree of extension, a discriminant function analysis was conducted with IBM® SPSS® version 22. The significance level was considered to be $p<0.05$.

5.3 RESULTS

5.3.1 Repeatability

Lin's concordance correlation coefficient of repeatability showed the following pc values: TD (0.9997) and VD (0.9988). Values for pc range from 0 to 1 and a value close to 1 indicates a high degree of repeatability. All pc values obtained were greater than 0.9, which indicates that the correlation between repeated measurements was high and thus inter-observer error was minimal.

5.3.2 Extension Angle

The average extension angle for this sample was 173^{o} (hypoextension). Differences were observed between individuals having the STA and those lacking the feature. When the STA was present, the extension angle was significantly greater than when it was absent ($\overline{X}$=175.4^{o} and $\overline{X}$=171^{o} respectively, p<0.001) (Fig. 5.3A). When the STA was present, the extension angle was greater on the left ($\overline{X}$=176.9^{o}) than when it occurred on the right ($\overline{X}$=173^{o}) (Fig. 5.3B).

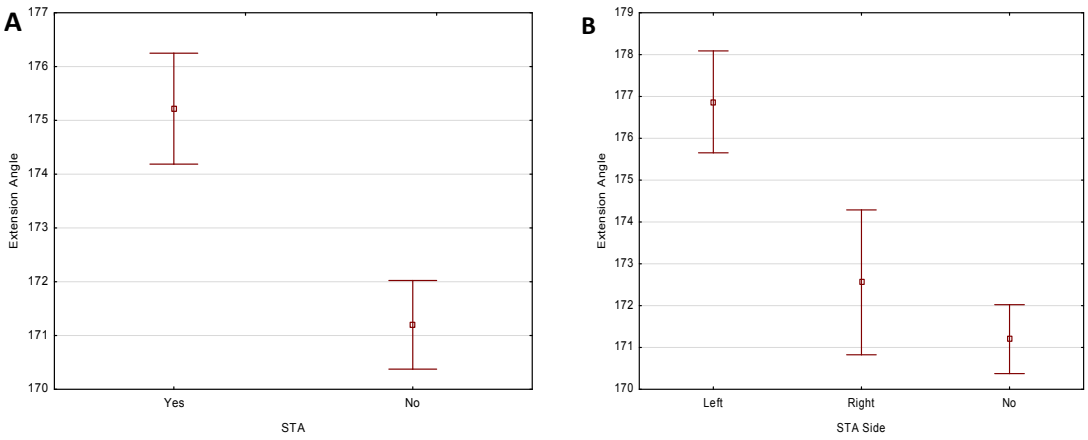


Figure 5.3: Extension angle and the presence of STA (A) and by side (B)

Females had a significantly greater extension angle than males irrespective of the STA status ($\overline{X}$=174.5^{o} and $\bar{X}$=171.3^{o} respectively, p<0.001) (Fig. 5.4). Among males, the angle of extension was greater when the STA was present than when it was absent although there was no significant difference ($\overline{X}$=173.6^{o} and $\overline{X}$=170.4^{o} respectively, p=0.10). In contrast, females showed a significantly greater extension angle when the STA was present than when it was absent ($\overline{X}$=179^{o} and $\overline{X}$=174.2^{o} respectively, p=0.001).

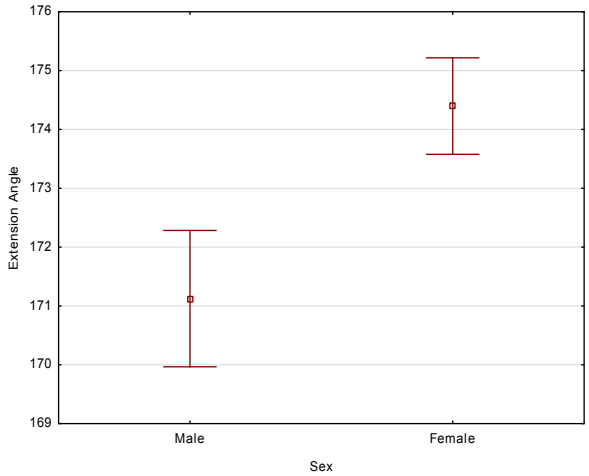


Figure 5.4: Extension angle in males and females

Among males, the extension angle was greater when the STA occurred on the left ($\overline{X}$=173.6^{o}) than on the right ($\overline{X}$=170,4^{o}) and was marginally lower when the STA was absent with a mean of 170.3^{o} (Fig. 5.5). However, there was no statistically significant difference between the sides (p=0.071). In contrast, females had a significantly greater extension angle with the STA on the left ($\overline{X}$=179^{o}) compared to the right ($\overline{X}$=174.2^{o}) being

marginally lower when it was absent ($\overline{X}$=173.3^{o}) (p>0.001 between the sides) (Fig. 5.5).

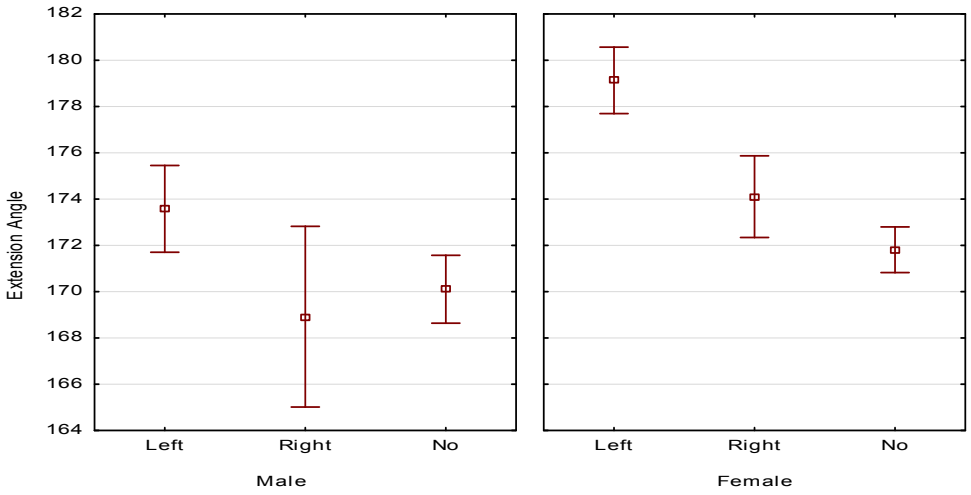


Figure 5.5: Extension angle and the side of STA in males and females

5.3.3 Magnitude of Extension

Although some of the limbs exhibited hyperextension (13%), the majority of them showed hypoextension (76%) and only a small proportion (11%) exhibited normal levels of extension (Fig. 5.6). More females (15%) exhibited hyperextension than males (11%). Hypoextension was significantly more prevalent in males (82%) than in females (71%) (X^2=42, df=1, p<0.001).

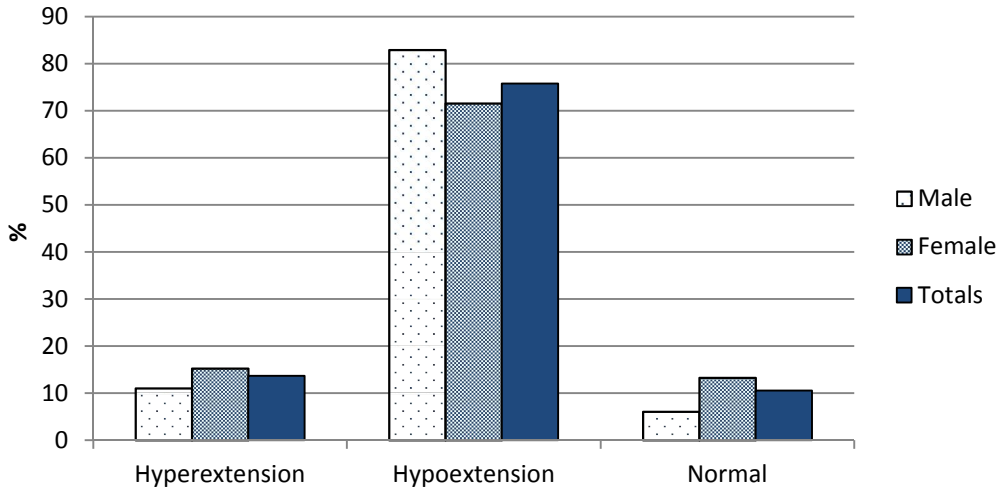


Figure 5.6: Elbow extension in males and females

Some limbs (24%) bearing the STA were able to extend beyond 180^{o} (hyperextension) at the elbow whereas only 3% of those without the STA was able to hyperextend (Fig. 5.6). The ability to hyperextend was dependent on the estimated size of the STA. Thus, when the STA was small, the ability to hyperextend was the least (20%) compared to when it was estimated to be medium (28%) or large (29%). These differences were statistically significant (X^2=449, df=3, p<0.001). Conversely, hypoextension was observed significantly more (X^2=43.46, df=2, p<0.001) when the STA was absent (88%) compared to when it was present (64%). However, hypoextension was exhibited in similar proportions when the STA was small (65%), medium (61%) or large (63%).

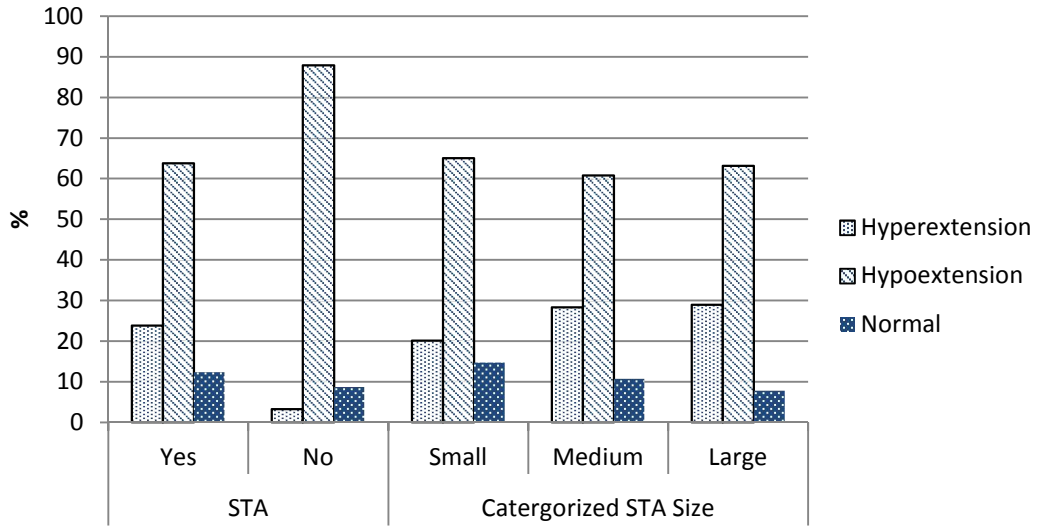


Figure 5.7: Magnitude of extension and STA parameters

5.3.4 Factors influencing the presence of the STA

Discriminant analysis was conducted to predict the presence of the STA and the side on which it occurred. The humeral parameters predicting STA status were midshaft circumference, olecranon fossa depth, and head circumference. The ulnar predictor variables were notch depth, olecranon-coronoid distance, olecranon length. In addition, the extension angle was also a factor in prediction of STA status (Table 5.2). The discriminant analysis yielded two functions with a significant association between groups and all predictors. Function 1 accounted for 94% of the variability whereas Function 2 accounted for only 6%. However, only notch depth and olecranon-coronoid distance were the main predictors in Function 1, while only extension angle was the only main predictor in Function 2. The cross-validated classification showed that overall 62.3% of humeri were correctly classified according to their STA status. The model

correctly classified 72% of the humeri as lacking the STA, yet when the STA was present it could not reliably predict whether the STA was on the left or right (Table 5.3 and Fig. 5.8).

Table 5.2: Correlations between variables discriminating STA status and standardized canonical discriminant functions
The contributing variables are arranged in descending order according to Function 1, with major contributors in bold (above .3).

Structure Matrix

Predictors	Function	
	1	2
Ulnar notch depth	**.886**	.355
Olecranon-coronoid distance	**.578**	.080
Extension angle	**.378**	.818
Olecranon length	**.324**	.079
Humerus midshaft circumference	**.306**	.024
Olecranon fossa depth	.191	.003
Humerus head circumference	.187	.130

Table 5.3: Classification of STA by presence and STA side

		STA Side	Predicted Group Membership			Total
			No	Left	Right	
Original	Count	No	166	44	16	226
		Left	17	105	18	140
		Right	20	50	17	87
	%	No	73.5	19.5	7.1	100
		Left	12.1	75	12.9	100
		Right	23	57.5	19.5	100
Cross-validated[b]	Count	No	164	45	17	226
		Left	17	104	19	140
		Right	22	51	14	87
	%	No	**72.6**	19.9	7.5	100
		Left	12.1	**74.3**	13.6	100
		Right	25.3	58.6	**16.1**	100

a. 63.6% of original grouped cases correctly classified.

b. Each case is classified by the functions derived from all cases other than that case.

c. 62.3% of cross-validated grouped cases correctly classified.

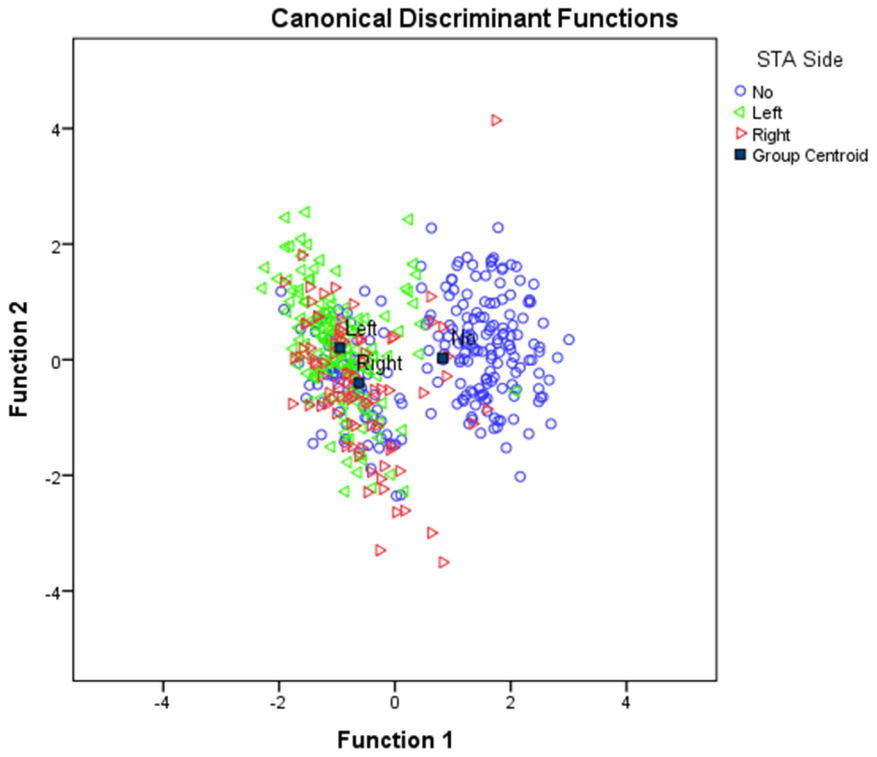


Figure 5.8: Classification of limbs by STA presence and absence

5.3.5 Variables predicting the degree of elbow extension

To determine which variables predict the degree of elbow extension, a second discriminant function analysis was conducted. Predictor variables were STA transverse and vertical diameters, humerus length, epicondylar breadth, ulnar length, olecranon-coronoid distance and ulnar notch depth (Table 5.4). The discriminant model yielded two functions with a significant association between groups and all predictors. Function 1 accounted for 76.8% of the variability whereas Function 2 accounted for 23.2%. The transverse and vertical diameters were the main predictors in Function 1 whereas the olecranon-coronoid distance and ulnar length were the main predictors in Function 2 (Table 5.4). The cross-validated classification showed that overall 74.7% of the cases were correctly classified to the degree of extension. Hypoextension was correctly predicted for 94% of the limbs while none of the limbs were correctly classified as capable of normal extension (Table 5.5 and Fig. 5.9). However, the centroids were clearly separated (Fig.5.9).

Table 5.4: Correlations between variables predicting degree of extension and standardized canonical discriminant functions

Structure Matrix		
Predictors	**Function**	
	1	**2**
Transverse diameters	**.874**	.024
Vertical diameters	**.854**	.061
Ulnar notch depth	**.564**	.461
Olecrano-coronoid distance	**.422**	.732
Ulnar length	**.324**	.566
Humerus length	**.317**	.453
Epicondylar breadth	**.310**	.171

Table 5.5: Classification according to degree of extension

		Extension Angle	Predicted Group Membership			Total
			Hypoextension	Normal	Hyperextension	
Original	Count	Hypoextension	332	2	7	341
		Normal	47	0	3	50
		Hyperextension	48	1	10	59
	%	Hypoextension	97.4	0.6	2.1	100
		Normal	94	0	6	100
		Hyperextension	81.4	1.7	16.9	100
Cross-validated[b]	Count	Hypoextension	329	2	10	341
		Normal	47	0	3	50
		Hyperextension	51	1	7	59
	%	Hypoextension	**96.5**	0.6	2.9	100
		Normal	94	**0**	6	100
		Hyperextension	86.4	1.7	**11.9**	100

a. 76.0% of original grouped cases correctly classified.

b. Each case is classified by the functions derived from all cases other than that case.

c. 74.7% of cross-validated grouped cases correctly classified.

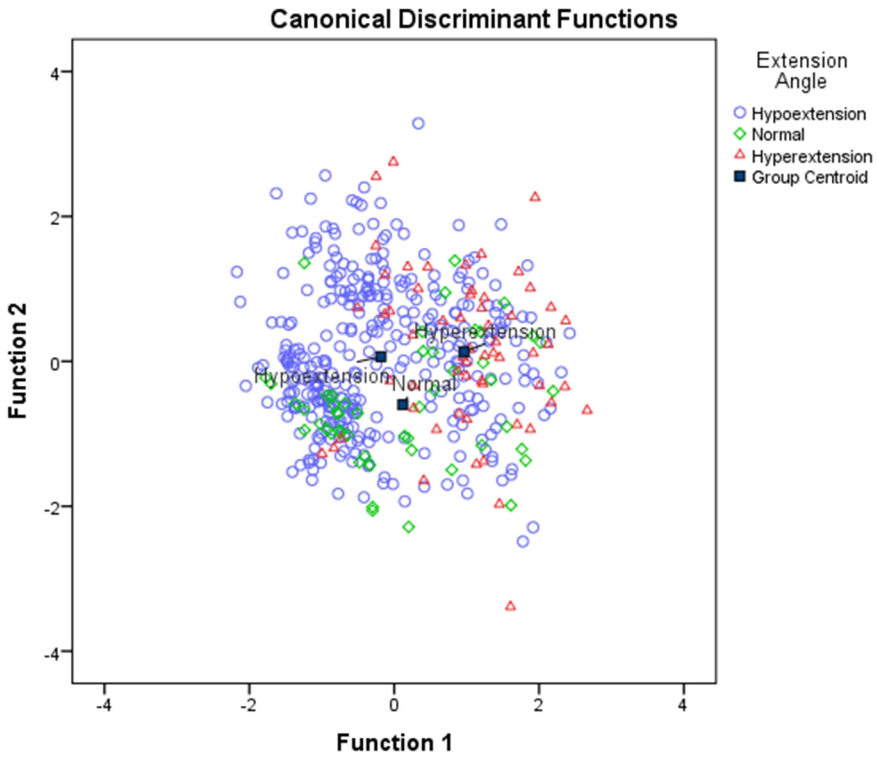


Figure 5.9: Classification of limbs by degree of extension

5.4 DISCUSSION

We investigated the association between STA presence and elbow extension angle in dry bones of males and females. Although some individuals exhibited hyperextension, the average extension angle was below 180° (hypoextension) in the present study. Females exhibited a greater angle of extension than males and the left side showed increased capability to extend although the average angle was still below 180°.

When the STA was present, a greater angle of extension was obtained compared to the cases with no STA. Additionally, hyperextension was more prevalent when the STA was present. This observation supports previous research such as Mays (2008) who attributed these findings to the ability of the ulnar coronoid and olecranon processes to enter the STA during flexion and extension, respectively. This indicates that the STA may expand the range of motion at the elbow joint. This is achieved when the ulnar processes enter the STA to permit an increased range of elbow motion.

The average extension angle below 180° observed in the present study is consistent with the results of previous research that used living human participants (Rouleau et al., 2012; Soucie et al., 2011). Locking of the ulnar olecranon process into the olecranon fossa, as in full extension, may potentially have energy saving benefits as no muscles would be active in this state. Unfortunately, these *in vivo* studies do not have the means of

showing whether the olecranon process fully occupies the STA during full extension.

We found sex differences in the magnitude of elbow extension, with females exhibiting greater degrees of extension than males. This result is consistent with recent findings in living participants (Chapleau et al., 2013). Since males are generally more muscular than females (Akagi et al., 2010), this could explain the smaller range of motion in males as the muscles crossing the joint could impede joint flexibility. Conversely, females have more laxity in joints that allows a greater range of motion about the elbow. While the present study lacks data on arm and forearm circumference, the findings of Chapleau et al. (2013) that these two parameters negatively correlate with flexion suggests that extension may also be constrained.

Gunal et al. (1996) found greater elbow extension angles on the left than on the right side in living children. Similarly, the present study found a greater extension angle on the left regardless of the STA status. We also noted that when the STA was on the left, a greater extension angle was obtained compared to when the STA was on the right and when the STA was absent. Therefore, our findings demonstrate that the left limb has a propensity for a greater extension angle irrespective of STA status.

A greater range of motion at the elbow has been associated with generalized hyperlaxity as measured through the Beighton and Horan Joint Mobility Index (Chapleau et al., 2013; Smits-Engelsman et al., 2011).

This implies that the greater angle of extension on the left and in females may not be solely attributed to the STA as it is possible that other joints may also have a greater range of motion. Our results are consistent with studies in living humans (Chapleau et al., 2013), this further supports our interpretation that the elbow extension angle is influenced by skeletal morphology in addition to the soft tissues such as muscles (Akagi et al., 2010) and joint capsule.

The discriminant function for predicting the presence and side of the STA showed that the olecranon process is among the predictors of STA in addition to other variables such as ulnar notch depth and olecranon-coronoid distance. This finding supports the mechanical theory of STA formation as the ulnar morphology appears to play a major role in the presence of the STA. The mechanical theory proposes that the STA is formed as a consequence of perforation of the septum separating the olecranon from the coronoid fossa. This is thought to result from articulation of the ulna processes with distal aspect of the humerus during extension (Mays, 2008; Singhal and Rao, 2007)

Further, the discriminant function analysis for classifying limbs according to their degree of extension showed that the transverse and vertical diameters of the STA contribute the most to the degree of extension. This result is in agreement with the proposition that limbs with the STA have a greater elbow extension angle (Mays, 2008).

5.5 CONCLUSIONS

We found that the presence of the STA permits a greater angle of extension. Therefore, the STA may be a contributing factor in enabling elbow joint hyperextension. The results show that females have a greater range of motion at the elbow joint than males and that the left side has a greater range of extension compared to the right. While impaired movement at the elbow joint may limit an individual's activities, it is not clear whether a greater range of extension at the elbow joint would be beneficial for most activities. Additionally, it cannot be deduced from the present study whether the degrees of extension found could impact daily living activities. Ulnar morphology has an association with the presence of the STA, thus limbs that have the STA have a greater angle of extension. This study could be of benefit to orthopedic surgeons and physiotherapists when deciding on interventions in cases of elbow deformities, as it contributes to their knowledge of the normal elbow range of motion.

5.6 ACKNOWLEDGEMENTS

We are very grateful to Brendon Billings for access to the skeletal collection and Thokozani Zwane for assistance with data collection. The funds for the project came from the National Research Council (South Africa), University of the Witwatersrand Faculty Research Council, the Wits WHC dividend, and the JJJ Smieszek Fellowship.

CHAPTER 6

Characterization of the tissue crossing the supratrochlear aperture of the humerus using histochemical techniques

Presented at the 18th Congress of the International Federation of Associations of Anatomists (IFAA) 2014, August 8 - 10, Beijing, China

Table of Contents

6.0 ABSTRACT 155
6.1 INTRODUCTION 156
6.2 MATERIALS AND METHODS 158
6.2.1 Sample from cadavers 158
6.2.2 Identification of the STA *in vivo* 159
6.2.3 Tissue harvesting 162
6.2.4 Tissue processing and staining 164
6.4 DISCUSSION 166
6.5 CONCLUSIONS 168
6.6 ACKNOWLEDGEMENTS 168

6.0 ABSTRACT

The supratrochlear aperture (STA) is the opening observed in the septum that separates the olecranon from the coronoid fossae. While numerous studies have shown that there is considerable variation in the occurrence of this feature within and among populations, it has not been studied by histochemical means before. Cadavers (n=43) were assessed for the presence of the STA by means of X-ray. Ten samples of STA bearing bones and an equal number of controls without STA were obtained from cadavers using a hole saw. These samples were decalcified, fixed in formalin and processed for histological assessment in differing (ascending) grades of alcohol before being embedded in paraffin wax. Sections (10μm thick) were stained with Heamatoxylin and Eosin (H&E) for general architecture as well as the Rapid One-Step Mallory-Heidenhain stain for bone and connective tissue. The STA samples exhibited an abundance of connective tissue arranged in regular bundles of fibers across the STA. In contrast, the controls showed only bone tissue in the septum. The arrangement of connective tissue fibers organized in regular bundles is a characteristic of strength, which may indicate that the STA is under sustained stress or pressure from the olecranon and coronoid processes of the ulna. It remains debatable whether the STA should continue to be considered as a foramen in life as we demonstrate that it is obliterated by connective tissue. It contains no neurovascular structures, making it unlike other structures defined as foramina.

6.1 INTRODUCTION

The occasional perforation of the septum that separates the olecranon and coronoid fossae is known as the supratrochlear aperture (STA). Both skeletal and radiographic studies using X-ray and Computed Tomography (CT) scans have been conducted to clarify the frequency, shape and size of this structure in both archaeological and cadaveric samples (Christos et al., 2011; De Wilde et al., 2004; Nayak et al., 2009). The frequency differs substantially in human populations, from as low as 0.3% among Greeks and up to 58% in Arkansas Indians (Nayak et al. 2009). It has been consistently found to occur predominantly on the left side and in females (Krishnamurthy et al., 2011; Mahajan, 2011; Ndou et al., 2013), making it plausible to propose that small-bodied individuals are prone to STA formation (Benfer and McKern, 1966; Mays, 2008).

There is no consensus as to the etiology of the STA. However, there is a school of thought that suggests the mechanical interaction of the ulna with the humerus during flexion and extension at the elbow joint could be the cause (Mays, 2008; Singhal and Rao, 2007). Observed variation across populations led other scholars to argue that the STA is a genetic trait (Koyun et al., 2011). Additionally, nutritional deficiencies have been implicated in STA formation (Koyun et al., 2011). While both genetic and environmental influences are thought to be involved, it remains to be determined to what extent nutrition, occupation or other cultural activities contribute to STA formation. It is not clear whether the etiology is

multifactorial or if a single cause may result in the formation of this aperture.

A foramen is defined as an opening in bone (Moore et al., 2014) that usually serves to allow neurovascular structures to pass through (White et al., 2012). No anatomical structure is known to pass through the STA. Instead, in life the foramen is reported to be covered by a membrane (Nayak et al., 2009). This membrane makes it difficult to visually observe the STA without the use of radiography. The histological characteristics of this membrane are currently unknown. We expect it to be able to withstand the pressure from the ulnar process in elbow flexion and extension.In the present study, a procedure for identifying STAs in cadavers and harvesting the tissue that crosses the STA is presented and the histological characteristics of the STA are described.

6.2 MATERIALS AND METHODS

6.2.1 Sample from cadavers

Paired humeri from 43 cadavers, housed at the University of the Witwatersrand, Johannesburg for use by medical students in 2013, were assessed for the presence or absence of the STA. Of the 43 cadavers, 7 had STA and were thus used in the study with an equal number of controls without STA. A total of 10 samples were collected from these 7 individuals with STA because three individuals had bilateral expressions. Of the individuals with unilateral expression, two had an STA on the left and the remaining two had it on the right (Table 6.1). In unilateral cases, the side without an STA served as the control.

Table 6.1: Samples taken from cadavers. The number of individuals assessed and the distribution of the observed STA on the left and right as well as bilaterally is shown. The last column presents the total number of samples collected.

	Individuals assessed		**Individuals used in the study**			**Number of samples**
Group	STA		Left	Right	Bilateral	Total
Experimental	Yes	7	2	2	3	10
Control	No	36	2	2	3	10
	Total	**43**	**4**	**4**	**6**	**20**

6.2.2 Identification of the STA *in vivo*

Since determination of the STA by physical observation *in vivo* is generally not possible, a portable dental X-ray machine (ARIBEX NOMAD® CE eXaminer) was used. The following problems were encountered: (i) determination of the appropriate or optimal distance from the X-ray machine barrel to the subject (elbow), (ii) establishing the correct exposure to distinguish with certainty between humeri bearing STA and those not, (iii) stability of the X-ray machine during radiography. In order to standardize the distance between the barrel of the X-ray machine and the bone being radiographed, a wooden table was constructed to position and stabilize the machine during the image acquisition (Fig. 6.1).

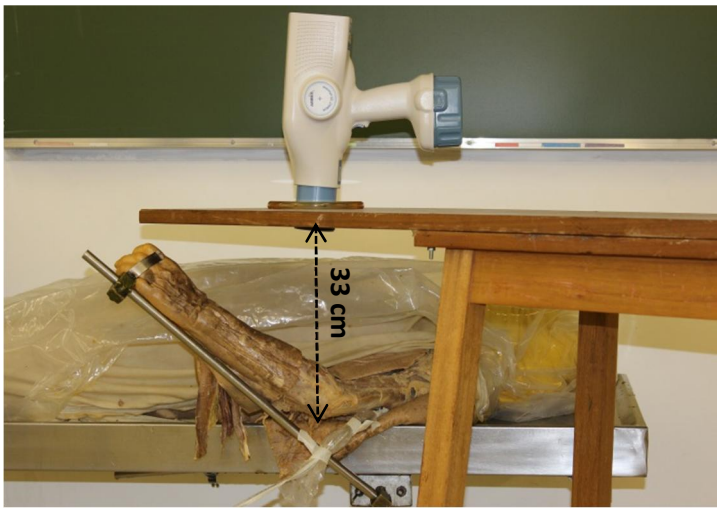


Figure 6.1: The setup of the equipment used to radiograph
A table was designed with an extension on the side where the barrel of the X-ray machine was secured in a circular opening. A distance of 33 cm was maintained between the top of the table and the barrel of the X-ray machine. The elbow was flexed at 135^{o} -140^{o} to keep the olecranon process out of the olecranon fossa.

As the septum is thin, a high radiation exposure may give a false positive STA (i.e. may give an impression that an STA is present while in actual fact it is not). Therefore, a dry humerus with a visible STA was used to determine the parameters in question (i – iii above). The standardized distance (33 cm) and exposure (40kv) that enabled visualization of the STA in this dry bone was used for the cadavers to test for the presence of STA (Fig 6.2).

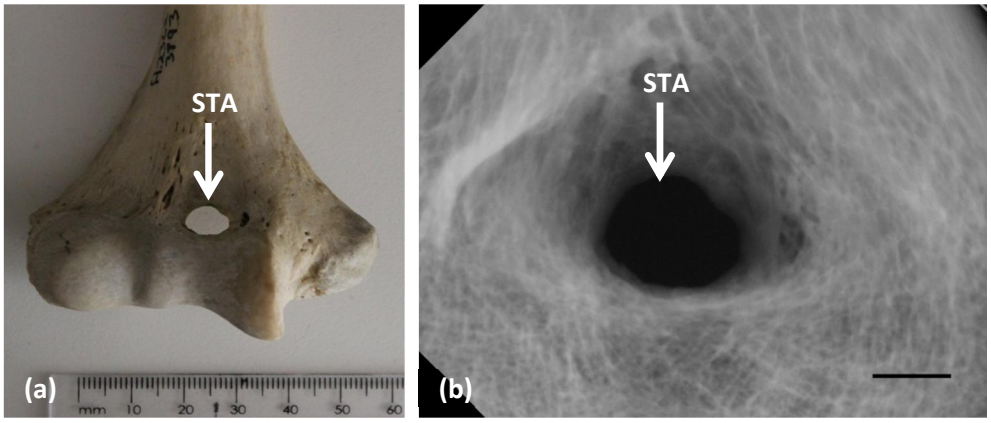


Figure 6.2: A dry bone used for radiographic standardization
(a) A dry bone with an STA.
(b) An anteroposterial (AP) radiograph of the dry bone in '(a)' with the STA visible Scale bar = 5 mm.

In the cadavers, the brachioradialis and the brachialis muscles were separated from the rest of the flexors anteriorly, and the triceps brachii was detached from its distal attachment on the olecranon, posteriorly. This was to simulate the situation of the dry bone. The elbow joint was flexed at 135^{o} - 140^{o} as measured using a goniometer to displace the olecranon process of the ulna from the olecranon fossa. This allowed proper positioning of the sensor directly under the olecranon fossa on the

posterior aspect. Due to the limited size of the X-ray sensor (35mm X 27mm), the entire distal humerus, including the medial and lateral condyles, could not be radiographed at once. Notwithstanding this, the entire olecranon fossa was in view as the sensor was of sufficient dimensions to cover this area. The STA was considered to be present when a clear boundary that surrounded a darker area devoid of visible trabecular bone was observed (Fig 6.3a). In contrast, the STA was considered to be absent when the entire septum exhibited trabecular bone throughout (Fig 6.3b). For the purpose of illustrating the difference between bones with and without STA, two humeri were defleshed and detached from an individual with unilateral STA and radiographed using an X-ray machine with a bigger sensor (Fig. 6.3c and d).

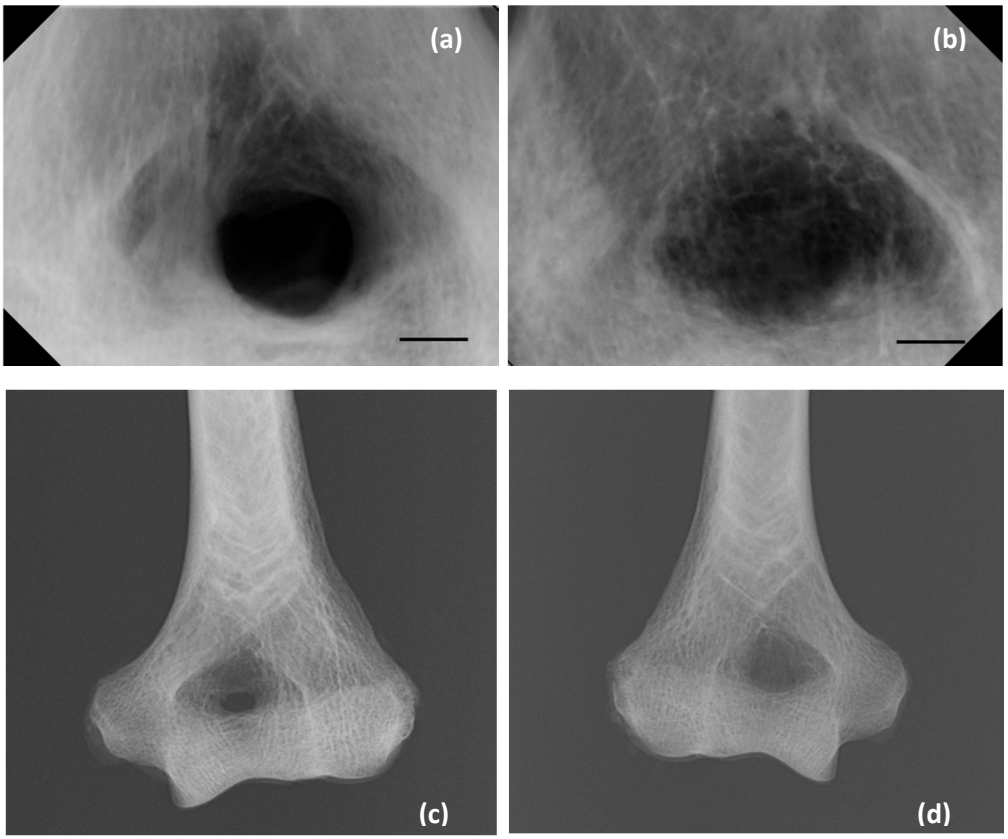


Figure 6.3: Identification of the STA in radiographs; (a) STA as viewed from a cadaver after standardization of the radiography procedure. The borders of the olecranon fossa are clearly visible as well as the trabecular bone within the septum. The margin of the STA is visible as it surrounds a darker area without bone. (b) The STA is absent as the entire septum exhibits bone. Scale bar = 5 mm. Using the MOBILE ART EVOLUTION – SHIMADZU® MUX 200 with a bigger sensor for the same individual with an STA on the left (c) and no STA on the right (d) is shown.

6.2.3 Tissue harvesting

When harvesting the tissue, the objective was to include the area with the STA as well as the surrounding bony areas in order to ascertain that the sample included the entire STA as desired (Fig. 6.4a). When the STA was observed, a metal paper clip cut to resemble a 'U' shape was positioned on the humerus to enclose either side of the STA (Fig. 6.4b) and was

subsequently radiographed (Fig. 6.4c). When the paper clip was confirmed to demarcate the STA, a scalpel was used to mark the location of the wire as an indication of the STA boundaries. These marks served as a guide to position the hole saw appropriately when harvesting the tissue so as to avoid cutting through the area of the STA.

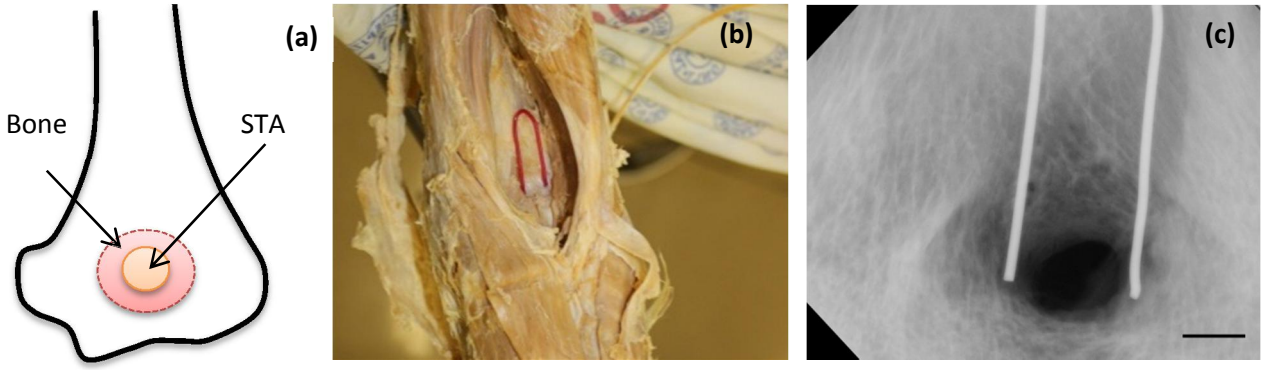


Figure 6.4: Demarcating the area of interest on the humerus for tissue harvesting; (a) The illustration indicates the objective of sampling, showing the STA surrounded by bone. The dotted line encompasses the area intended for drilling to extract the tissue. (b) Paper clip cut to resemble an elongated 'U' shape and strategically positioned on the bone to partially enclose the STA region. (c) Radiograph showing the STA partially enclosed by the paper clip that indicates the extent of the STA for ease of marking on the bone prior to tissue harvesting. Scale bar = 5 mm.

It was previously shown that the STA has an average transverse diameter of 6.3mm (±2.9) and a vertical diameter of 4.1mm (±1.7) in this South African population (Ndou et al., 2013). Therefore, a 10mm hole saw was used to harvest the tissue as it would likely include most of the STA and the surrounding bone (Fig. 6.5a). The tissue samples were radiographed together with a piece of thin wire and the position of the wire was then

marked using a scalpel to indicate where the tissue would subsequently be bisected following decalcification (Fig. 6.5b).

6.2.4 Tissue processing and staining

The tissue samples were decalcified for 24 hours before being processed for histological assessment. Making certain that the STA site remained sandwiched between areas of bone on either side, the tissue samples were then bisected with a scalpel (Fig. 6.5b). An automatic processor was used to take the tissue through different grades of alcohol before embedding the tissue in wax blocks. Cross sections (10μm thick) were cut with a microtome and stained with Hematoxylin and Eosin (H&E) for general morphological assessment and Rapid One-Step Mallory-Heidenhain stain (Cason, 1950) for connective tissue identification.

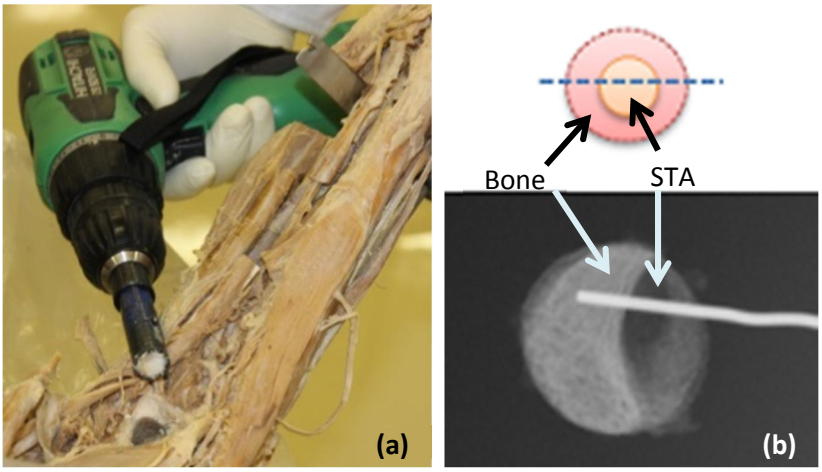


Figure 6.5: Harvesting and bisecting the tissue samples
A 10mm hole saw (a) was used to extract the tissues. (b) The horizontal dotted line on the illustration (top) corresponds to the metal wire positioned to indicate the area of the sample to be bisected in preparation for histological tissue processing.

6.3 RESULTS

The tissue in the STA is composed of dense regular connective tissue labelled C in Fig. 6.6a. The connective tissue consists of both collagen fibers and fibrin. This connective tissue is attached to the bone in a manner resembling the way tendons attach to bone (Fig. 6.6b). The controls show bone throughout the septum (Fig. 6.7).

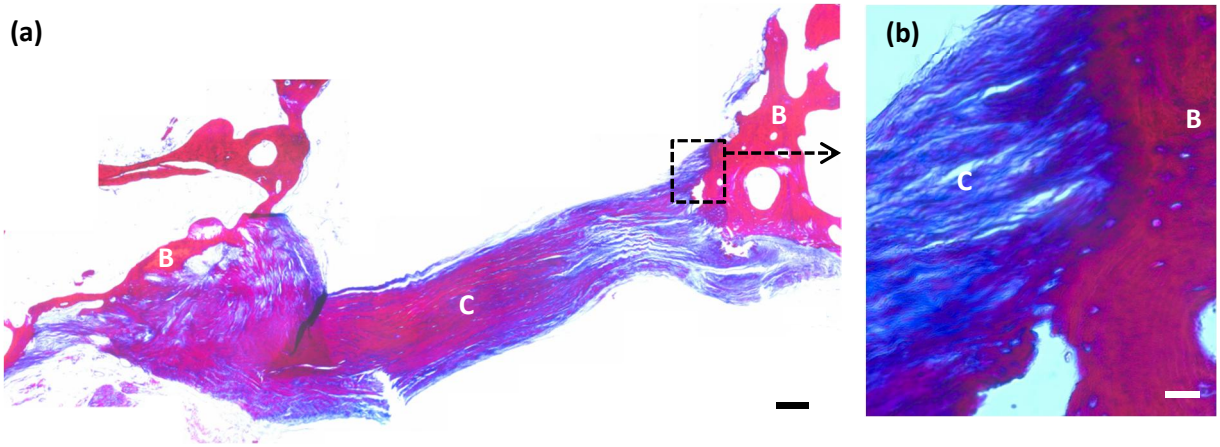


Figure 6.6: STA (composite image) stained with Rapid One-Step Mallory-Heidenhain
(a) Tissue that occupies the STA exhibits an abundance of connective tissue (C) fibers of collagen and fibrin arranged in a regular manner. Scale bar = 500μm. Bone (B) is seen surrounding this connective tissue
(b) A higher magnification showing the attachment of connective tissue to bone. Scale bar = 200μm.

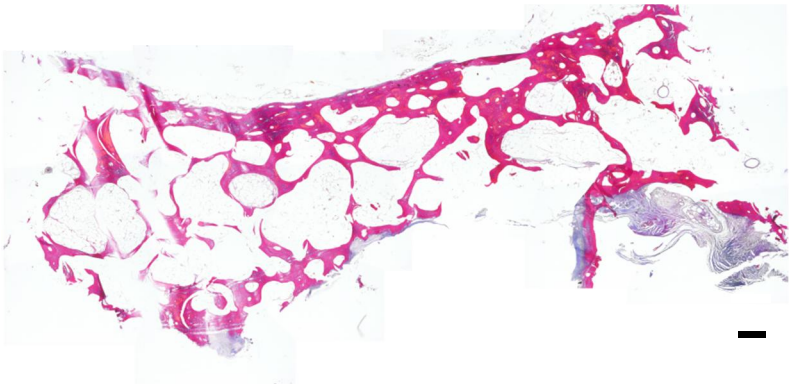


Figure 6.7: Control sample stained with Rapid One-Step Mallory-Heidenhain (composite image)
The STA is absent as indicated by the presence of bone throughout. Scale bar = 500μm.

6.4 DISCUSSION

Histochemical methods were used here for the first time to understand the characteristics of the tissue that occupies the STA *in vivo*. The differences in the radiological and histological features and staining characteristics of the controls compared to the STA samples indicate that we have been able to effectively identify and differentiate between individuals with STA and those without.

As is well known, there is no anatomically functional structure that passes through the STA, and none was observed in this study. Dense regular connective tissue closes the gap created by the bone deficient septum in STA cases. The septum is composed of bone, which suggests that structural strength is required in that area. This may explain why dense regular connective tissue is exhibited when there is a deficiency in the bony septum. The connective tissue may function to provide strength, support and some form of resistance to the movement of the olecranon process of the ulna during flexion and extension. In the present study, we observed both collagen and fibrin in the connective tissue occupying the STA. Previous studies demonstrate that a complimentary relationship exists between these tissues (Lai et al., 2012; Rowe and Stegemann, 2006; Rowe and Stegemann, 2009), with fibrin giving substantial extensibility (Guthold et al., 2007; Liu et al., 2006) while collagen provides stiffness (Lai et al., 2012). It is therefore understandable why both collagen and fibrin are present in the STA as the collagen would help with stiffness while the fibrin allows for stretching. This is particularly important for

extension of the elbow joint as the olecranon process of the ulna could potentially impinge into the STA and stretching would provide room for the olecranon process.

The presence of the dense connective tissue found crossing the aperture appears to be a feature unique to the elbow joint. It is possible that the STA forms as a result of incomplete remodeling in response to pressure from the olecranon process. The result would be bone resorption and subsequent osteoblastic secretion of collagen, but no incorporation of hydroxyapatite occurs. This would allow the aperture region to be pliant and able to withstand the continuing force of the olecranon during joint motion.

The manner in which the connective tissue attaches to the surrounding bony septum resembles the strong character of tendon-bone attachments. This observation suggests that this connective tissue may provide some form of structural integrity despite a deficiency in the bony septum. Additionally, this structure may withstand the tension during elbow extension when the olecranon process of the ulna locks into the olecranon fossa.

The fact that connective tissue occupies the STA foramen makes it debatable as to whether the STA should continue to be considered and defined as a “foramen”. It is understandable why it has been described as a foramen in the past as it has been identified as an opening through bone in cadaveric and archeological human remains and in clinical settings.

Cadaveric remains are subjected to maceration, which may lead to the loss or the removal of the connective tissue occupying the STA when defleshing the bones. Similarly, in archeological material, decomposition of softer tissues would destroy the connective tissue. In radiology (as in clinical settings), the difference in the relative density of bone and connective tissue may explain why characteristics (appearing dark on radiographs) consistent with a foramen are observed. This is because connective tissue present in the STA will appear darker than bone, and thereby resembling a true foramen.

6.5 CONCLUSIONS

In the present study, the STA is shown to be occupied by tissue that may be of considerable strength in light of its dense regular connective tissue composition. This tissue is strongly attached to the bony septum in a manner comparable to the way tendons attach to bone, suggesting a need for structural strength. As the etiology of the STA remains unknown, this study contributes significantly to the basis of future studies that may seek to understand how the STA is formed. Long-term studies of the olecranon fossa at various stages of growth and development are needed to elucidate the etiology of the STA and the possible involvement of T-box genes is worth exploring in future studies.

6.6 ACKNOWLEDGEMENTS

We are very grateful to Alison Mortimer, Hasiena Ali and Monica Gomes for assistance with sectioning and staining of the tissue. The following

students took part in the project as part of their undergraduate training: Lindsay Kaberry, Daniel Mak and Ivan Jovanovic. Tony Meadows and Leon Du Plessis assisted with image processing. The funds for the project came from the National Research Council (South Africa), University of the Witwatersrand Faculty Research Council, the Wits WHC dividend, and the J.J.J Smieszek Fellowship.

CHAPTER 7

Generalized Discussion

and Conclusion

Table of Contents

7.0 GENERALIZED DISCUSSION 172
7.1 STA prevalence and characteristics in South Africa 173
7.3 Investigation of STA etiology and function 174
7.4 Clinical implications for intramedullary fixation 176
7.5 CONCLUSIONS 177

7.0 GENERALIZED DISCUSSION

The present study investigated several questions pertaining to the possible etiology and function of the supratrochlear aperture using a sample of South African populations. First, we documeneted the frequency of the aperture and its size and shape variability. Then, tested the hypothesis that gracility of their bones may predispose individuals to aperture formation (Benfer and McKern, 1966; Mays, 2008). We subsequently tested the mechanical etiology hypothesis that the length of the ulnar coronoid and olecranon processes and their spatial relationship are implicated in STA formation as these structures are thought to impinge on the olecranon fossa during elbow extension (Glanville, 1967; Mays, 2008). The internal humeral structure was studied with respect to the mediolateral medullary canal width and cortical bone thickness as information from orthopedic practice suggests that these dimensions may vary according to STA status (Mays, 2008; Singhal and Rao, 2007). To address the possible functions of the STA, we documented extension ability of humeroulnar joints. Finally, we examined the tissue that occupies the STA in life.

Despite the STA being a subject of study for over a century, no single study attempted to systematically investigate the above questions in a large skeletal collection of known sex, age and ancestry. Many past studies relied on archeological material with single and often fragmented humeri, unpaired arm elements, and undocumented demographics. Such studies have to use osteological features to estimate sex, age and skeletal associations. In the present study, sex and ethnicity are known, age was

usually known, and the majority of the individuals had the left and right humeri and ulnae present.

7.1 STA prevalence and characteristics in South Africa

Prior to Ndou et al. (2013), there were no studies on STA frequency in South African populations. In the present study the prevalence of the STA across six South African groups was found to be 32.5%. The aperture occurred predominantly on the left and more frequently in females (19.5%) than in males (13%), as is commonly observed in other populations (Ndou et al., 2013)

Whites (16%) exhibited the lowest prevalence of STA, followed by the Mixed group (31%) with almost twice the prevalence. Of the South African indigenous Black groups, the Sotho (41%) had the highest prevalence followed by the Tswana (39%), Zulu (33%) and Xhosa (33%). Additionally, the shape of the STA was assessed. The most common form being the oval, whereas the triangular form was the least common observed.

7.2 Characteristics of bones with STA

Most measures of overall humeral size, such as epicondylar breadth, humeral head circumference and the three shaft circumferences, were significantly larger when the STA was absent in all three populations. This supports the general proposition that smaller-bodied individuals are prone to septal perforation. However, an important result of our study is the finding from our discriminant analyses that determinants of STA status are population specific. For Blacks and the Mixed group, the olecranon process length was the sole main contributor to STA status. Lower

loadings for this variable were found for the Mixed group. Therefore, this variable can more reliably predict STA status in Blacks compared to the Mixed group. In Whites, with a lower prevalence of the STA, more parameters are required for STA prediction compared to the Mixed group or Blacks. These additional parameters were proximal humeral shaft circumference (right) and trochlear notch depth (left).

The differences in the discriminant analysis loadings for the left and right humeral variables in STA status predictions could be a result of handedness or predominant utilization of one arm. Occupational and other behaviors are some of the causes of extensive usage of one arm that may result in our observed STA and bone size asymmetries.

7.3 Investigation of STA etiology and function

To evaluate whether humerus and ulna articulation may result in STA formation, dimensions of the olecranon and coronoid processes and the olecranon fossa were compared by STA status. The olecranon process was longer and the olecranon fossa was shallower when the STA was present, whereas the coronoid process length did not differ by STA status. This illustrates that the olecranon process, and not the coronoid process, may be implicated in STA etiology. The best explanation for this result is the difference in the musculature surrounding the elbow. Muscles in the anterior compartment of the arm and forearm may limit elbow flexion so that the coronoid process does not engage with the septum to the same extent as the olecranon process does posteriorly.

The depth of the olecranon fossa also varied among the groups studied. Whites had a deeper mean olecranon fossa compared to the others; Blacks and the Mixed ethnic group had similar fossa depths. Whites also had a lower prevalence of STA than Blacks and the Mixed ethnic group. If the mechanical theory of STA formation is correct, it would be expected for Whites to have shorter mean olecranon lengths than Blacks and individuals of Mixed ethnicity. However, a long olecranon process coupled with a deeper olecranon fossa would permit sufficient room for elbow extension without septal perforation. Taken together, these results support the mechanical theory of STA formation as a deeper olecranon fossa may provide sufficient room for the ulnar olecranon process in elbow extension. It follows that, with sufficient olecranon fossa depth, the process may not impinge upon the septum, thereby reducing the likelihood of mechanical perforation.

The presence of the dense connective tissue found crossing the aperture needs to be explained as it appears to be a feature unique to the elbow joint. It is possible that remodeling may be initiated in response to pressure from the olecranon process, however, sufficient time may not be available for complete remodeling resulting in STA formation. The result would be bone resorption and subsequent osteoblastic secretion of collagen, but no incorporation of hydroxyapatite occurs – rendering the aperture region pliant and able to withstand the continuing force of the olecranon during joint motion. As to the function of the STA covering tissue, it may be of considerable strength in light of its dense regular connective tissue composition. It is strongly attached to the bony septum

in a manner comparable to the way tendons attach to bone, suggesting a need for structural strength. One explanation for this particular feature of the tissue may be that it functions to prevent locking the olecranon process in the joint.

An additional aspect to be considered regarding function of the STA is that the mean extension angle in the STA bearing arms is greater. This implies that the olecranon process tip may penetrate the aperture (as observed on many dry bone specimens), permitting a greater extension angle. It follows that the elbow range of motion is greater in STA individuals.

7.4 Clinical implications for intramedullary fixation

We did not find differences in the proportion of the mediolateral medullary canal width with respect to STA status when the canal width was standardized by humeral length or diameter. The smaller medullary canal width observed in STA humeri is due to the bone size differences rather than the presence of the STA. We therefore propose that bone size be the major factor to consider when making choices of a rod for intramedullary fixation.

Limitations

The sample for Whites was relatively small and there was a general lack of individuals above the age of 75 years and those in teenage years. It would have been interesting to see if there were differences in cortical thickness in teenagers and adults above the age of 75 years.

The radiographic measurements were taken only in the mediolateral aspect. It is possible that different results would have been obtained if it

was possible to take the measurements in the anteroposterior aspect. Further studies using CT scans may be more appropriate for investigation of this relationship.

Measurements of the extension angle were done on dry bones, which means that the angles obtained might not be the same as in the living. This is because there are soft tissues in the living such as muscles, tendons and cartilage that may impact on the resultant elbow range of motion.

7.5 CONCLUSIONS

In summary, the following seven conclusions can be drawn from this study:

1. The prevalence of the STA is higher in South African Black and Mixed populations compared to Whites (Chapter 2).
2. The occurrence of a long olecranon process with a shallow olecranon fossa was associated with the presence of the STA, and as such, supports the role of the olecranon process as the mechanical basis for STA formation (Chapter 3).
3. Measures of humeral size are greater in individuals without the STA, verifying that smaller bones are prone to STA formation (Chapter 3).
4. We did not find differences in the proportion of the mediolateral medullary canal width with respect to STA status when bone size

was factored in, indicating that bone size, and not the STA, was correlated with medullary canal mediolateral width (Chapter 4).

5. There is no correlation between medullary canal mediolateral width and cortical bone thickness among individuals exceeding 75 years of age; this suggests that the remodeling cycle may be different for individuals of this age cohort (Chapter 4).
6. A greater elbow extension angle occurs in arms bearing the STA (Chapter 5).
7. Dense regular connective tissue attached to the surrounding bone occupies the STA and no neurovascular structures were found. Therefore, the feature should be referred to as an aperture and not a foramen (Chapter 6).

7.6 GENERAL ACKNOWLEDGMENTS

I am very grateful to my supervisor, Professor L. A Schepartz, for her guidance and assistance throughout the entire project.

8.0 REFERENCES

Akabori E. 1934. Septal apertures in the humerus in Japanese, Ainu and Koreans. Am J Phys Anthropol 18:395-400.

Akagi R, Takai Y, Kato E, Wakahara T, Ohta M, Kanehisa H, Fukunaga T, Kawakami Y. 2010. Development of an equation to predict muscle volume of elbow flexors for men and women with a wide range of age. Euro J Appl Physiol 108:689-694.

Akpinar F, Aydinlioglu A, Tosun N, Dogan A, Tuncay I, Unal O. 2003. A morphometric study on the humerus for intramedullary fixation. Tohoku J Exp Med 199:35-42.

Alt Murphy M, Willen C, Sunnerhagen KS. 2011. Kinematic variables quantifying upper-extremity performance after stroke during reaching and drinking from a glass. Neurorehabil Neural Repair 25:71-80.

Amft EN, Buckley CD, Ralston SH. 2013. Physiology & pathology of the musculoskeletal system, 2nd ed. Toronto: Mosby Elsevier.

Baker JB, Dupras LT, Tocheri W. 2005. The Osteology of Infants and Children

1st ed. Texas A&M University Press.

Basson CT, Bachinsky DR, Lin RC, Levi T, Elkins JA, Soults J, Grayzel D, Kroumpouzou E, Traill TA, Leblanc-Straceski J, Renault B, Kucherlapati R, Seidman JG, Seidman CE. 1997. Mutations in human TBX5 cause limb and cardiac malformation in Holt-Oram syndrome. Nat Genet 15:30-35.

Benfer RA, McKern TW. 1966. The correlation of bone robusticity with the perforation of the coronoid-olecranon septum in the humerus of man. Am J Phys Anthropol 24:247-252.

Binkley N, Bone H, Gilligan JP, Krause DS. 2014. Efficacy and safety of oral recombinant calcitonin tablets in postmenopausal women with low bone mass and increased fracture risk: A randomized, placebo-controlled trial. Osteoporos Int:Epub ahead of print.

Bland MD, Beebe JA, Hardwick DD, Lang CE. 2008. Restricted active range of motion at the elbow, forearm, wrist, or fingers decreases hand function. J Hand Ther 21:268-274.

Bronner F, Farach-Carson M. 2004. Bone formation. London ; New York: Springer.

Bryce CD, Armstrong AD. 2008. Anatomy and biomechanics of the elbow. Orthop Clin North Am 39:141-154.

Cason JE. 1950. A rapid one-step Mallory-Heidenhain stain for connective tissue. Stain Technol 25:225-226.

Cauley JA, Lui LY, Ensrud KE, Zmuda JM, Stone KL, Hochberg MC, Cummings SR. 2005. Bone mineral density and the risk of incident nonspinal fractures in black and white women. JAMA 293:2102-2108.

Chapleau J, Canet F, Petit Y, Sandman E, Laflamme GY, Rouleau DM. 2013. Demographic and anthropometric factors affecting elbow range of motion in healthy adults. J Shoulder Elbow Surg 22:88-93.

Chapman DL, Garvey N, Hancock S, Alexiou M, Agulnik SI, Gibson-Brown JJ, Cebra-Thomas J, Bollag RJ, Silver LM, Papaioannou VE. 1996. Expression of the T-box family genes, Tbx1-Tbx5, during early mouse development. Dev Dyn 206:379-390.

Christos P, Marios P, Apostolos S. 2011. Rare cases of humerus septal apertures in Greeks. Trends Med Res 6:178-183.

Colbert RA. 2007. Genes and common diseases: Genetics in modern medicine. New York: Cambridge University Press.

Crockett JC, Rogers MJ, Coxon FP, Hocking LJ, Helfrich MH. 2011. Bone remodelling at a glance. J Cell Sci 124:991-998.

Dayal MR, Kegley ADT, Štrkalj G, Bidmos MA, Kuykendall KL. 2009. The history and composition of the Raymond A. Dart Collection of Human Skeletons at the University of the Witwatersrand, Johannesburg, South Africa. American Journal of Physical Anthropology 140:324-335.

De Groot JH, Angulo SM, Meskers CG, van der Heijden-Maessen HC, Arendzen JH. 2011. Reduced elbow mobility affects the flexion or extension domain in activities of daily living. Clin Biomech 26:713-717.

De Wilde V, De Maeseneer M, Lenchik L, Van Roy P, Beeckman P, Osteaux M. 2004. Normal osseous variants presenting as cystic or lucent areas on radiography and CT imaging: A pictorial overview. Eur J Radiol 51:77-84.

De Wit E, Delport W, Rugamika CE, Meintjes A, Moller M, Van Helden PD, Seoighe C, Hoal EG. 2010. Genome-wide analysis of the structure of the South African Coloured Population in the Western Cape. Hum Genet 128:145-153.

Ellenbecker TS, Roetert EP. 2003. Isokinetic profile of elbow flexion and extension strength in elite junior tennis players. J Orthop Sports Phys Ther 33:79-84.

Gartner PL, Hiatt JL. 2014. Color Atlas of Histology, 5th ed. Philadelphia: Lippincott Williams & Wilkins.

Glanville EV. 1967. Perforation of the coronoid-olecranon septum. Humero-ulnar relationships in Netherlands and African populations. Am J Phys Anthropol 26:85-92.

Govoni KE, Lee SK, Chadwick RB, Yu H, Kasukawa Y, Baylink DJ, Mohan S. 2006. Whole genome microarray analysis of growth hormone-induced gene expression in bone: T-box3, a novel transcription factor, regulates osteoblast proliferation. Am J Physiol Endocrinol Metab 291:28-36.

Govoni KE, Linares GR, Chen ST, Pourteymoor S, Mohan S. 2009. T-box 3 negatively regulates osteoblast differentiation by inhibiting expression of osterix and runx2. J Cell Biochem 106:482-490.

Gray DJ, Gardner E. 1969. The prenatal development of the human humerus. Am J Anat 124:431-445.

Gunal I, Kose N, Erdogan O, Gokturk E, Seber S. 1996. Normal range of motion of the joints of the upper extremity in male subjects, with special reference to side. J Bone Joint Surg Am 78:1401-1404.

Guthold M, Liu W, Sparks EA, Jawerth LM, Peng L, Falvo M, Superfine R, Hantgan RR, Lord ST. 2007. A comparison of the mechanical and structural properties of fibrin fibers with other protein fibers. Cell Biochem Biophys 49:165-181.

He M, Wen L, Campbell CE, Wu JY, Rao Y. 1999. Transcription repression by Xenopus ET and its human ortholog TBX3, a gene involved in ulnar-mammary syndrome. Proc Natl Acad Sci U S A 96:10212-10217.

Hirsch IS. 1928. On a Foramen in the Lower Extremity of the Humerus. Radiology 10:199-208.

Hirsh IS. 1927. The supratrochlear foramen: Clinical and anthropological considerations. Am J Surg 2:500-505.

Ho PW, Goradia A, Russell MR, Chalk AM, Milley KM, Baker EK, Danks JA, Slavin JL, Walia M, Crimeen-Irwin B, Dickins RA, Martin TJ, Walkley CR. 2014. Knockdown of PTHR1 in osteosarcoma cells decreases invasion and growth and increases tumor differentiation in vivo. Oncogene:Epub ahead of print.

Isaac A, Rodriguez-Esteban C, Ryan A, Altabef M, Tsukui T, Patel K, Tickle C, Izpisua-Belmonte JC. 1998. Tbx genes and limb identity in chick embryo development. Development 125:1867-1875.

Keating J. 2013. Fracture management. In: Luqmani R, Robb J, Poter D, Joseph B, editors. Textbook of Orthopaedics, Trauma and Rheumatology, 2nd ed. Toronto: Mosby. p 117-139.

Kierszenbaum AL, Tres LL. 2012. Histology and cell biology : An introduction to pathology, 3rd ed. Philadelphia, PA: Saunders.

Koyun N, Aydinlioglu A, Gumrukcuoglu FN. 2011. Aperture in coronoid-olecranon septum: A radiological evaluation. Indian J Orthop 45:392-395.

Krishnamurthy A, Yelicharla A, Takkalapalli A, Munishamappa V, Bovinndala B, Chandramohan M. 2011. Supratrochlear foramen of humerus – A morphometric study. Int J Biol Med Res 2:829-831.

L'Abbe EN, Loots M, Meiring JH. 2005. The Pretoria Bone Collection: a modern South African skeletal sample. Homo 56:197-205.

Lai VK, Lake SP, Frey CR, Tranquillo RT, Barocas VH. 2012. Mechanical behavior of collagen-fibrin co-gels reflects transition from series to parallel interactions with increasing collagen content. J Biomech Eng 134:011004.

Lamb D. 1980. The olecranon perforation. Am Anthropol 3:159-174.

Laval-Jeantet AM, Bergot C, Carroll R, Garcia-Schaefer F. 1983. Cortical bone senescence and mineral bone density of the humerus. Calcif Tissue Int 35:268-272.

Lee TC, Staines A, Taylor D. 2002. Bone adaptation to load: Microdamage as a stimulus for bone remodelling. J Anat 201:437-446.

Leonard MB, Elmi A, Mostoufi-Moab S, Shults J, Burnham JM, Thayu M, Kibe L, Wetzsteon RJ, Zemel BS. 2010. Effects of sex, race, and puberty on cortical bone and the functional muscle bone unit in children, adolescents, and young adults. J Clin Endocrinol Metab 95:1681-1689.

Liu W, Jawerth LM, Sparks EA, Falvo M, Hantgan RR, Superfine R, Lord ST, Guthold M. 2006. Fibrin fibers have extraordinary extensibility and elasticity. Sci 313:634.

Magermans DJ, Chadwick EK, Veeger HE, van der Helm FC. 2005. Requirements for upper extremity motions during activities of daily living. Clin Biomech 20:591-599.

Mahajan A. 2011. Supratrochlear foramen: Study of humerus in North Indians. Professional Med J 18:128-132.

Mays S. 1996. Age-dependent cortical bone loss in a medieval population. Int J Osteoarchaeol 6:144-154.

Mays S. 2008. Septal aperture of the humerus in a mediaeval human skeletal population. Am J Phys Anthropol 136:432-440.

Meiring RM, Avidon I, Norris SA, McVeigh JA. 2013. A two-year history of high bone loading physical activity attenuates ethnic differences in bone strength and geometry in pre-/early pubertal children from a low-middle income country. Bone 57:522-530.

Mescher AL. 2013. Connective Tissue. In: Junqueira's Basic Histology, 13e. New York: The McGraw-Hill Companies.

Ming-Tzu PA. 1935. Septal apertures in the humerus in the Chinese. Am J Phys Anthropol 20:165-170.

Miyamoto I, Tsuboi Y, Wada E, Suwa H, Iizuka T. 2005. Influence of cortical bone thickness and implant length on implant stability at the time of surgery - clinical, prospective, biomechanical, and imaging study. Bone 37:776-780.

Moore K, Dalley A, Agur A. 2014. Clinically oriented anatomy, 7th ed. New York: Lippincott Williams & Wilkins.

Nayak SR, Das S, Krishnamurthy A, Prabhu LV, Potu BK. 2009. Supratrochlear foramen of the humerus: An anatomico-radiological study with clinical implications. Ups J Med Sci 114:90-94.

Ndou R, Smith P, Gemell R, Mohatla O. 2013. The supratrochlear foramen of the humerus in a South African dry bone sample. Clin Anat 26:870-874.

Niinimaki S, Soderling S, Junno JA, Finnila M, Niskanen M. 2013. Cortical bone thickness can adapt locally to muscular loading while changing with age. Homo 64:474-490.

O'Neill OR, Morrey BF, Tanaka S, An KN. 1992. Compensatory motion in the upper extremity after elbow arthrodesis. Clin Orthop Relat Res 281:89-96.

Ortner D. 2003. Identification of pathological conditions in human skeletal remains, 2nd ed. London: Academic Press.

Ovalle WK, Nahirney PC. 2013. Netter's Essential Histology, 2nd ed. Philadelphia: Saunders.

Paraskevas GK, Papaziogas B, Tzaveas A, Giaglis G, Kitsoulis P, Natsis K. 2010. The supratrochlear foramen of the humerus and its relation to the medullary canal: A potential surgical application. Med Sci Monit 16:119-123.

Parfitt AM. 1984. Age-related structural changes in trabecular and cortical bone: cellular mechanisms and biomechanical consequences. Calcif Tissue Int 36 Suppl 1:S123-128.

Paulsen DF. 2010. Connective Tissue. In: Histology & Cell Biology: Examination & Board Review, 5th ed. New York: The McGraw-Hill Companies.

Pearson OM, Lieberman DE. 2004. The aging of Wolff's “law”: Ontogeny and responses to mechanical loading in cortical bone. American Journal of Physical Anthropology 125:63-99.

Provins KA, Salter N. 1955. Maximum torque exerted about the elbow Joint. J Appl Physiol 7:393-398.

Raggatt LJ, Partridge NC. 2010. Cellular and molecular mechanisms of bone remodeling. J Biol Chem 285:25103-25108.

Ross MH, Edward R, Romrell L. 1989. Histology: A colour text and atlas, 2nd ed.

Ross MH, Pawlina W. 2011. HIstology: A text and atlas, 6th ed. Philadelphia: Lippincott Williams & Wilkins,.

Rouleau DM, Canet F, Chapleau J, Petit Y, Sandman E, Faber KJ, Athwal GS. 2012. The influence of proximal ulnar morphology on elbow range of motion. J Shoulder Elbow Surg 21:384-388.

Rowe SL, Stegemann JP. 2006. Interpenetrating collagen-fibrin composite matrices with varying protein contents and ratios. Biomacromolecules 7:2942-2948.

Rowe SL, Stegemann JP. 2009. Microstructure and mechanics of collagen-fibrin matrices polymerized using ancrod snake venom enzyme. J Biomech Eng 131:061012.

Rubin C, Judex S, Hadjiargyrou M. 2002. Skeletal adaptation to mechanical stimuli in the absence of formation or resorption of bone. J Musculoskelet Neuronal Interact 2:264-267.

Ruff C, Holt B, Trinkaus E. 2006. Who's afraid of the big bad Wolff?: "Wolff's law" and bone functional adaptation. Am J Phys Anthropol 129:484-498.

Sahajpal DT, Pichora D. 2006. Septal aperture: an anatomic variant predisposing to bilateral low-energy fractures of the distal humerus. Can J Surg 49:363-364.

Sajantila A, Lahermo P, Anttinen T, Lukka M, Sistonen P, Savontaus ML, Aula P, Beckman L, Tranebjaerg L, Gedde-Dahl T, Issel-Tarver L, DiRienzo A, Paabo S. 1995. Genes and languages in Europe: an analysis of mitochondrial lineages. Genome Res 5:42-52.

Silveira F, Junior V, Fazan V. 2007. Anthropometric evaluation of the humerus in the presence and absence of the septal foramen. Int J Morphol 25:158 (Abstract).

Simon H. 1999. T-box genes and the formation of vertebrate forelimb- and hindlimb specific pattern. Cell Tissue Res 296:57-66.

Singhal S, Rao V. 2007. Supratrochlear foramen of the humerus. Anat Sci Int 82:105-107.

Smits-Engelsman B, Klerks M, Kirby A. 2011. Beighton score: a valid measure for generalized hypermobility in children. J Pediatr 158:119-112

Soucie JM, Wang C, Forsyth A, Funk S, Denny M, Roach KE, Boone D. 2011. Range of motion measurements: Reference values and a database for comparison studies. Haemophilia 17:500-507.

Steyn M, Iscan MY. 1999. Osteometric variation in the humerus: sexual dimorphism in South Africans. Forensic Sci Int 106:77-85.

Stull KE, L'Abbé EN, Steiner S. 2013. Measuring distortion of skeletal elements in Lodox Statscan-generated images. Clin Anat 26:780-786.

Sunday O, Olusegun O, Oluwabunmi B. 2014. The supratrochlear foramen of the humerus: implications for intramedullary nailing in distal humerus. J Bio, Agri Healthcare 4:136-139.

Thandrayen K, Norris SA, Pettifor JM. 2009. Fracture rates in urban South African children of different ethnic origins: the Birth to Twenty cohort. Osteoporos Int 20:47-52.

Trotter M. 1934. Septal apertures in the humerus of American Whites and Negroes. Am J Phys Anthropol 19:213-227.

Vasen AP, Lacey SH, Keith MW, Shaffer JW. 1995. Functional range of motion of the elbow. J Hand Surg Am 20:288-292.

Vidulich L, Norris SA, Cameron N, Pettifor JM. 2006. Differences in bone size and bone mass between black and White 10-year-old South African children. Osteoporos Int 17:433-440.

Volkman SK, Galecki AT, Burke DT, Paczas MR, Moalli MR, Miller RA, Goldstein SA. 2003. Quantitative trait loci for femoral size and shape in a genetically heterogeneous mouse population. J Bone Miner Res 18:1497-1505.

White TD, Black MT, Folkens PA. 2012. Human Osteology, 3rd ed. San Diego: Elsevier Academic Press.

Wilk K, Andrews J. 2001. Rehabilitation of Elbow Injuries. In: Puddu G, Giombini A, Selvanetti A, editors. Rehabilitation of Sports Injuries: Springer Berlin Heidelberg. p 73-93.